ISTANBUL TECHNICAL UNIVERSITY ★ GRADUATE SCHOOL OF SCIENCE

EVALUATION OF SEISMIC HEALTH MONITORING SYSTEM OF GOLDEN HORN METRO BRIDGE

M.Sc. THESIS

Eray TEMUR

Department of Civil Engineering

Structural Engineering Programme

JULY 2019

ISTANBUL TECHNICAL UNIVERSITY ★ GRADUATE SCHOOL OF SCIENCE

EVALUATION OF SEISMIC HEALTH MONITORING SYSTEM OF GOLDEN HORN METRO BRIDGE

M.Sc. THESIS

Eray TEMUR
(501161008)

Department of Civil Engineering

Structural Engineering Programme

Thesis Advisor: Asst. Prof. Barış ERKUŞ

JULY 2019

İSTANBUL TEKNİK ÜNİVERSİTESİ ★ FEN BİLİMLERİ ENSTİTÜSÜ

HALİÇ METRO KÖPRÜSÜNÜN SİSMİK SAĞLIK İZLEME SİSTEMİNİN DEĞERLENDİRİLMESİ

YÜKSEK LİSANS TEZİ

Eray TEMUR
(501161008)

İnşaat Mühendisliği Anabilim Dalı

Yapı Mühendisliği Programı

Tez Danışmanı: Asst. Prof. Barış ERKUŞ

TEMMUZ 2019

Eray TEMUR, a M.Sc. student of ITU Graduate School of Science Engineering and Technology student ID 501161008 successfully defended the thesis entitled "EVALUATION OF SEISMIC HEALTH MONITORING SYSTEM OF GOLDEN HORN METRO BRIDGE", which he prepared after fulfilling the requirements specified in the associated legislations, before the jury whose signatures are below.

Thesis Advisor :	**Asst. Prof. Barış ERKUŞ** Istanbul Technical University	.....
Jury Members :	**Assoc. Prof. Barlas Özden ÇAĞLAYAN** Istanbul Technical University	.....
	Prof. Dr. Erdal ŞAFAK Boğaziçi University	.....

Date of Submission : **3 May 2019**
Date of Defense : **11 July 2019**

In the memory of my father,

FOREWORD

First of all, I would like to express my sincere gratitude to my supervisor Asst. Prof. Dr. Barış Erkuş, for his support and encouragement.

I would like to thank my jury members, Assoc. Prof. Dr. Barlas Özden Çağlayan for his guidance and continuous contribution during this thesis and Prof. Dr. Erdal Şafak for his precious comment and suggestions.

I would like to express my special thanks to my dear friends İrem Topal, Taygun Güngör, Barış Burnak, and Burak Uçar for their continuous support throughout my thesis.

I am also grateful to my research group friends Barış Kasapoğlu, Ömer Galip Pınar, Ceyda Ergül, and Kubilay Çiçek for their cooperation.

I must also express my very profound gratitude to my family for their unconditional love and support.

Most of all, I owe my deep and sincere gratitude to my wife, Derya for her continuous encouragement and unending patience. This journey would not have been possible without her.

July 2019

Eray TEMUR
(Civil Engineer)

TABLE OF CONTENTS

Page

ABBREVIATIONS

AASHTO : American Association of State Highway and Transportation Officials
ASCE : American Society of Civil Engineers
GHB : Golden Horn Bridge
DBYBHY : Deprem Bölgelerinde Yapılacak Binalar Hakkında Yönetmelik
FEMA : Federal Emergency Management Agency
PEER : Pacific Earthquake Engineering Research Center
PP : Peak Picking
BFD : Basic Frequency Domain
FDD : Frequency Domain Decomposition
SSI : Stochastic Subspace Identification
SSI-DATA : Data Driven Stochastic Subspace Identification
SSI-COV : Covariance Driven Stochastic Subspace Identification
MAC : Modal Assurance Criterion
ARMA : Auto Regressice Moving Average
CMIF : Complex Mode Indication Function
ITD : Ibrahim Time Domain
DFT : Discrete Fourier Transform
FEM : Finite Element Method
FFT : Fast Fourier Transform
FRF : Frequency Response Function
MACEC : Modal Analysis on Civil Engineering Constructions
SVD : Singular Value Decomposition
PSD : Power Spectral Density
SI : System Identification
SHM : Structural Health Monitoring
PSD : Power Spectral Density
FEE : Functional Evaluation Earthquake
SEE : Safety Evaluation Earthquake
RS : Response Spectrum
CSB : Cable-Stayed Bridge

SYMBOLS

$\mathbf{C}$	:	Damping Matrix
$\mathbf{K}$	:	Stiffness Matrix
$\mathbf{M}$	:	Mass Matrix
μ	:	Mean
$E[\cdot]$	:	Expectation Operator
σ_x	:	Standard Deviation
$R_{xy}(\tau)$	:	Crosscorrelation of x and y
$R_x(\tau)$	:	Autocorrelation of x
$\mathbf{R}_x(\tau)$	:	Correlation matrix of x
$S(f)$	:	Power Spectral Density Function
Σ	:	Singular Values Matrix
$\mathbf{U}$	:	Left Singular Values Matrix
$\mathbf{V}$	:	Right Singular Values Matrix
$x[\cdot]$	:	Discrete system input
$y[\cdot]$	:	Discrete system output
$x(\cdot)$	:	Continuous system input
$y(\cdot)$	:	Continuous system output
$\mathbf{A}_c$	:	Continuous State Matrix
$\mathbf{B}_c$	:	Continuous Input Matrix
$\mathbf{C}_c$	:	Continuous Output Matrix
$\mathbf{D}_c$	:	Continuous Feedforward Matrix
$\mathbf{A}_d$	:	Discrete State Matrix
$\mathbf{B}_d$	:	Discrete Input Matrix
$\mathbf{C}_d$	:	Discrete Output Matrix
$\mathbf{D}_d$	:	Discrete Feedforward Matrix
$\mathscr{L}(\cdot)$	:	Laplace Transform
f	:	Frequency (Hz)
ω	:	Circular Frequency (rad/s)
K	:	Kalman Gain Matrix
Q, R	:	Factors of QR factorization
$y(t)$	:	Output at time t
$x(t)$	:	State at time t
$\mathscr{F}(\cdot)$	:	Fourier Transform
$\mathscr{P}$	:	Controllability Matrix
$\mathscr{O}$	:	Observability Matrix
$\mathscr{O}_{i-1}$	:	Extended Observability Matrix
$\mathscr{N}(\mu, \sigma)$:		Gaussian Distribution with mean μ and standard devitaion σ

$H(\cdot)$	:	Transfer Function
$X(s)$	:	State in the Laplace Domain
s	:	Laplace Domain Variable
$X(z)$	:	State in the z Domain
$p(\cdot)$	:	Probability Density Function
z	:	z Domain Variable
q	:	Modal Displacement
ξ	:	Damping Ratio
$\hat{\mathbf{X}}$	:	Kalman State Matrix
Q, R, S	:	Process and Measurement Noise Covariance Matrices
$(\cdot)^{\dagger}$	:	Moore-Penrose pseudo-inverse of a matrix
$(\cdot)^{\mathrm{H}}$	:	Complex Conjugate Transpose of a matrix
$(\cdot)^{\mathrm{T}}$	:	Transpose of a Matrix
Ψ	:	Mode shape matrix
Λ_{d}	:	Eigenvalue Matrix

LIST OF TABLES

Page

LIST OF FIGURES

Page

EVALUATION OF SEISMIC HEALTH MONITORING SYSTEM OF GOLDEN HORN METRO BRIDGE

SUMMARY

Performance-based design is an established approach in civil engineering. In this context, it is required to estimate the performance of the building at any time both after the design and during the service period. For example, the new performance level should be determined in damaged structures. System identification can be performed to ascertain the behavior of a given structure using specific parameters. However, structural element capacities are reduced and the forces to be resisted are increased in the design of structures. Therefore, in case of critical structures, such as bridges, system identification should be performed immediately after design and when encountering sudden loads. Thus, the source of the changing dynamic behavior of the structure can be detected in order that more realistic results can be obtained to analyze the structure.

In structural health monitoring studies, acceleration and displacement measurements are used to predict structural behavior. Modal properties of the structure can be obtained from sensor data using system identification algorithms, and they provide a reference point in order to compare the theoretical and real physical models of the structure. In this way, those models can be brought closer to each other. This method is primarily used to determine whether the structure is damaged. In case there is damage then its location should be found. If the damage can be located, it can be repaired without any loss. Upon the damage and location are identified, the damage level of the structure should also be determined, which will provide the reparability of the structure. Lastly, the remaining service life of the structure should be established, since it may ensure safer use of the structure and can serve to avoid possible negative consequences.

In this study, system identification of the Golden Horn Metro Crossing Bridge was realized and the performance of the bridge was assessed. The construction of the Golden Horn Bridge was started in 2009, and the bridge was opened in 2014. The bridge has been used for metro crossing of Hacıosman-Yenikapı M2 metro line. The Golden Horn Bridge consists of five separate bridges: cable-stayed bridge, swing bridge, single-span bridge, Beyoglu approaching bridge, and Unkapanı approaching bridge. Beyoglu and Unkapanı approaching bridges are made of reinforced concrete, while other bridges are constructed as steel structures. The bridge design was made by Wiecon, and there is a permanent health monitoring system on the bridge, which was established by Vienna Consulting Engineers (VCE). The permanent bridge health monitoring system includes sensors and GPSs for temperature displacement, slope and acceleration measurement. The data measured by the sensors are collected at the Metro Istanbul Headquarters. In addition, the first measurements were made by VCE using temporary sensors after the construction of the bridge. Based on the first measurements, the suitability of the bridge to design projects and the permanent

health monitoring system were tested. However, no software developed for system identification is currently available for the bridges. This study aims to evaluate the current system of the bridge by the software to be developed specifically for the Golden Horn Bridge and to present a framework to evaluate the health of a building when it is subjected to loads throughout its service life.

In this study, system identification methods are also compared using experimental and numerical studies. Additionally, system identification methods are implemented in the Golden Horn Bridge. Comparison of structural acceleration measurements involves field studies on the Golden Horn Bridge based on the sensor measurements of the structure, comparison of system identification algorithms on the Golden Horn Bridge and finally the determination of the performance of the Golden Horn Bridge were performed. Moreover, Average Normalized Power Spectral Density, frequency domain decomposition and Stochastic Subspace Identification were used as compared system identification algorithms, which were programmed using MATLAB software. These three different algorithms, which are widely used in the system identification of bridge structures in the literature, were compared in terms of the effect of different sensor numbers on the system identification within the experiments performed in ITU Steel Laboratory. Moreover, two-dimensional structural analysis program that was also programmed using MATLAB software was developed, and its accuracy was compared with SAP2000 software. System identification was performed by applying different levels of Gaussian white noise on the numerical model.

HALİÇ METRO KÖPRÜSÜNÜN SİSMİK SAĞLIK İZLEME SİSTEMİNİN DEĞERLENDİRİLMESİ

ÖZET

Performansa dayalı tasarım anlayışı inşaat mühendisliğinde kabul görmüş bir yaklaşımdır. Bu çerçevede yalnızca tasarım sonrasında değil yapı hizmet süresi içinde herhangi bir zamandaki yapının performansının da tahmin edilebilmesi gerekmektedir. Örneğin, Hasar görmüş yapılarda yeni performans seviyesinin belirlenmesi gerekebilir. Sistem tanılama ise verilen bir yapının davranışının belirli parametreler ışığında tespit edilmesinde kullanılabilmektedir. Öte yandan yapıların tasarımında da yapısal eleman kapasiteleri azaltılır gerekli karşı koyulması gereken kuvvetler ise artırılmaktadır. Bu yaklaşım da yapıların dinamik davranışını öngörülen davranıştan uzaklaştırabilir. Bu sebeple önemli yapılarda sistem tanılama tasarımın hemen ardından ve/veya ani yüklemelere karşılaştıktan sonra uygulanabilir. Bu sayede yapının değişen dinamik davranışının kaynağı bulunabilmektedir. Buradan hareketle, yapısal sistem tanılama yapının performans seviyesinin belirlenmesi ile beraber kullanıldığında daha gerçekçi sonuçlar elde edilebilmektedir.

Yapısal sağlık izleme çalışmalarında yapısal davranış tahmini için ivme ve yerdeğiştirme ölçümlerinden yararlanılmaktadır. Sistem tanılama algoritmaları yardımıyla sensor verilerinden yapının modal özellikleri elde edilebilmektedir. Yapının modal özellikleri ise yapının teorik modeli ile gerçek fiziksel model arasında benzerlik açısından karşılaştırabilmek üzere bir referans noktası sunar. Bu sayede yapının fiziksel modelinden alınan özellikler ile teorik modeli birbirlerine yaklaştırılabilmektedir. Bu yöntem ile ulaşılmak istenilen öncelikli olarak yapının hasarlı olup olmadığının saptanmasıdır. Hasarlı olduğu anlaşılırsa, yapının hasarının lokasyonunu bulmak gerekmektedir. Hasar lokasyonu bulunursa herhangi bir kayıp vermeden yapısal hasar onarılabilecektir. Ayrıca yapısal hasarın ve lokasyonunun bulunmasının ardından yapının hasar seviyesinin tespitidir. Yapının hasar seviyesinin tespit edilmesi yapının onarılabilirliğinin de değerini verecektir. Nihai amaç ise yapının kalan ömrünün tespit edilmesidir. Yapının kalan hizmet ömrünün tespit edilmesi, yapıların daha güvenli kullanımlarını sağlayabilir ve muhtemel olumsuz sonuçlardan kaçınılmasına hizmet edecektir.

Bu çalışmada Haliç Metro Geçiş Köprüsünün sistem tanılaması ve performans seviyesinin belirlenmesi uygulanmıştır. Haliç köprüsü inşaatı 2009 yılında başlamış, 2014 yılında kullanıma açılmış olan ve demiryolu metro geçişi için kullanılan eğik askılı çelik bir köprüdür. Eğik askılı çelik köprü, açılır/kapanır köprü, tek açıklıklı köprü, Beyoğlu yaklaşım köprüsü ve Unkapanı yaklaşım köprüsü olmak üzere 5 ayrı bölümden oluşmaktadır. Bu bölümlerden Beyoğlu ve Unkapanı yaklaşım köprüleri betonarme ve diğer köprüler çelik olarak inşa edilmiştir. Hacıosman-Yenikapı M2 metro hattı için kullanılmaktadır. Köprü tasarımı Wiecon firması tarafından yapılmış olup, köprü üzerinde Vienna Consulting Engineers isimli firma tarafından kurulmuş olan kalıcı bir sağlık izleme sistemi mevcuttur. Haliç köprüsü sağlık

izleme sisteminde sıcaklık yerdeğiştirme, eğim, ivme ölçümü için kullanılan sensörler ve GPS'ler bulunmaktadır. Bu sensorlerde ölçülen veriler Metro İstanbul ana merkezinde toplanmaktadır. Ayrıca VCE firması tarafından, yapının yapım aşaması sonrasında ilk ölçümler geçici sensörlerle gerçekleştirilmiştir. İlk ölçümler ile hem yapının tasarım projelerine uygunluğu test edilmiş hem de kalıcı sağlık izleme sistemi test edilmiştir. Ancak halihazırda sistem tanılama sisteminin yapılması için geliştirilmiş bir yazılım köprü işletmesi bünyesinde bulunmamaktadır. Bu çalışmanın amacı Haliç Köprüsü özelinde geliştirilecek bir yazılımın köprünün mevcut sistemini değerlendirmek hem de yapı ömrü boyunca karşılaştığı yüklemeler sonrasında da yapı sağlığını değerlendirecek bir çatı sunmaktır.

Bu çalışmada ivme ölçümleriyle yapılarda kullanılan sistem tanılama algoritmalarının deneysel ve nümerik olarak karşılaştırılması, Haliç köprüsünde yapılan saha çalışmalarıyla elde edilen yapısal ivme ölçümlerinin, yapıda bulunan sensör ölçümleri ile karşılaştırılması, sistem tanılama algoritmalarını Haliç köprüsü üzerinde uygulanarak karşılaştırılması ve son olarak da Haliç köprüsü performans seviyesinin belirlenmesi gerçekleştirilmiştir.

Karşılaştırılan sistem tanılama algoritmaları, Ortalama normalize spektral güç yoğunluğu, frekans alanında dekompozisyon ve stokastik altuzay tanılamasıdır. Sistem tanılama algoritmaları MATLAB yazılımı kullanılarak programlanmıştır. Literatürde köprü yapılarının sistem tanılamasında yaygın olarak kullanılan bu 3 ayrı sistem tanılama algoritması, ITU Çelik Laboratuvarında hazırlanmış deney düzeneğinde farklı sensor sayılarının sistem tanılamaya etkisi açısından karşılaştırılmıştır. Ayrıca yine MATLAB yazılımı kullanılarak programlanan 2 boyutlu yapısal analiz programı geliştirilmiş, doğruluğu SAP2000 programı ile karşılaştırılmıştır. Nümerik model üzerine farklı seviyelerde gauss beyaz gürültüsü uygulanarak sistem tanılama algoritmalarına gürültü seviyesi etkisi araştırılmıştır. Ayrıca kurulan deney düzeneğinde iki farklı ivme ölçerden alınan titreşim verileri karşılaştırılmıştır. Bu çalışmada ivme ölçer ölçümlerinden deplasman sinyaline geçişte filtreleme ve referans doğrulama (baseline correction) etkisi araştırılmıştır. Öte yandan bu algoritmalar Haliç köprüsü kalıcı sağlık sisteminde test edilmiş ve gerekli parametreler elde edilememiştir. Bu sebeple Haliç Köprüsü tabliyesinde öğlen pik saatlerde saha ölçümleri yapılmış ve modal parametreler başarı ile elde edilmiştir. Böylece mevcut kalıcı yapısal sağlık izleme sistemi ve saha ölçümleri sonucunda elde edilen veriler de karşılaştırılmıştır. Saha ölçümü sonucunda elde edilen yapısal modal parametrelerin ilk ölçümlerde elde edilen parametrelere yakın olduğu görülmüştür.

Son olarak yapısal sonlu eleman modeli mevcut tasarım raporları, proje çizimleri ve geoteknik raporları ışığında toprak etkisini de dikkate alacak şekilde kurulmuştur. Yapısal analizler genel olarak kabul görmüş bir yapısal analiz programı olan SAP2000 programı kullanılarak gerçekleştirilmiştir. Verilen deprem etkisi altında doğrusal davranışa geçmesi öngörülen yapı bölgeleri tasarım raporlarına göre sünek davranış kabulu yapılan yapı bölgeleri olarak seçilmiştir. Yapının doğrusal olmayan davranışı SAP2000 yazılımı kullanılarak rijit-plastik mafsal olarak modellenmiştir. Kurulan yapısal modelin modal analizleri statik itme ve zaman tanım alanında analizler yapılmış ve yapının tasarım raporlarına da uygun olarak doğrusal olmayan davranışa geçtiği gözlemlenmiştir. Karşılaştırılan sistem tanılama algoritmalarının yüksek gürültü seviyelerinde ve sensor sayısının da yakalanmak istenen mode sayısına bağlı olmak üzere elde edilen sonuçların kabul edilebilir mertebe olduğu görülmüştür.

Sonuç olarak, Haliç Metro Köprüsü yapısal sağlık izleme sisteminin deprem etkilerine yönelik kullanılması açısından mevcut sistem değerlendirilmiş ve mevcut sistemin deprem sonrası karar alma süreçlerinde kullanımı için geliştirilmesi gerektiği sonucuna ulaşılmıştır.

1. INTRODUCTION

1.1 Overview

It is known that the population of metropolises has increased significantly in recent decades. The growing population and economy result in demand for the larger urban infrastructure for more civilized and social living. It is also needed buildings for accommodation purposes in the limited land and transportation infrastructures that may be in a difficult geographic condition. To solve these problems, humanity comes up with tall buildings and bridges as a solution. Thanks to recent technological advances, the bridges may be constructed to get over with the very strong obstacles such as a valley or body of water. The major transportation and accommodation requirement must be solved for increasing the welfare of society. Moreover, transportation without traffic is another prerequisite for modern life, and the bridges are used to decrease the traffic.

The importance of civil engineering structures such as bridges depends on not only the invested high amount of money but also utilization by the great number of people daily. Bridges are widely constructed in today's metropolises. The bridges can have many different properties. Bridges can be classified into 5 major categories: beam bridges, cantilever bridges, arch bridges, suspension bridges and cable-stayed bridges. Suspension bridges and cable-stayed bridges are widely used for transportation purposes. Generally, cable-stayed bridges are built to serve railway transportation. Any time the train passes, the bridge is loaded axially and these stresses are carried by the cables. Stayed-cables are placed diagonally and attached to pylons directly. These type bridges are easily reparable and constructible since they are constructed without main cable. Usually, mid-span bridges are built as cable-stayed.

The main aspect of the civil engineering design is optimizing the material used without any compromise on safety. However, the structures like bridges are highly sensitive to the dynamic loads. Dynamic loads can cause vibration-induced structural failures

and serviceability problems. That emphasizes the importance of the performance assessment of the structures that have been built. After any structure has been built, the performance should be validated based on the assumption made at the design stage. Also, the probable earthquake event or the undesired situation have many other uncertainties. Structures like bridges or tall building need to be investigated in terms of structural performance. Dynamic behavior of structures subjected to the random vibrations might alter in time. Failure or collapse mechanisms of various dynamical systems has been investigated by many engineers and scientists. Furthermore, structural health monitoring (SHM) methods may be used for estimating the structural response properties in the effects of dynamic loads.

In the earthquake prone areas, structures are designed as resistant to the earthquake. Although the earthquake performance assessment has many uncertainties. One of these uncertainties is dependence on whether structural mathematical model the same as the real structure or not. The mathematical properties of the structure can be extracted using SHM and finite elements model updating can be used to obtain the real structural model. So, the mathematical model of the structures can be used for the performance assessment of the structures. The main purpose of the performance assessment of a structure is the damage level estimation after a probable earthquake. Therefore, SHM is valuable civil engineering tool to assess the performance.

The Golden Horn (Metro Crossing) Bridge (GHB) located in Istanbul, has been investigated in this study. Istanbul, one of the biggest metropolitan cities in the world, is prone to seismic action. So that the structures located in Istanbul need to be assessed in terms of earthquake resistance. System identification, FEM model updating, and performance assessment of the GHB are presented in this study.

1.2 Literature Review

1.2.1 Structural Health Monitoring

Doebling *et al.* reviewed the literature up to 1996 and classified the structural health monitoring methods [3]. This review was based on the classification defined by Rytter [4]. According to this classification, damage identification may be divided into four main classes as follows [4];

- Determination of existence of the damage in existing structure,
- Determining spatial location of damage,
- Quantification of the damage level
- Forecasting the remaining life of the structure.

The review conducted by Doebling *et al.* emphasized that the damage level of structures can be defined based on structural parameters change in order to investigate the existence of damage, such as frequency change, mode shape change, mode shape curvature change, and flexibility change. On the other hand, almost all methods depend on availability of accurate finite element model or the undamaged data sets. With no available data for the undamaged structures, structural health monitoring may not be applicable. Moreover, finite element models utilized as undamaged structural properties source evaluated from linear structural models. Nonlinear models or nonlinear structural response may not be taken advantage of as a damage index. Also, the importance of the sensor number to be placed and their location has been highlighted to proper identification of damage location. The survey recommends the structural health monitoring community to apply the methods on real structures in operating environments. Structure-specific studies need to be applied to support the utility of methods [3].

Sohn *et al.* conducted another review summarized and compared the works carried out from 1996 to 2001 [5]. Comparatively to the recent review, structural health monitoring problem was dealt with the solution of the inverse problem. To solve the inverse problem linear structural model was used. Dependency on the linear structural model and its uncertainties could not be fully coped with. However, some researchers conducted unsupervised learning paradigm, in order to avoid the dependency. In addition to the unsupervised learning approach, neural network paradigm which is supervised learning is also used, even though the common training methods have not been agreements on. Another important progress in the structural health monitoring has been improvement and decrement of prices of the microelectromechanical sensors (MEMS). The price of MEMS being affordable means that the sensor number is not a great deal for structural health monitoring [5].

Carden and Fanning present another review on structural health monitoring literature [6]. The same classification of damage identification was used defined by Rytter. The studies of interest are the ones conducted between 1996 and 2003. In this interval, there has not been an agreement on the damage identification methods to use structural health monitoring of real structures. The researchers used the laboratory test to validate the algorithms but the scientists suggested that the algorithms shall be evaluated using real scale structures. However, the laboratory-scale test helps to develop the algorithms but the real measurements still have uncertainties. Also, while some of the algorithms work for one damage types, other algorithms work for other types in locating damage. On the other hand, some researchers use statistical pattern recognition paradigm but the method's usage was limited to only level 1 of damage identification namely determination of damage existence [6].

Fan and Qiao provide a review on the beam-type and plate-type structures [7]. Some of the civil engineering structures may be simplified as beam-type and plate-type structures. These structures may also be the benchmark problem to be used for the more complex structures. Authors stated that frequency change-based methods may be successfully used to identify small damages in simplified structures, but in more complex structures, these methods have some limitations. For the localize the damage mode shape-based methods which depend on the optimization algorithms need to be used. Moreover, the situations subjected to the environmental noise, the development of robust damage detection algorithms and its extension to the quantification of damage found to be necessary for the future studies [7].

1.2.2 System identification

System identification is a systematic study of evaluation of mathematical models through measurements. Generally system identification methods are divided into two major parts. These are parametric methods and non-parametric methods. In parametric methods, the structural model is represented the limited number of parameters such as state-space matrix entries, while the single tabulated form is the all representation of the structural behavior, in the non-parametric methods. In other words, parametric and non-parametric methods are named as model based and non-model based methods, respectively. Another classification of system identification methods widely used is

based on its domain; time and frequency domain even though almost every time domain methods have equivalent of frequency domain method. In this thesis, time and frequency domain classification is used [8].

Peak picking is widely used system identification methods in civil engineering structures. Peak picking technique, basic frequency domain in other words, is named for when applying from FRF obtained is used for selecting local maximum. Because of its simplicity and intuitiveness, the basic frequency domain method is one of the most common system identification methods. Peak picking technique defined by Felber, is suggested to use for ambient vibration cases and the method has some limitations, such that structure should be linear, lightly damped, and he modes of interest should be well separated and excited [9]. However, these methods may not be applicable to all kinds of structures, it may be used to provide information about the structures of interests [9]. This method is based on obtaining transfer function of structures and power spectral densities. This method is used within the scope of this thesis, and explained broadly in Chapter 2.

Frequency Domain Decomposition (FDD) is another frequency domain system identification method. The method was first proposed by Brincker *et al.* [10]. This method is also applied in this thesis and explained how to apply in Chapter 2. But there are many counterparts of this method in the literature. FDD method has a very close relationship with those method uses peak picking technique. It also involves the singular value decomposition of the PSD matrix. This part is a very common step in system identification methods. The technique called complex mode indication function proposed by Shih *et al.* also include SVD of FRF matrix [11]. These methods are robust for the data contaminated with noise [11].

In the time domain system identification methods, general development approach is that first, the input-output system identification method has been developed and then it is converted to the output-only case [12]. One of these methods is called Natural Excitation Technique (NExT). NExT procedure was first proposed by James and Carne (1995) [13]. Although some of the system identification methods were suggested for the impulse responses, these algorithms may be applied through NExT procedure. This procedure involves the calculation of cross and auto correlation functions which explained in Chapter 2. Since the correlation function of the recorded signal may be

defined as sum of decaying sinusoidal signals, so the impulse response analogy can be supported. Most of the impulse response system identification methods may be used for structural parameter estimation. The methods which could be used with NExT procedure are mainly ITD and ERA methods.

One of the earliest techniques for multi output structural identification is Ibrahim Time Domain (ITD) proposed by S.R. Ibrahim [14]. Like the earlier methods suggested that free vibration response of a structure can be expressed as linear combination of mode shapes and exponential decays, the method considered correlation functions as well. Time domain system identification methods based on state-space model generally is applied to estimate system matrices. Similarly, ITD technique also estimates the system matrix. From the system matrices, it can be performed the eigenvalue analysis to obtain the structural parameters [12, 15].

Another system identification methods depending on impulse response, is the Eigensystem Realization Algorithm (ERA). ERA was first proposed by Juang and Pappa [16]. The method involves the system realization algorithm introduced by Ho and Kalman [17] and implementation of singular value decomposition proposed by Zeiger and McEwen [18]. The main objective of ERA is to estimate the system matrices similar to ITD. The techniques use the Hankel matrix to obtain controllability and observability matrices. Observability and controllability matrices are obtained by performing singular value decomposition, then the system matrices can be used on ERA method is primarily used for free decaying responses, but also it may be used for ambient response with the extension of NExT [13]. It has been also proposed to use ERA with observer Kalman identification (OKID) known as OKID/ERA for identifying structural parameters from noisy measurements, by Juang *et al.* [19] although it has been reported that OKID algorithm is statistically inconsistent [8].

Stochastic system identification is mainly related to system realization problem. System realization problem is to obtain the minimum realization of system estimation from input/output measurements and this problem was solved for input/output and deterministic case by Ho and Kalman (1966) [17]. The system realization technique has been enhanced by performing singular value decomposition for the noisy measurements by Zeiger and McEwen (1974) [18]. The system realization problem was extended to output-only case for the white noise stationary input by

Akaike (1974) [20]. Finally, Benveniste proposed the modal parameter estimation from stochastic realization [21]. Stochastic subspace algorithm may be implemented as either data-driven (SSI-DATA) or covariance-driven (SSI-COV). These methods are broadly explained in the book written by Van Overschee and De Moor [22]. Moreover, the SSI methods have been proposed an enhancement using reference sensor by Peeters *et al.* [23]. The implementation of data-driven stochastic subspace identification method was broadly explained in Chapter 2.

1.2.3 System identification of buildings

Although the scope of this thesis is limited to the system identification of bridges, only major studies are included. Frequency domain decomposition method is applied to identification of modal parameters of a tall building located in Istanbul by Kaynardağ and Soyöz [24]. Moreover, ambient vibration analysis of transamerica building is tested, and the seismic response analysis of the building was investigated through earthquake ground motion records [25, 26]. Also, the system identification of MIT Green Building has been applied using blind source separation for modal identification [27]. The review on Ambient Vibration Tests (AVT) and Operational Modal Analysis (OMA) on heritage building were presented, and as a results scientists stated that frequency and time domain identification methods for this type of structures should be performed and evaluated simultaneously [28].

1.2.4 System identification of bridges

In the literature, there are so many system identification applications of bridges. Herein, only major applications are summarized. First of all, Melk bridge M6 located in Austria is multi-span composite bridge. The bridge is investigated for the vibration analysis and assessing noise emission during the train passage. For this purpose ambient and forced vibration tests are conducted. Then the system identification methods applied for the bridge is stochastic subspace identification. Another application of system identification for bridges is Porr Bridge. Porr Bridge is located in Vienna, Austria. The bridge which is post-tensioned box girder was constructed in 1975. Sensor number used for monitoring is 36. System identification of bridge is applied through stochastic subspace identification using MACEC software.

Another example of system identification for the bridge structures is Warth Bridge located in Austria. This bridge is multi-span and post-tensioned structure. Acceleration sensor number of the SHM system of the bridge is 4. The s ystem identification algorithm is applied through basic peak picking method to structural parameter identification. The Szechenyi bridge located in Hungary has also SHM system since 2003 and the bridge is multi-span concrete bridge. Type of analysis to define the modal parameter identification is Fourier analysis realized using ORIGIN 6.0. The Bridge Z24 is also investigated using system identification methods. Z24 Bridge which is medium-span, prestressed concrete bridge is located in Koppigen-Utzenstorf, Switzerland. For the system identification of Z24 bridge, the total number of acceleration sensor is 20 (15 on deck, 2 on a pylon, and 3 as reference channels). The system identification algorithm used in this analysis is the stochastic subspace identification method and the model updating is also used for this bridge [29]. In the study conducted by Sabamehr *et al.* the ambient vibration analysis of a pre-stressed concrete box girder bridge was made and the system identification analysis namely Frequency Domain Decomposition was implemented [30]. Feng *et al.* have conducted research on long-term performance variation of bridges [31]. Although the vibration information of bridge are measured as displacement and acceleration separately, the structural identification can be implemented using data fusion [32, 33]. Moreover, the system identification of bridges have been applied using recorded earthquake ground motion response [34, 35].

In Turkey, there are so many bridge having structural health monitoring system. These are summarized in the study conducted by Bas *et al.* [36]. Also, the system identification of Bosphorus suspension bridges are implemented in normal condition and during the hanger replacement [37, 38]. Finally Golden Horn (metro-crossing) bridge which will be mentioned in the following chapters have permanent structural health monitoring system [39, 40]. In this thesis, system identification results and performance assessment of the bridge will be presented.

1.2.5 Performance assessment of structures

Performance based design of structures has been practiced since 1908 Messina (Italy) and 1923 Kanto (Japan) earthquake. After these earthquakes, scientists have studied

on new approach; the earthquake forces is approximately 10 percent of the structure's weight in both countries. This approach was also accepted by Uniform Building Code (UBC) in the United States in 1927 [41]. Moreover, response spectrum approach is also added to codes beginning with the 1958 UBC. With this approach, it has been noticed that the earthquake response is related to the natural vibration period of structure, introduced by Housner [42]. Then the earthquake force coefficient is defined as the variable depending on the period of structures. The variable indicating the occupancy classification is also defined in UBC 1958 [43]. After the 1971 San Fernando earthquake which is milestone event for the structural engineering society, the damages of structures were unexpected for the community and it affected the structural design concepts, it also causes establishing the Advanced Technology Council (ATC) in 1973 in order to investigate the consequences of the damages caused by earthquake and enhance the existing codes.

1989 San Francisco earthquake caused extensive damages to not only buildings but also the infrastructure and industrial facilities. It emphasized performance-based design concept [41]. Hence, firstly Vision 2000 document published by SEAOC in 1995, its main goal is to define design of structures with predictable seismic performance or adaptation of multiple performance objectives [44]. In Vision 2000, five performance levels are also defined. The second document which defines the performance-based design is Applied Technology Council ATC 40 published in 1996. Although ATC 40 is limited to concrete buildings, it defines the performance based design procedure. The procedure involves the construction of capacity and demand spectra [45]. To construct the capacity spectrum, the force-displacement curve of a structure may be obtained through nonlinear static (pushover) analysis. Forces and displacements are transformed to the spectral accelerations and spectral displacement using equivalent single-degree of freedom (SDOF) system. Earthquake demands are defined by elastic spectra. At the performance point, it assumed that the seismic capacity of the structures equals to the demand. Then the acceleration and displacement can be obtained as strength and the demand. Finally, the probability of earthquake level is highly related to the damage occurrence probability [46]. Another, documents which should be taken to the account for the performance assessment or performance based design of structures belong to the Federal Emergency Management

Agency. FEMA 273 documents published in 1996 defines the variety of performance objectives based on the probabilistic ground motions [47]. The performance objectives of the structures differ from the linear static analysis to the nonlinear time history analysis [46]. Even though the ATC 40 and FEMA 273 documents focus on nonlinear static analysis which considers the structural response based on the limited number of modes primarily, nonlinear time history is the best available tool for predicting the structural response at different earthquake levels [48]. Nonlinear response history method depends on the simulation of the noteworthy deformations and deterioration of the structures. Although, the practical constraints is not allow to simulate nonlinear behavior of structures fully, the members expected to be exhibit nonlinear behavior can be chosen to be analyzed [48].

1.3 Objective

Finite element model of the structures is generally used to design the structures. Although the mathematical model of the structures is obtained by making very critical assumptions, these assumptions create the uncertainties about the structures designed. Hence the FEM model of the structures should be modified to more realistic FEM model representing the real structure behavior. To obtain the model representing the real structural response has been still an open question. Also, in order to assess the performance of the structures, the realistic FEM model is a necessary need.

So the SHM can be used to validate and modify the FEM model and then the performance assessment can be applied to more realistic results. The results of the performance assessment provide probabilistic information about the damage level of the structure after an earthquake.

In this study, SHM system of the GHB was investigated using the permanent and initial measurements. The field study is also realized for the deck of the GHB. System identification (SI) methods used are Peak Picking (PP), Frequency Domain Decomposition (FDD), Stochastic Subspace Identification (SSI). The structural parameter identification using SI methods was carried out. First of all, FEM model was developed using technical drawing and structural and geotechnical design report. After the implementation of system identification, FEM model updated through structural parameter obtained with system identification algorithms.

After updating the FEM model, using code based spectrum, nonlinear time history analysis was conducted with 11 different earthquake records.

1.4 Scope

This study involves 6 chapter. The first chapter gives a general overview of the study, literature review of structural health monitoring, system identification, and performance assessment of structures.

Chapter 2, introduces the background information to use system identification algorithms mainly probability, correlation, system theory and system identification algorithms. The system identification methods used within this study, is explained in details.

In Chapter 3, the comparison of the system identification is presented using experimental setup and numerical model. Experimental setup (simply supported beam) used for investigating the sensor number effects, and the numerical model is used to compare the system identification algorithms in terms of noise level.

In Chapter 4, the structural properties of GHB, structural health monitoring system of the bridge is introduced and the initial SHM results are presented. Also system identification algorithms for GHB is indicated, and it is compared for the 3 different system system identification methods results.

In Chapter 5, the performance assessment through nonlinear time-history analysis for 11 different earthquake records is presented.

In Chapter 6, summary of results, conclusion and brief suggestions for future studies are presented.

2. THEORETICAL BACKGROUND

2.1 Introduction

While studying on any measurement data, there is generally large amount of discrete point. This data is considered as a random variable. Due to the fact that there is no way without use of probability in the existence of a random variable, some basis of probabilistic definitions will be explained shortly in this chapter.

2.2 Probability

Probability is the only method for dealing with the uncertainties on the many aspects of engineering. In the example of coin tossing, the probable results can be determined based on either observations or some assumptions. Probability can be defined using three different background. In this subsections, these definitions will be briefly discussed chronologically.

2.2.1 Classical Definition

Classical Definition of probability has constituted the basis of probability theory, for long time. This concept mainly is based on some assumptions and there is no need to experiment. The possible outcomes are equally-likely for this definition. If so, the probability of any given outcome can be expressed as the 2.1.

$$\frac{N_S}{N} \tag{2.1}$$

where the N is number of possible outcomes N_S number of desired outcome.

2.2.2 Frequentists definition

In the frequentists definition, the main parameter is the relative frequency between the possible outcomes. Let A be an event of interest. When experiments have been performed n times, n_A is the number of times that event A appears. Infinite numbers

of experiments can not be conducted but in principle, when the number of experiments approaches the infinity, the relative frequency of possible outcomes can be obtained.

$$lim_{n_A \to \infty} \frac{n_A}{n} \tag{2.2}$$

2.2.3 Axiomatic definition

Axiomatic definition of probability is the relatively latest definition of probability [49]. This definition is based on three major axioms. [50, 51]

Probability of an event is positive and equal or smaller than unity,

$$P(A) \geq 0 \tag{2.3}$$

Probability of a certain event is must be unity,

$$P(A) = 1 \tag{2.4}$$

Let B be another event and A and B are mutually exclusive

$$P(A+B) = P(A) + P(B) \tag{2.5}$$

Otherwise,

$$P(A+B) = P(A) + P(B) - P(A \cap B). \tag{2.6}$$

2.2.4 Expectation and probability density

The mean value (also called expected value or average value) of a random variable is the weighted average of its own values. When the probability density function of a variable is given, the mean value of the variable can be calculated according to the equation 2.7.

$$E[x(k)] = \int_{-\infty}^{\infty} xp(x)dx = \mu_x \tag{2.7}$$

When the probability density is known, the expected value of a random variable can be calculated. But if the data to be analyzed is discrete, generally the drastic assumption is made such that probability density functions is known. If the data which is working on, is discrete, the expected value of a given discrete random variable should be calculated with equation 2.7.

Since the measurement record is generally zero mean, the expected value is not considered for processing the data. Also, the $p(x)$ is the probability density function

and the probability density function of the signals measured is not given and hard to be obtained [15].

Probability density function $p(x)$ is about the probability of the event that the random variable is in the small interval $[x;x+dx]$. Let X be a random variable;

$$Pr[X \in [x,x+dx]] = p(x)dx \tag{2.8}$$

$$\int_{-\infty}^{\infty} p(x)dx = 1 \tag{2.9}$$

Once the probability density function is obtained, the statistical parameters such as the expected value, variance and also probability distribution function can be obtained easily with the following equations;

$$E[X] = \int_{-\infty}^{\infty} xp(x)dx = \mu_x \tag{2.10}$$

$$E[(X-\mu_x)^2] = \int_{-\infty}^{\infty} (x-\mu_x)^2 p(x)dx = \sigma_x \tag{2.11}$$

$$P(x) = \int_{-\infty}^{x} p(u)du \tag{2.12}$$

Since what we are dealing with are the observed signals, density function can not be obtained using equation 2.7 without knowing the density function. To estimate the probability density function of a discrete signal, it should be applied time averaging according to equations 2.13, 2.14, 2.15 [15].

$$Pr[x(t) \in [x_n;x_n+\Delta x_n]] = p(x_n)\Delta x_n = \frac{\sum_k \Delta t_{n,k}}{T} \tag{2.13}$$

$$E[x(k)] = \sum_{i=0}^{N} xp(x)dx = \mu_x \tag{2.14}$$

$$E[x(t)] = \sum_{n=-\infty}^{\infty} x_n p(x_n)\Delta x_n = \sum_{n=-\infty}^{\infty} x_n \frac{\sum_k \Delta t_{n,k}}{T} \tag{2.15}$$

Four most commonly used probability density functions are given as follows [52].

- Gaussian distribution,
- Rayleigh distribution,

- Uniform distribution,
- Laplacian distribution.

2.2.5 Median

Median is the middle value of the data sorted in order from smallest to largest. However, median value finding differentiate if the number of the data is odd or not, the value can be found in both cases. If the number of data is odd, median will be middle value of the sorted data, if not median value will be average of two value in the middle of the sorted in order from smallest to largest.

2.2.6 Probability distribution function

While the probability density function is estimated, using the aforementioned probability distribution function integration formula 2.12 can be used numerically. Basically probability distribution function is the cumulative summation of the probability density function.

$$P(x) = \int_{-\infty}^{x} p(u)du \tag{2.16}$$

2.2.7 Joint distributions

Joint distribution function of two random variables defines the probability density function of two variables in two dimension. Thus the probability of two or more joint event can be obtained using joint distributions graph. [50]

$$Pr[X \in [x, x+dx]Y \in [y, y+dy]] = p_{xy}(x,y)dxdy \tag{2.17}$$

$$p_x(x) = \int_{-\infty}^{\infty} p_{xy}(x,y)dy \tag{2.18}$$

$$p_y(y) = \int_{-\infty}^{\infty} p_{xy}(x,y)dx \tag{2.19}$$

Also for more of the joint statistics rather than the joint distributions, further reading can be found in [50].

2.3 Correlation

2.3.1 Correlation coefficient

Correlation is a term which provides information about how compatible the two data are. One can show the relation between two series by using the correlation coefficient. The correlation coefficient can be obtained with this formula;

$$\rho_{xy} = \frac{E[xy]}{\sigma_x \sigma_y} \tag{2.20}$$

2.3.2 Autocorrelation

Autocorrelation is used for evaluation of the correlation with itself. And it is also used for evaluating how relevant the signal by itself with respect to τ variable. τ variable is defined as time shifting of the signals. Therefore it can be expected that correlation of a signal decreases as τ increases. Furthermore, in the case of the uncorrelated signals, correlation sharply decreases to the zero. for the non-zero value of τ.

$$R_x(\tau) = \frac{1}{T}\int_0^T x(t)x(t+\tau)dt = E[x(t)x(t+\tau)] \tag{2.21}$$

2.3.3 Crosscorrelation

Correlation also can be applied two series. In this application, correlation obtained will be a matrix form. And if these two time series are different, correlation matrix obtained is namely cross correlation (2.1).

$$R_{xy}(\tau) = \frac{1}{T}\int_0^T x(t)y(t+\tau)dt = E[x(t)y(t+\tau)] \tag{2.22}$$

Also one can investigate the correlation of a time series by itself and it is called autocorrelation;

$$R_x(\tau) = \frac{1}{T}\int_0^T x(t)x(t+\tau)dt = E[x(t)x(t+\tau)] \tag{2.23}$$

2.3.4 Power spectral density

Power spectral density function can be found by using three different ways [53]. These are;

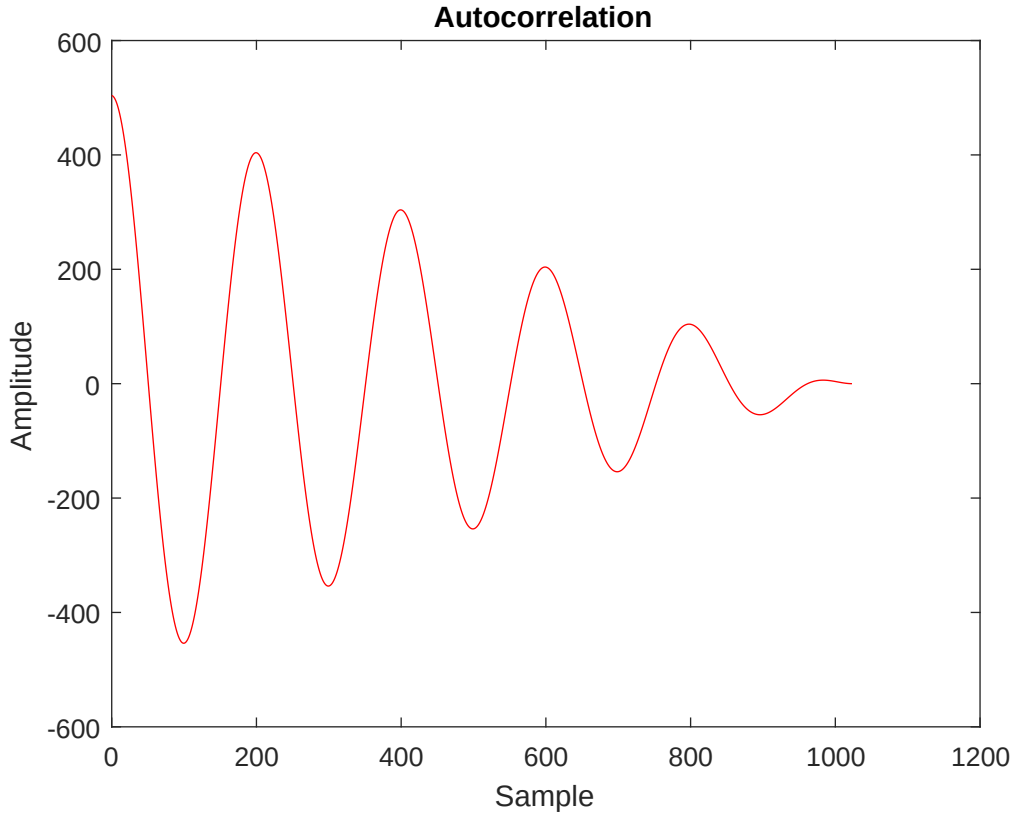

Figure 2.1 : Autocorrelation function of a sine wave.

- spectra via correlation function,
- spectra via Fourier transform,
- spectra via analog filtering.

2.3.4.1 Spectra via correlation function

Power spectral density function can be calculated Fourier transform of the correlation function;

$$S_{xy}(\tau) = \frac{1}{T}\int_{-\infty}^{\infty} R_{xy}(\tau)e^{-j2\pi nk/N}dt \tag{2.24}$$

2.3.4.2 Spectra via Fourier transform

It can be obtained also by using the Fourier transform;

$$X_k(f,T) = \int_{n=0}^{N-1} x(t)e^{-j2\pi nk/N} \tag{2.25}$$

$$Y_k(f,T) = \int_{n=0}^{N-1} y(t)e^{-j2\pi nk/N} \tag{2.26}$$

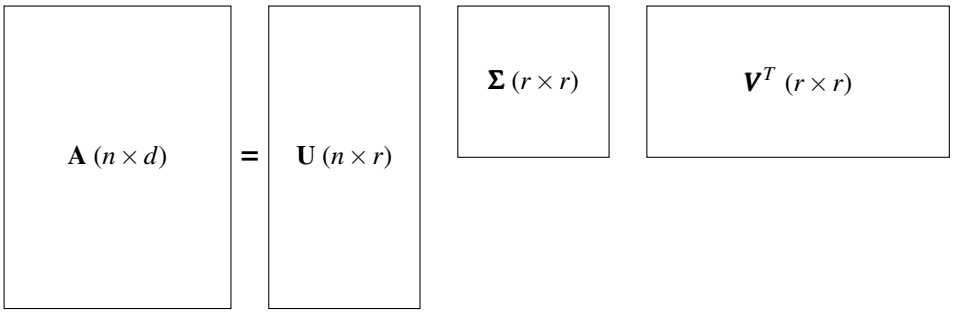

Figure 2.2 : Singular Value Decomposition of a matrix.

$$S_{xy}(\tau) = \lim_{T\to\infty} \frac{1}{T} E[X_k(f,t) * Y_k(f,t)] \tag{2.27}$$

2.3.4.3 Spectra via analog filtering

Thanks to developing digital signal processing software and equipment, spectral density functions can be estimated, with analog wave analyzers [53]. Auto spectral density function estimate is applied with following equation;

$$S_{xx}(f) = \frac{1}{(\Delta f)T} \int_0^T x^2(f,\Delta f,t)dt \tag{2.28}$$

2.3.4.4 Spectral density function estimate

Spectral density functions of measurement results can be obtained with several methods [52].

- Unwindowed periodogram
- Modified periodogram,
- BT periodogram,
- Barlett, Welch periodograms,
- Daniel periodogram.

2.3.5 Singular value decomposition

Singular value decomposition is generally eigenvalue decomposition for Hermitian matrix. SVD can be applied by decomposition of three different matrix, namely **U**, **V** and Σ. **U** is left singular vectors, V is right singular vectors, and Σ is non-negative singular values of A in descending order [15].

$$\mathbf{A} = \mathbf{U}\boldsymbol{\Sigma}\mathbf{V}^{\mathrm{T}} \tag{2.29}$$

$$\mathbf{U} = [\mathbf{u}_n] \tag{2.30}$$

$$\mathbf{V} = [\mathbf{v}_n] \tag{2.31}$$

$$\boldsymbol{\Sigma} = [\mathbf{s}_n] \tag{2.32}$$

Singular value decomposition unlike the eigenvalue decomposition are defined for the rectangular matrix. It is also closely related to eigenvalues.$\boldsymbol{\Sigma}$ is the matrix which is the diagonal matrix and having singular values. The rectangular matrix have $\boldsymbol{\Sigma}$ matrix and its dimensions are based on the rank of the matrix $\mathbf{A}$. For the square matrix, singular values of the matrix are eigenvalues of itself. The singular value decomposition of a matrix can be performed through the equations 2.34 and 2.35.

$$\mathbf{A}\mathbf{A}^{\mathrm{T}} = \mathbf{U}\boldsymbol{\Sigma}\mathbf{V}^{\mathrm{T}}\mathbf{V}\boldsymbol{\Sigma}^{\mathrm{T}}\mathbf{U}^{\mathrm{T}} \tag{2.33}$$

$$\mathbf{A}\mathbf{A}^{\mathrm{T}} = \mathbf{U}\boldsymbol{\Sigma}\boldsymbol{\Sigma}^{\mathrm{T}}\mathbf{U}^{\mathrm{T}} \tag{2.34}$$

$$\mathbf{A}\mathbf{V} = \mathbf{U}\boldsymbol{\Sigma} \tag{2.35}$$

Singular value decomposition is a useful tool for the following areas;

- Principal Component Analysis,
- Compression Algorithm,
- Spectral Decomposition,
- Discrete Optimization Problem.

2.4 LTI Systems and Signals

In general, signals are data sets carrying information and represented as function of one or more variable mathematically. For instance, while earthquake record is function of time, a video is a function of spatial coordinates and time. Signals can be classified into two main categories. These are analog and digital signals. Moreover any physical process can be represented as a input/output relationship of signals. Systems are classified according to the signals that they processed and, the linearity properties and also their time invariance. This chapter signals and systems, classification, properties and their usage in terms of system identification will be discussed briefly.

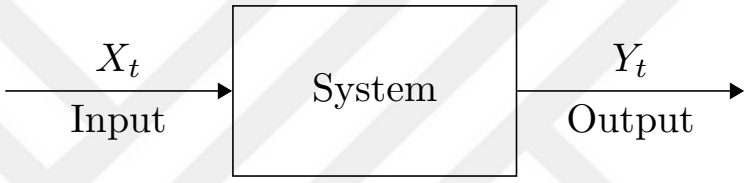

Figure 2.3 : Single input single output system (SISO).

2.4.1 Signals classification

Signals can be categorized mainly two categories. These are digital and analog signals. Analog signals are continuous functions of time. Generally continuous signals are represented using independent variable. Such as wind velocity or speech signals are continuous signals as in nature. But our measurement techniques make them discrete. Measured signals should be treated as discrete data since the any measurement device can never measure in continuously. In structural health monitoring or system identification, the measured signals are also discrete in nature and one should be aware of this. Discrete and continuous signals are mainly called analog and digital signals respectively. Analog and digital signals can be converted between them using appropriate filter [54]. These methods will be discussed later.

2.4.2 Systems

A system can be evaluated as the any process which takes an input and provides an output based on input [54]. According to this definition, any physical system or process

can be modelled by configuring some basic system elements. Here it is important the way the physical system is modeled. A physical process can be modeled decoupling system the subsystems. Subsystems are connected differently in order to generate the real system. Interconnections of subsystems can be parallel, serial or combination of them. In the modeling real process, it is important that not only interconnections of subsystems but also mathematical representations. Mathematical representation of a system will be discussed later. The properties of system will be explained briefly.

2.4.2.1 Memoryness

A system can be defined as either with memory or memoryless. If the system's output at any time depends on only the input at the same time only. The system is said memoryless. On the contrary, if the system's output depends on not only the input at the same time but also earlier input, the system can be called the system with memory.

$$y[n] = ax[n] \tag{2.36}$$

$$y[n] = a_k x[n] + a_{k-1} x[n-1] + ... \tag{2.37}$$

where x and y is the input and output of the system, respectively and a is also weighting coefficients. The memoryless system is represented as equation 2.36; likewise, the system with memory is represented as equation 2.37.

2.4.2.2 Invertibility

As was discussed before, a system has output based on input. If the input can be obtained exactly using output, it is said that the system is invertible. Mathematical representation of inverse systems can be indicated as equation 2.39. It is clear that equation 2.39 is the inverse system of the system having the equation 2.38.

$$y[n] = 4x[n] \tag{2.38}$$

$$w[n] = \frac{1}{4} y[n] \tag{2.39}$$

2.4.2.3 Causality

A system also have the properties of causality depends on the way dependence on past and/or future inputs. A system is said to be causal if the output of any time depends on present and past inputs. The important factor to define a causality properties of a system is the dependence of future inputs. All the memoryless systems are always causal system, since the output is based on only present input.

$$y[t] = 0 \quad for \quad y \leq 0 \tag{2.40}$$

$$y(t) = 0 \quad for \quad y \leq 0 \tag{2.41}$$

2.4.2.4 Stability

For bounded input, if the output is also bounded in other words, it is not divergent, the system is said to be stable. Generally stability is the results of the damping. Stability of a system can be classified into three major types.These are asymptotically stable, marginally stable and unstable system. For example, for single degree of freedom system,

$$\int_{-\infty}^{\infty} |y(t)|dt < \infty \tag{2.42}$$

$$\sum_{-\infty}^{\infty} |y[t]|dt < \infty \tag{2.43}$$

2.4.2.5 Time invariance

The time invariance property defines that two identical input constitutes same output no matter when they are applied. When the system input is shifted then the output is shifted but the resulting signal is the same for the time invariant systems.

2.4.2.6 Linearity

Linear system is a system that sum of inputs yields the equivalent output comparing to the sum of outputs for each single inputs. This leads the superposition principle of the system. Every linear system has the superposition principle and that helps to evaluate the input and output relations using subdivision into simple parts. According to superposition principle, one can investigate the input signal as sum of discrete data

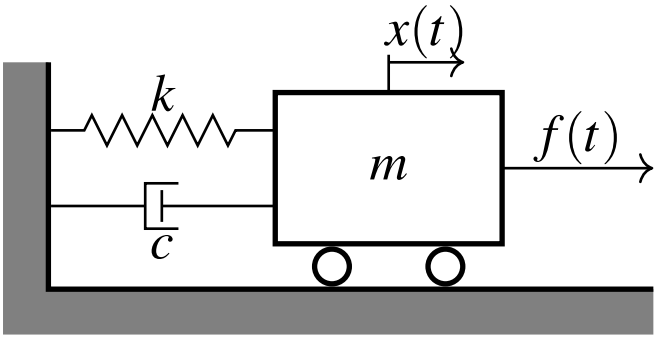

Figure 2.4 : Single Degree of Freedom System

for discrete time signals and infinitesimal point for continuous signals. This property provide us to convolution sum that is going to be explained later.

2.4.3 Mathematical representations of systems

Systems can be modeled in three different ways. A system can be represented mathematically using three different approach these are differential equation, transfer function and state-space formulation. In this part, the mathematical formulation of a system will be derived for single degree of freedom mass spring dash-pot system. In structural mechanics, equation of motion is a second order differential equation and can be solved analytically in terms of transient and steady state solution, separately. Equation of motion can be defined using free body diagram for the single degree of freedom system as shown in the figure.

$$m\ddot{x} + c\dot{x} + kx = f(t) \tag{2.44}$$

$$\ddot{x} + \frac{c}{m}x + \frac{k}{m}x = f(t) \tag{2.45}$$

$$\ddot{x} + 2\xi\omega_n\dot{x} + \omega_n^2 x = f(t) \tag{2.46}$$

where ξ is the viscous damping ratio and ω_n^2 is the natural frequency. The resulting equation 2.46, is solved according to whether free or forced vibration and damping properties. Also the displacement of a system can be calculated using the Duhammel (convolution) integral. The Duhammel integral is basically uses the linear time invariant system properties, $f(t)$ is divided to infinitesimal part and the response of the system is calculated summing response of these infinitesimal inputs. It is also

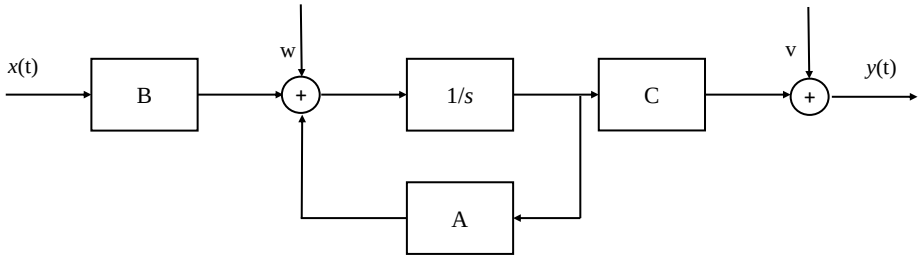

Figure 2.5 : State-space flow diagram.

called convolution sum in interdisciplinary areas [54]. The Duhammel integral was well defined in structural dynamics book [55, 56] [57].

$$x(t) = \int_0^t \frac{h(t-\tau)}{m} f(t)dt \tag{2.47}$$

where the h(t) is the impulse response function of single degree of freedom system given in the figure 2.4. And the $h(t)$ is defined as,

$$h(t) = \frac{1}{\omega_n} e^{-\xi\omega_n t} sin(\omega_d t) \tag{2.48}$$

When the $h(t)$ is substituted to the equation to equation 2.47, structural response is obtained using convolution sum or Duhammel integral,

$$x(t) = \int_0^t \frac{1}{m\omega_n} e^{-\xi\omega_n(t-\tau)} sin(\omega_d(t-\tau)) f(t)dt \tag{2.49}$$

2.4.3.1 Linear state space equation

The second order equation of motion could be converted to the state equation from control theory. Second order differential equation is transformed into first order form through state equation [58];

$$\dot{x}(t) = \mathbf{A}_c x(t) + \mathbf{B}_c u(t), \tag{2.50}$$

where

$$\mathbf{A}_c = \begin{Bmatrix} 0 & \mathbf{M}^{-1} \\ \mathbf{M}^{-1}\mathbf{K} & \mathbf{M}^{-1}\mathbf{C} \end{Bmatrix}, \qquad \mathbf{B}_c = \begin{Bmatrix} 0 \\ \mathbf{M}^{-1}\mathbf{K} \end{Bmatrix}. \tag{2.51}$$

Also the observer equation;

$$y(t) = \mathbf{C}_c x(t) + \mathbf{D}_c u(t). \tag{2.52}$$

2.4.4 Transforms

Transforms are essential topics for the signal processing also commonly used for system identification in civil engineering. In this study, Fourier transform, the Laplace transform and the Z transform will be briefly explained and will be used in the system identification part later. Especially for output only system identification, output acceleration records sometimes are evaluated based on their periodicity properties. Periodicity evaluation is the most critical part for OMA in order to obtain modal properties for a structure. One can use the transform techniques to accomplish signal processing part for system identification.

2.4.4.1 Fourier transform

Fourier Transform mainly divides a signal into periodic signals with different frequency properties. It mainly depends on the assumption that any signal can be simplified to sum of sinusoidal signals. The transform is the reversible process so inverse Fourier transform also can be applied. Fourier transform is also important for the system analysis, input and output of any system can be represented as a linear combination of basic signals. Periodic basic signals is simple to evaluate and superpose. So the superposition of basic signals are the important part of the signal processing. For the periodic signals can be said:

$$x(t) = x(t+T) \tag{2.53}$$

Basic periodic functions are classified to two major types;

$$x(t) = sin\omega_o t \tag{2.54}$$

or

$$x(t) = e^{j\omega_0 t} \tag{2.55}$$

So any finite length stable signal can be represented;

$$x(t) = \sum_{n=-\infty}^{\infty} a_k e^{jn\omega_0 t} \tag{2.56}$$

In the equation 2.56, the actual problem is finding the $a_k$coefficient. These coefficient can be found using following operations. When the equation 2.56 is multiplied by $e^{-jn\omega_0 t}$;

$$x(t)e^{-jn\omega_0 t} = \sum_{n=-\infty}^{\infty} a_k e^{jn\omega_0 t} e^{-jn\omega_0 t}. \tag{2.57}$$

Then the both sides is integrated for the given time interval;

$$\int_0^T x(t)e^{-jn\omega_0 t}dt = \int_0^T \sum_{n=-\infty}^{\infty} a_k e^{jn\omega_0 t}e^{-jn\omega_0 t}dt. \tag{2.58}$$

When the equation is simplified and rearranged;

$$\int_0^T x(t)e^{-jn\omega_0 t}dt = \sum_{n=-\infty}^{\infty} a_k \int_0^T e^{jn\omega_0 t}e^{-jn\omega_0 t}dt. \tag{2.59}$$

and using Euler's formula, following equation is obtained;

$$\int_0^T e^{jn\omega_0 t}e^{-jn\omega_0 t}dt = j\int_0^T sin(k-n)\omega_0 t dt + \int_0^T cos(k-n)\omega_0 t dt. \tag{2.60}$$

Finally, Fourier coefficient is formulated;

$$a_n = \frac{1}{T}\int_0^T x(t)e^{-jn\omega_0 t}dt. \tag{2.61}$$

Also it can be shown that $e^{-jn\omega_0 t} = 1$ when $t = 0$ and $a_0$is;

$$a_0 = \frac{1}{T}\int_0^T x(t)dt. \tag{2.62}$$

It should be noted that equation 2.62 is also aforementioned mean equation. The main text of Fourier equations are actually

By now the equations derived are for continuous-time signals and for discrete-time signal Fourier coefficient. And also it can be derived Fourier transform for discrete-time signals as follows;

$$x[n] = e^{j\omega_0 n} \tag{2.63}$$

$$x[n] = \frac{1}{N}\sum_{n=0}^{N-1} a_r e^{-jr2\pi nk/N} \quad r = 0,1,2,...,N \tag{2.64}$$

$$a_r = \frac{1}{N}\sum_{n=0}^{N-1} a_n e^{-j2\pi rn/N} \quad r = 0,1,2,...,N \tag{2.65}$$

$$f_k = \frac{kF_s}{N} \tag{2.66}$$

$$x(n) = \frac{1}{N}\sum_{n=0}^{N-1} x(k)e^{j2\pi nk/N} for 0 \leq n \leq N-1 \tag{2.67}$$

2.4.4.2 Properties of Fourier transform

In this section only the formulas about the important properties of the Fourier Transform will be given, for more information reader is referred to the textbooks [54] and [53]

Linearity of the Fourier transform is the most important property, since the superposition principle comes from the linearity;

$$a_1 x_1[n] + a_2 x_2[n] \overset{F}{\longleftrightarrow} a_1 X_1(e^{j\omega}) + a_2 X_2(e^{j\omega}) \tag{2.68}$$

The Fourier transform has periodicity property that means;

$$X(e^{j(\omega+2\pi)}) = X(e^{j\omega}). \tag{2.69}$$

The Fourier transform can also be shifted in time domain or frequency domain;

$$x[n] \overset{F}{\longleftrightarrow} X(e^{-j\omega}) \qquad \Longrightarrow \qquad x[n-n_0] \overset{F}{\longleftrightarrow} e^{-\omega n_0} X(e^{j\omega}). \tag{2.70}$$

When the conjugation process is needed to apply, it could be seen that the Fourier transform has the conjugation symmetry;

$$x[n] \overset{F}{\longleftrightarrow} X(e^{-j\omega}) \qquad \Longrightarrow \qquad x^*[n] \overset{F}{\longleftrightarrow} X^*(e^{j\omega}). \tag{2.71}$$

Moreover, as the Fourier transform is applied to a signal, the energy of the signal can not be changed. So the Parseval's Theorem is conserved;

$$\sum_{n=-\infty}^{\infty} |x[n]|^2 = \frac{1}{2\pi} \int_{2\pi} |X(e^{j\omega})|^2 d\omega. \tag{2.72}$$

Last but not least the Fourier transform is also reversible operation;

$$X(e^{j\omega}) \overset{F}{\longleftrightarrow} x(t). \tag{2.73}$$

The Fourier transform has also convolution property which helps for the system identification and signal processing. The aforementioned equation 2.47, convolution integral could be converted to the multiplication in frequency domain such that;

$$y[n] = x[n] * h[n], \tag{2.74}$$

$$Y(e^{j\omega}) = X(e^{j\omega}) H(e^{j\omega}), \tag{2.75}$$

where the $Y(e^{j\omega})$,$X(e^{j\omega})$ and $H(e^{j\omega})$ is defined as the Fourier transform of the y, x, and h, respectively.

2.4.4.3 Laplace transform

It could be said that Laplace transform is generalization of Fourier transform. As it is shown before, in LTI systems, response can be written as;

$$x(t) = H(s)e^{st}. \tag{2.76}$$

where $H(s)$ is;

$$H(s) = \int_{-\infty}^{\infty} h(t)e^{-st}dt \tag{2.77}$$

where s is completely imaginary $(s = j\omega)$ equation 2.77 is converted to the Fourier transform. So the s can be substituted any values, generally s is taken to the account as $s = \sigma + i\omega$ where the σ is the real part and the ω is the imaginary part. So the Laplace transform of any signal $x(t)$ is written as;

$$X(s) = \int_{-\infty}^{\infty} x(t)e^{-st}dt. \tag{2.78}$$

$$X(s) \mid_{s=j\omega} = \int_{-\infty}^{\infty} x(t)e^{-j\omega t}dt = \mathscr{F}(x(t)) \tag{2.79}$$

$$X(\sigma + j\omega) = \int_{-\infty}^{\infty} x(t)e^{-(\sigma+j\omega)}dt = \mathscr{F}(x(t)e^{-\sigma}) \tag{2.80}$$

Also it can be said that the Laplace transform is the Fourier transform of a signal $x(t)$ multiplied by $e^{-\sigma}$real exponential. This real exponential can be either decaying or growing in time.

2.4.4.4 The properties of Laplace transform

The Laplace transform have similar properties like the Fourier transform. Since the Laplace transform is the generalization of the Fourier transform.

Linearity properties can be indicated that;

$$a_1x_1[n] + a_2x_2[n] \overset{\mathscr{L}}{\longleftrightarrow} a_1X_1(s) + a_2X_2(s). \tag{2.81}$$

Laplace transform also has the time reversal and time shifting property;

$$e^{-st_0}X(-s) \overset{\mathscr{L}}{\longleftrightarrow} x(-t). \tag{2.82}$$

$$e^{-st_0}X(-s) \overset{\mathscr{L}}{\longleftrightarrow} x(t-t_0). \tag{2.83}$$

Moreover Laplace transform is reversible operation like the Fourier transform;

$$X(s) \overset{\mathscr{L}}{\longleftrightarrow} x(t). \tag{2.84}$$

2.4.4.5 Z transform

As it is mentioned that Laplace transform is the continuous time generalization of the Fourier transform. Likewise the Z transform is the discrete time extension of the Fourier transform. The z transform is the discrete time equivalent of the Laplace transform. Again the impulse response of a system can be expressed by using Z transform;

$$x[n] = H(z)z^{-n}, \tag{2.85}$$

where

$$H(z) = \sum_{n=-\infty}^{\infty} h[z]^{-n}. \tag{2.86}$$

In the equation 2.86, if the z is replaced with the $e^{j\omega}$, the Fourier transform for the $h(z)$ is obtained. Generally the z transform is formulated that;

$$z = re^{j\omega} \tag{2.87}$$

where the r is the magnitude and the ω is the angle. It could be shown that if $r = 1$, then $z = e^{j\omega}$so the expression 2.87 is returned to the Fourier transform;

$$X(z) \mid_{z=e^{j\omega}} = X(e^{j\omega}) = \mathscr{F}(x[n]). \tag{2.88}$$

As was shown the equation 2.87, z transform stability properties and the pole-zero plot are shown in the polar coordinates. And the unit circle boundaries are drawn with the Fourier transform. Inside the unit circle is defined as stable and vice versa.

2.4.4.6 The properties of Z transform

The z transform like every other aforementioned transforms, have mainly the linearity;

$$a_1x_1[n] + a_2x_2[n] \overset{\mathscr{Z}}{\longleftrightarrow} a_1X_1(z) + a_2X_2(z), \tag{2.89}$$

time reversal property;

$$X(\frac{1}{z}) \overset{\mathscr{Z}}{\longleftrightarrow} x[-n], \tag{2.90}$$

time shifting property;

$$z^{-m}X(-s) \overset{\mathscr{Z}}{\longleftrightarrow} x[n-m], \tag{2.91}$$

reversibility property;

$$X(z) \overset{\mathscr{Z}}{\longleftrightarrow} x[n], \tag{2.92}$$

and the convolution property;

$$x(z) * h(z) = X(z)H(z). \tag{2.93}$$

2.5 System Identification

System Identification is mainly used for extracting of structural properties. System identification used for the civil engineering structure,can be divided into two major parts. These are force vibration and ambient vibration testing. Since it is difficult to find a controllable input facilities, output only operational modal analysis is widely researched. Output only modal analysis techniques can be classified mainly two major groups. These are frequency domain and time domain techniques. In this Chapter, some of system identification techniques are explained in details and applied for the simply supported beam. Furthermore, the experimental modal parameters are compared with those found in SAP2000 v20 finite elements model in the Chapter 3.

2.5.1 Frequency domain system identification

In this section, some frequency domain system identification methods are reviewed. In the frequency domain techniques, generally Power Spectral Densities (PSD) of the measurements are using for the modal parameter estimation. Modal parameters modal frequency, mode shapes and modal damping ratios are extracted and compared with finite element model.

2.5.1.1 Basic frequency domain (Peak Picking)

Peak Picking technique is also called Basic Frequency Domain method. This method is broadly defined classical reference book written by Bendat and Piersol and PhD thesis of Felber [53, 59]. This is the one of the easiest to implement method in the output only modal parameter identification techniques. It is generally based on Power Spectral Density (PSD) of the sensor measurements. This method is considered as a SDOF in OMA methods, because of having some restriction. For the implementation

of BFD method, structure, whose structural modes of interest should be excited and it should be in linear region. Likewise, modes of interest should be well separated and lightly damped [12, 59]. While one mode is dominant in a wide frequency band, structural response can be proposed as approximately equal to modal response. So the response can be given:

$$\mathbf{y}(t) = \mathbf{a}q(t) \tag{2.94}$$

Where a and $q(t)$ is the mode shape vector and modal coordinates respectively. By using aforementioned definition of correlation, 2.94 can be written in this form.

$$\mathbf{R}(\tau) = E[y(t)y(t+\tau)^T] = \mathbf{a}E[q(t)q(t+\tau)]\mathbf{a}^{\mathrm{T}} = R_q(\tau)\mathbf{a}\mathbf{a}^{\mathrm{T}} \tag{2.95}$$

Where $\mathbf{S}_y(f)$, $S_q(f)$ are the spectral density matrix and the auto spectral density matrix respectively. It can be seen that the rank of the spectral density matrix is one. Moreover, any column of the PSD matrix corresponding frequency of the peak selected, is basically mode shape vector

$$\mathbf{S}_y(f) = S_q(f)aa^T \tag{2.96}$$

The reason why basic frequency domain is called Peak Picking method is apparently the modes frequency of interest is chosen by picking the peak of the trace of the power spectral density matrix graph. One column of the PSD matrix corresponding the chosen frequency is mode shapes [12, 15].

2.5.1.2 Frequency domain decomposition

The frequency-domain decomposition is the widely used method for the output-only system identification for civil engineering structures. This method is an extension of basic frequency domain method and primarily based on the estimation of power spectral density matrix, and singular value decomposition of PSD. Also, it should be noted that there are outstanding advantages. First, the FDD could identify the closely spaced modes, although the modes to be identified should be well separated and lightly damped in BFD. The technique was proposed by Brincker [60], [15]. For this method, the structural response is described in the modal space in the equation 2.97;

$$\mathbf{y}(t) = a_1q_1(t) + a_2q_2(t) + a_3q_3(t) + \ldots = \mathbf{A}q(t) \tag{2.97}$$

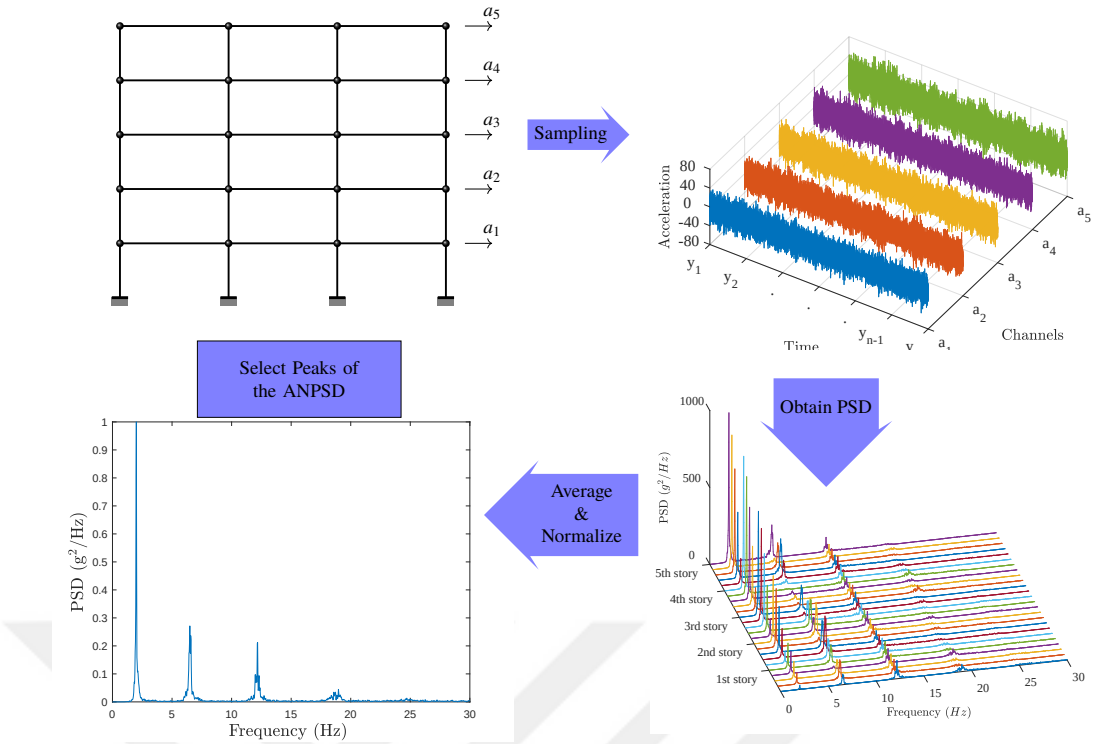

Figure 2.6 : Peak picking methods flow diagram.

where the A is the mode shapes matrix and the $q$is the modal coordinates matrix. it can be obtained the equation 2.98, using correlation factor matrix definition;

$$\mathbf{R}_{\mathrm{y}}(\tau) = E[y(t)y^T(t+\tau)], \tag{2.98}$$

and the scaling factors can be taken outside of the expectation operator;

$$\mathbf{R}_{\mathrm{y}}(\tau) = \mathbf{A}E[q(t)q^T(t+\tau)]\mathbf{A}^{\mathrm{T}}, \tag{2.99}$$

so the equation can be rewritten in terms of modal coordinates;

$$\mathbf{R}_{\mathrm{y}}(\tau) = \mathbf{A}\mathbf{R}_q(\tau)\mathbf{A}^{\mathrm{T}}, \tag{2.100}$$

that means that correlation matrix of the response matrix could be also defined by correlation of the modal coordinates matrix.Therefore the equation 2.100, can be written in the different form after performing the Fourier transform for both sides;

$$\mathbf{G}_{\mathrm{y}}(f) = \mathbf{A}\mathbf{G}_{\mathrm{q}}(f)\mathbf{A} \tag{2.101}$$

It has been already known that the modal coordinates are uncorrelated the $\mathbf{G}_q(f)$ matrix is diagonal and the positive valued, however it is also known that some complexity may occur in the mode shapes, the Hermitian could be used instead of transpose;

$$\mathbf{G}_{\mathrm{y}}(f) = \mathbf{A}[g_n^2(f)]\mathbf{A}^{\mathrm{H}}. \tag{2.102}$$

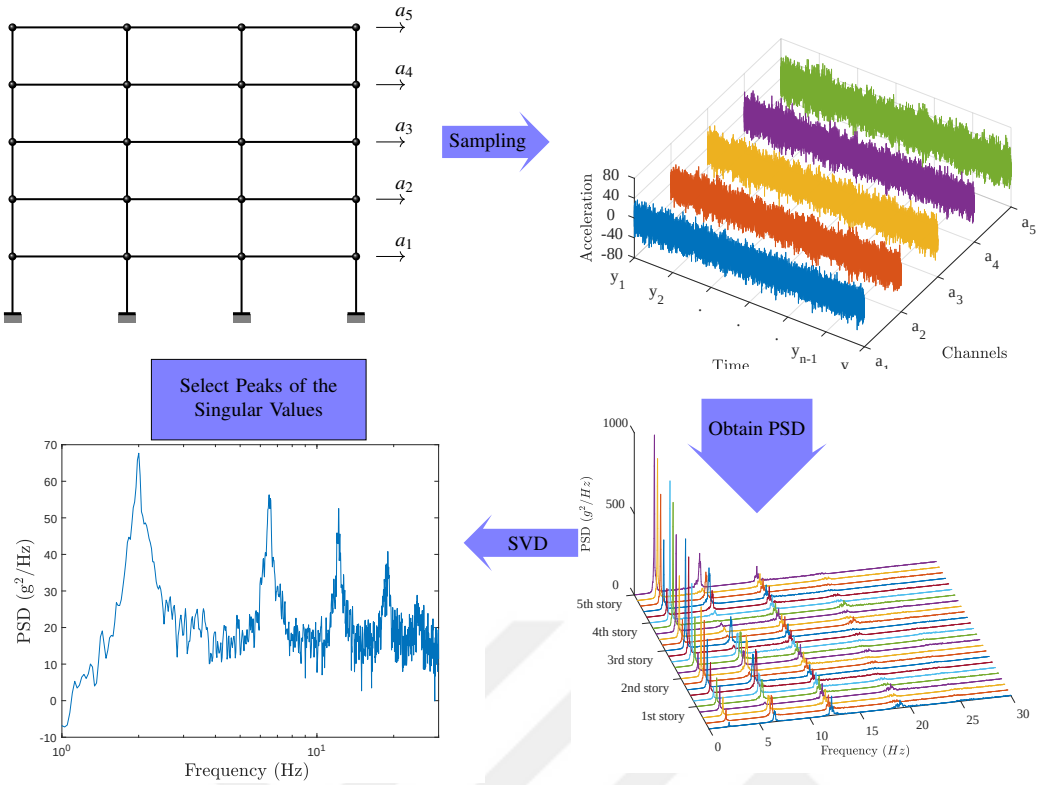

Figure 2.7 : FDD methods flow diagram.

Hence the singular value decomposition of the response matrix is performed;

$$\mathbf{G}_{\mathrm{y}}(f) = \mathbf{U}\mathbf{S}\mathbf{U}^{\mathrm{H}}, \tag{2.103}$$

again in the equation 2.103, **S** matrix diagonal and positive valued. As a results;

$$\mathbf{G}_{\mathrm{y}}(f) = \mathbf{U}[s_n^2]\mathbf{U}^{\mathrm{H}}, \tag{2.104}$$

where s_n can be defined as mode frequency, **U** is the matrix containing mode shapes.

2.5.1.3 Damping identification

In frequency domain system identification methods, generally half power bandwidth method is used for damping estimation. This method is based on frequency response function of single degree of freedom. It assumes that the ω_{a} and ω_{b} are forcing function at the left and right hand side of the resonant frequency, and these frequencies are found using the half power bandwidth of the corresponding frequency. More detailed information may be found in the Dynamics of Structures book [55].Parameters are shown in the figure 2.8; damping ratio can be found through following equations;

$$2\xi = \frac{\omega_{\mathrm{b}} - \omega_a}{\omega_{\mathrm{n}}}, \tag{2.105}$$

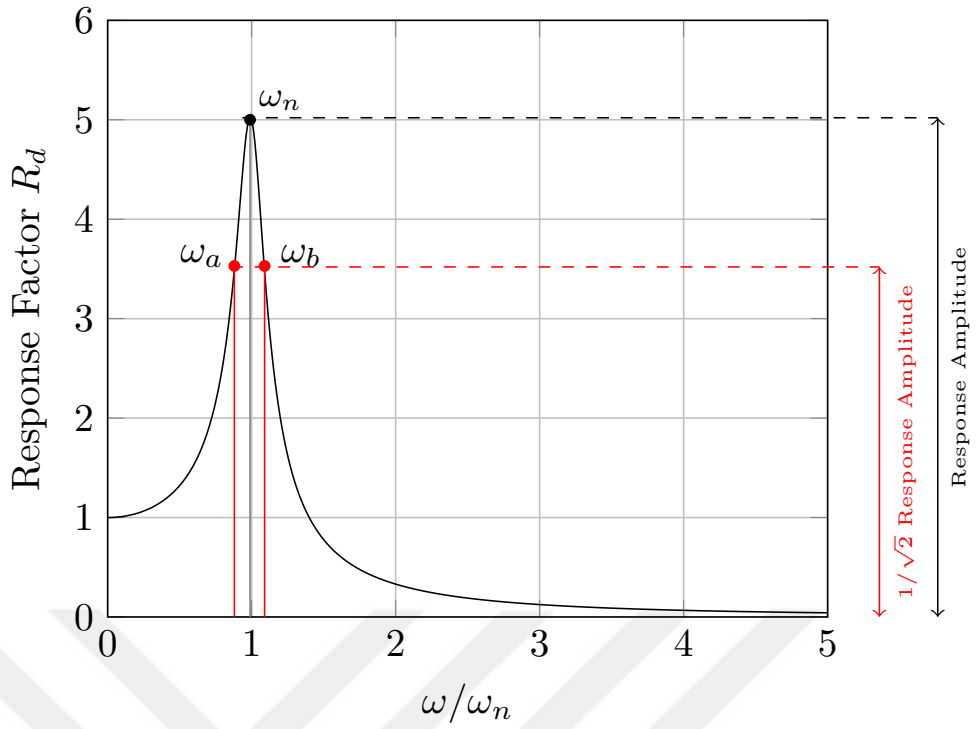

Figure 2.8 : Half power bandwidth method.

$$\xi = \frac{\omega_b - \omega_a}{2\omega_n} \quad or \quad \xi = \frac{f_b - f_a}{2f_n}. \tag{2.106}$$

2.5.2 Time domain system identification

Time domain system identification methods could be classified into two categories such as covariance driven methods and the data driven methods. Covariance driven time domain system identification methods requires the step of obtaining spectra or covariance which is very demanding step computationally. In this section, Stochastic Subspace Identification method reviewed.

2.5.2.1 Data-driven stochastic subspace identification (SSI-DATA)

Stochastic subspace identification techniques are well studied topics in the system identification literature. Interested readers are refered to textbooks such as Overshee and Moor ot Ljung [22,61] for the system identification and PhD thesis of Peeters [62] for system identification of civil engineering structures and damage assessment. Here, data-driven stochastic subspace identification technique is briefly explained and main advantages of the method is discussed.

Stochastic subspace identification is the time domain system identification methods which involves primarily Kalman filter estimation, QR factorization, SVD, and least squares. In stochastic identification, the main problem is the determination of system matrix. Once the system matrices have been determined, the rest of the identification is just an eigenvalue problem. First step of the SSI-DATA is the projection of the row space of the future inputs into row space of the past sensors. The actual SSI method uses the each sensor output as a reference sensor. However the method is presented in [63], uses some sensors as a reference, and the methods efficiency was discussed. Projection step is carried out through QR decomposition which is the mathematical technique known for its robustness. The projection to be applied for the stochastic subspace identification, is the orthogonal projection which could be expressed that;

$$\mathscr{P}_i = \mathbf{Y}_f/\mathbf{Y}_p = \mathbf{Y}_f(\mathbf{Y}_p)^{\mathrm{T}}(\mathbf{Y}_p(\mathbf{Y}_p)^{\mathrm{T}})^{\dagger}\mathbf{Y}_p. \tag{2.107}$$

The orthogonal projections is applied through QR decomposition, and in this method Q part is not used. Thus the Q part of the QR decomposition may not be computed in order to avoid the computational complexity. Then the projection is used to extract controllability matrix and Kalman states. To extract the Kalman states, the extended observability matrix should be known. By performing singular value decomposition to the projection to the projection, extended observability matrix and the Kalman states. The main theorem of the stochastic subspace identification techniques is the $\mathscr{P}_i$ could be defined as the multiplication of the extended observability matrix (O_i) and the non steady Kalman filter state ($\hat{X}_i$);

$$\mathscr{P}_i = \mathbf{O}_i\hat{\mathbf{X}}_i. \tag{2.108}$$

To obtain the Kalman filter states and the extended observability matrix, singular value decomposition is applied;

$$\mathscr{P} = \mathbf{U}_1\mathbf{S}_1\mathbf{V}_1. \tag{2.109}$$

And the $\mathbf{U}_1\mathbf{S}_1\mathbf{V}_1$ is the multiplication of O_i and $\hat{X}_i$;

$$O_i = \mathbf{U}_1\mathbf{S}_1^{1/2}, \tag{2.110}$$

$$\hat{\mathbf{X}}_i = \mathbf{O}_i\mathscr{P}_i^{\dagger}. \tag{2.111}$$

Also the another projection to be used for system identification is following;

$$\mathscr{P}_{i-1} = \mathbf{Y}_f^-/\mathbf{Y}_p^+ = O_{i-1}\hat{\mathbf{X}}_{i+1}. \tag{2.112}$$

The extended observability matrix for $i-1$ must be obtained. Moreover, O_{i+1} could be obtained deleting last rows corresponding to the time i. Therefore, Kalman states can be computed;

$$\hat{\mathbf{X}}_{i+1} = O_{i-1}^{\dagger} \mathscr{P}_{i-1}. \tag{2.113}$$

Now, $\hat{\mathbf{X}}_{i+1}$ and $\hat{\mathbf{X}}_i$ are obtained, then system matrix can be evaluated through following equation;

$$\begin{pmatrix} \hat{\mathbf{X}}_{i+1} \\ \mathbf{Y}_{i|i} \end{pmatrix} = \begin{pmatrix} \mathbf{A} \\ \mathbf{C} \end{pmatrix} \hat{\mathbf{X}}_i + \begin{pmatrix} \mathbf{W}_i \\ \mathbf{V}_i \end{pmatrix}. \tag{2.114}$$

The left hand side of the equation 2.114 is known as well as $\hat{\mathbf{X}}_i$. It should be noted that $\mathbf{W}_i$ and $\mathbf{V}_i$ is the residuals and known that uncorrelated with the Kalman states. Thus, the equation 2.114 could be solved through least square;

$$\begin{pmatrix} \mathbf{A} \\ \mathbf{C} \end{pmatrix} = \begin{pmatrix} \hat{\mathbf{X}}_{i+1} \\ \mathbf{Y}_{i|i} \end{pmatrix} \hat{\mathbf{X}}_i^{\dagger}. \tag{2.115}$$

Moreover, $\mathbf{Q}$, $\mathbf{S}$, and $\mathbf{R}$ are considered as the covariance of the least squares residuals;

$$\begin{pmatrix} \mathbf{Q} & \mathbf{S} \\ \mathbf{S}^T & \mathbf{R} \end{pmatrix} = \begin{pmatrix} \mathbf{W}_i \\ \mathbf{V}_i \end{pmatrix} \begin{pmatrix} \mathbf{W}_i^T & \mathbf{V}_i^T \end{pmatrix}. \tag{2.116}$$

After obtaining system matrices $\mathbf{A}$ and $\mathbf{C}$ eigenvalue analysis is applicable for the state matrix by taking into account whether continuous or not.

$$\mathbf{A} = \boldsymbol{\Psi} \boldsymbol{\Lambda}_{\mathrm{d}} \boldsymbol{\Psi} \tag{2.117}$$

$$\mathbf{U} = \mathbf{C} \boldsymbol{\Psi} \tag{2.118}$$

$$\xi_i = \frac{Re(\lambda_i)}{\mid \lambda_i \mid} \tag{2.119}$$

where $\boldsymbol{\Lambda}_{\mathrm{d}}$ is the discrete poles, $\boldsymbol{\Psi}$ is the mode shapes matrix, and $\mathbf{U}$ is the observed mode shapes. The system identification methods presented in [22], the matrices $\mathbf{B}$ and $\mathbf{D}$ are also identified. Since in the control literature, these matrices needs to be identified for optimal control. On the other hand, for the civil engineering structures, the main purpose is to obtain the observable poles for the systems and these poles are used for model updating.

3. COMPARISON OF SYSTEM IDENTIFICATION METHODS

3.1 Introduction

In the scope of this thesis, The system identification algorithms were implemented in the MATLAB environment. Also, the effects of sensor brand and system identification method selection were investigated. For the purpose of system identification methods comparison, the experimental setup numerical model and Golden Horn Bridge acceleration records have been used. In this section, the experimental setup used for sensor comparison and system identification, the numerical model is explained and the results are presented.

3.2 Sensor Comparison

For the system identification application, the sensor properties are essential parameters, since the system identification algorithms requires the sensitive sensors and usable data. Also todays' sensors are coming with the built-in properties. While Some of sensors may need data logger others may not. In this section, two sensors having different properties are compared and the resulting signals was processed.

3.2.1 Acceleration sensing

Acceleration sensors are classified mainly two parts. These are AC and DC response sensors. While AC response accelerometers can not be used for measure static acceleration such as gravity and centrifugal acceleration, DC response accelerometers can be used. Additionally, both of AC and DC response accelerometers can be used for measuring dynamic events. AC response accelerometers can be divided into two categories. These are charge mode piezoelectronics and voltage mode piezoelectronics. DC response accelerometers can be also classified into two categories such as capacitive and piezoresistive. AC response accelerometers are out of scope for this report. In the capacitive accelerometers, there are seismic mass and

Figure 3.1 : TLE acceleration sensor.

a spring and under effects of the acceleration, displacement of seismic mass creates change of capacitance. Piezoresistive accelerometers' working principle is based on resistance change in the strain gauge. One of the most important type of the DC response accelerometers is named Micro-Electro-Mechanical-Systems (MEMS). MEMS technology has decreased the prices and increased availability of sensors in the private sector. ILE and TLE sensors are both Force-Balance acceleration.

3.2.2 Accelerometers

Acceleration sensors to be compared, are International Leading Equipment (ILE) and Turkish Leading Equipment (TLE). While ILE does not need a data logger, since it has built-in digitizer, TLE needs data logger and the data logger used in this study belongs to TLE brand.

TLE acceleration sensor is shown in the figure 3.1. Also, TLE and ILE was placed almost the same location on the experimental setup which will be explained following subsection. Sensors deployment for the sensor comparison can be seen in Figure 3.2.

3.2.3 Experimental setup

In this study, accelerometers are compared with respect to their usage in Structural Health Monitoring (SHM). Therefore, this comparison is applied using simply

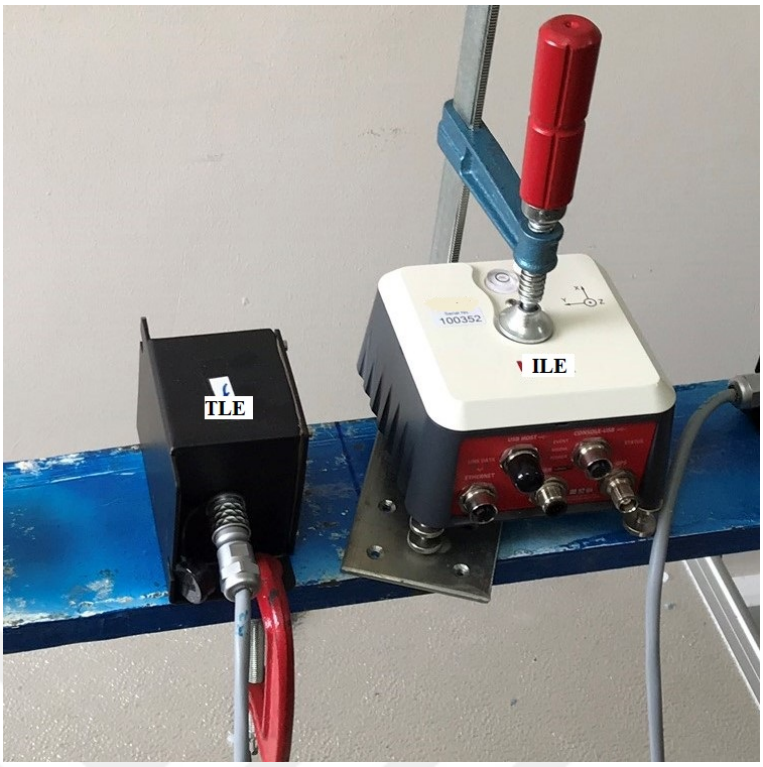

Figure 3.2 : Sensors to be compared side by side.

supported beam loaded impulsively. The simply supported beam's material is steel and its sectional dimensions are 2.06, 10, 242 cm and indicated in Figure 3.3. The main purpose of the SHM is modal parameter estimation and extracting the information whether the structure is damaged or not, using accelerometer signals. For this reason, accelerometer signals need to be doubly integrated in order to provide the displacement signal. Beam vibration records is obtained and sensors are located very close so acceleration records can be expected as approximate.

For comparing two different sensor data, it is necessary either the usage of same data logger or the availability local GPS data. In this study, GPS sensor for each acceleration is provided.

ILE sensor's output file format is mseed while TLE sensor's output file format is tdms. Mseed stands for mini Standard for the Exchange Earthquake Data. In order to obtain data from mseed file, the MATLAB tool namely mkmseed was used. Tdms file format is generally used for recording of simulation and measurement data in National Instruments software, such as LabVIEW. Moreover, npTDMS tool was used to obtain the acceleration data in the python environment. For both of the tdms and mseed data format, GPS data is embeded and can be easily synchronized to be compared.

Figure 3.3 : Sensor locations and simply supported beam

As a results, acceleration records were synchronized with the help of GPS and records were integrated over time in order to obtain velocity and displacement.

The baseline correction and high-pass filter was applied separately. Baseline corrected time history results was illustrated in Figure 3.5, while 3.4 indicates the raw time history recors. Moreover, Figure 3.6 shows the results of the Fourier transforms of the baseline corrected signals of acceleration, velocity, and displacement respectively.

3.3 Experimental study for system identification

In this part, to compare and determination effects of sensor number, series of experiments is carried out. Experiments performed using the simply supported beam whose material is steel and sectional dimensions are 2.06, 10, 242 cm. The boundary condition of the beam is set roller support in the one end and pinned support in the other. For all of the experiments, the same material and support conditions are used but different number of uni-axial acceleration sensors are utilized for the purpose of modal parameter estimation. Impulse loading is applied as excitation. As an example for the acceleration record is presented in the figure 3.8, and the other records are shown in Appendix A.1. In this study, the effects of sensor number is investigated. Three different system identification techniques is used namely Basic Frequency Domain (BFD), Frequency Domain Decomposition (FDD), and Stochastic Subspace Identification (SSI). Results are presented in Figures 3.7 3.8 3.9 3.103.123.14 for maximum number of sensors for system identification methods comparison and separately sensor number effects on modal parameter estimation.

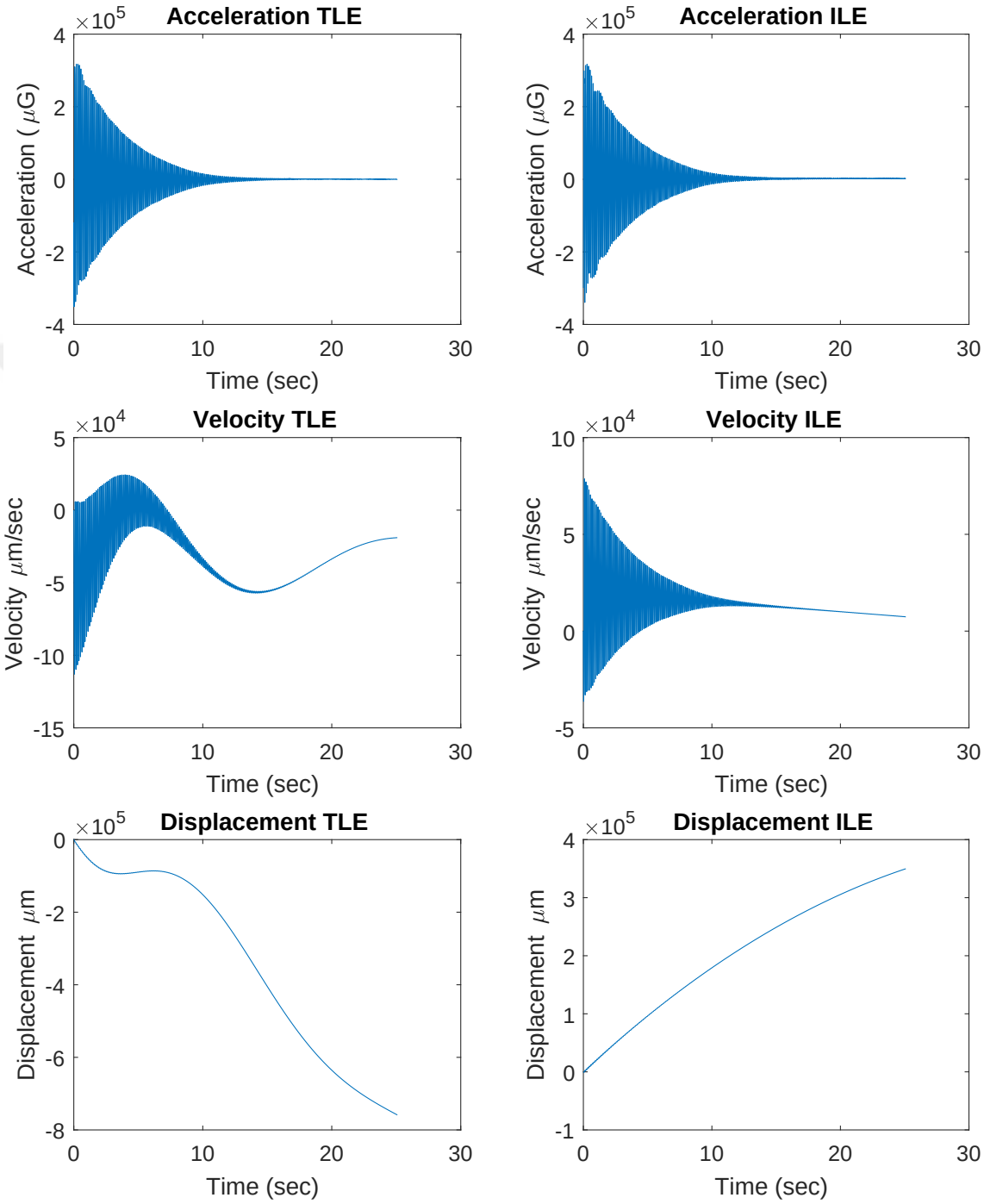

Figure 3.4 : Acceleration records and their integrals

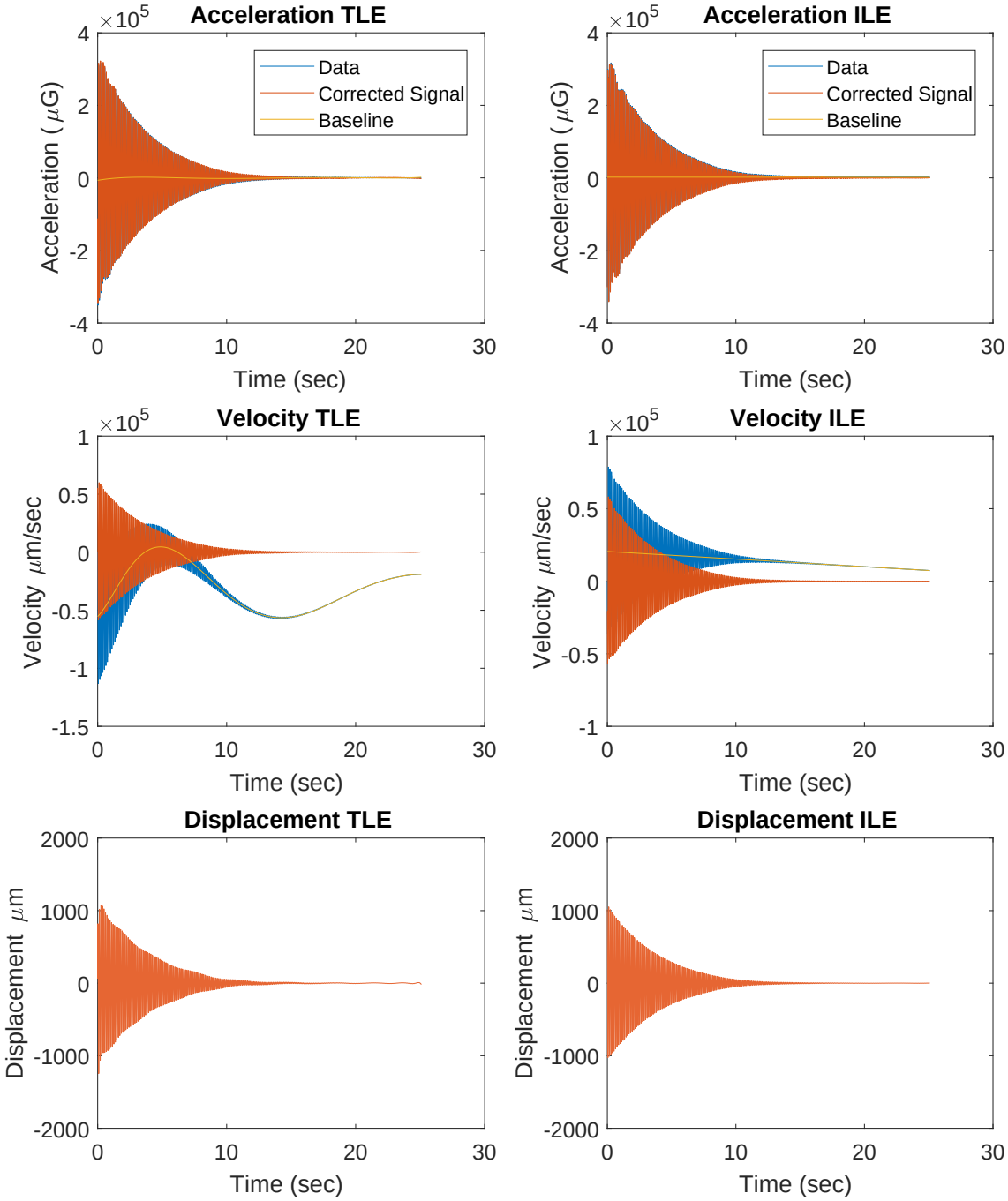

Figure 3.5 : Baseline corrected acceleration records.

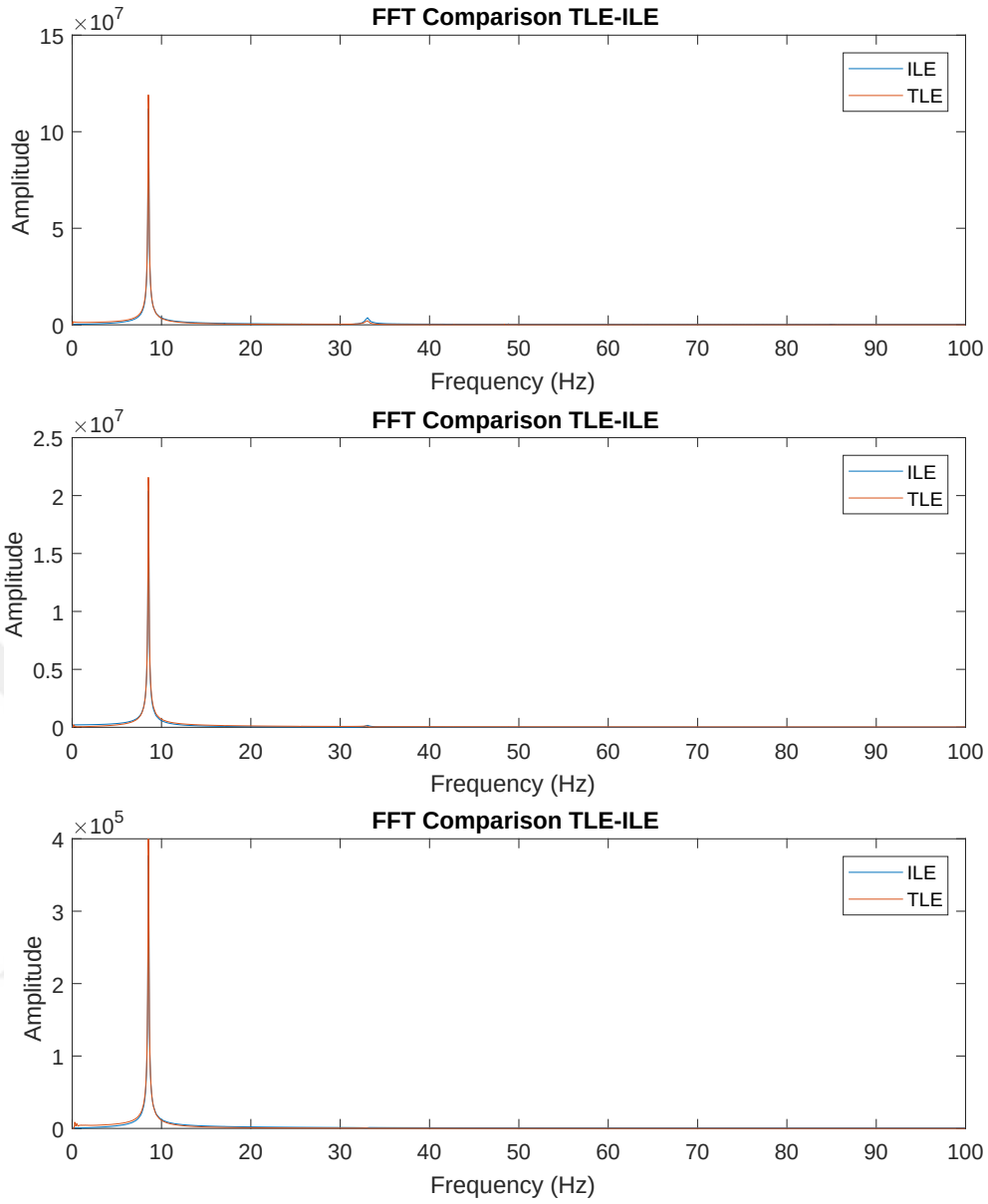

Figure 3.6 : Baseline corrected signals' Fourier transforms.

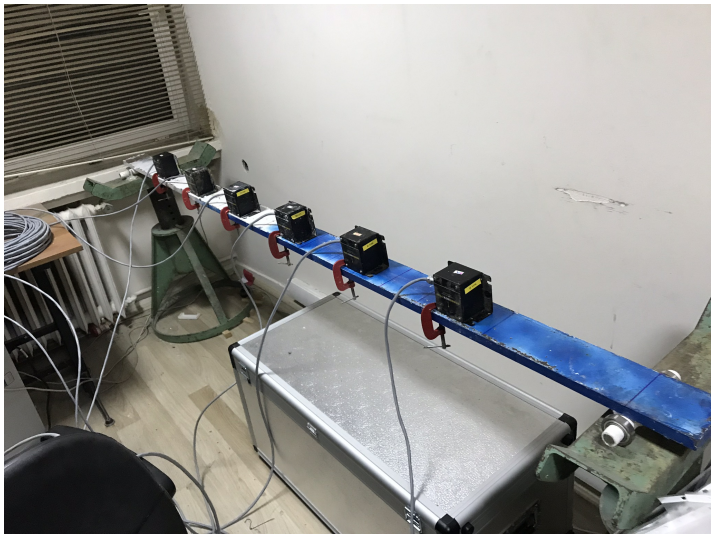

Figure 3.7 : Experimental setup for system identification.

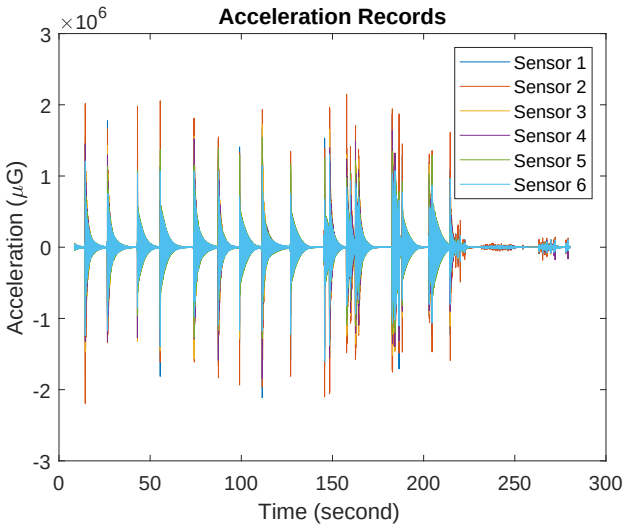

Figure 3.8 : 6 sensors acceleration records.

For the frequency domain system identification techniques, the power spectral densities can be found through aforementioned methods. Here, cpsd() function which uses welch methods is utilized in MATLAB environment. And the power spectral densities of the 6 sensors are shown in Figure 3.9. For the frequency domain methods, it can be applied either trace operation or singular value decomposition to find the modal frequencies. The trace of the PSD matrices is indicated in Figure 3.10.

The trace of the power spectral density matrices is generally used for basic frequency domain method. Moreover, to pick the fundamental frequency frequency domain decomposition method is more powerful and can be applied multi modal systems. The singular value decomposition of the power spectral density matrices are also shown in Figure 3.11.

3.4 Numerical Study

The sensors to be used for data acquisition, are quite sensitive devices and these devices subjected to environmental conditions, provides certain amount of noise. This noise affects the result of system identification. System identification methods are data quality dependent procedures. For this reason, it is important to avoid the sensor noise, if possible; however, more or less there will exist always some amount of noise, in real life applications. So, the noise effects to the structural parameter estimation is important topic. In this study, in order to change the measurement noise numerical model of the structure is created. The input of the structural model is Gaussian random

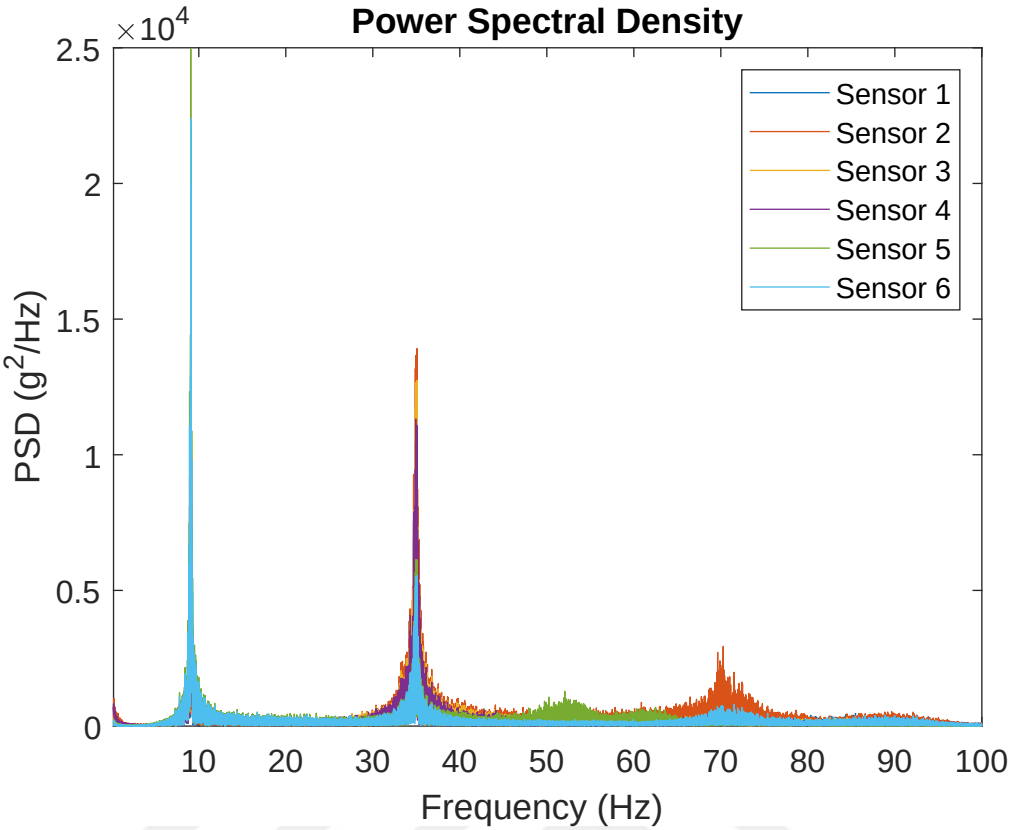

Figure 3.9 : Power spectral Densities.

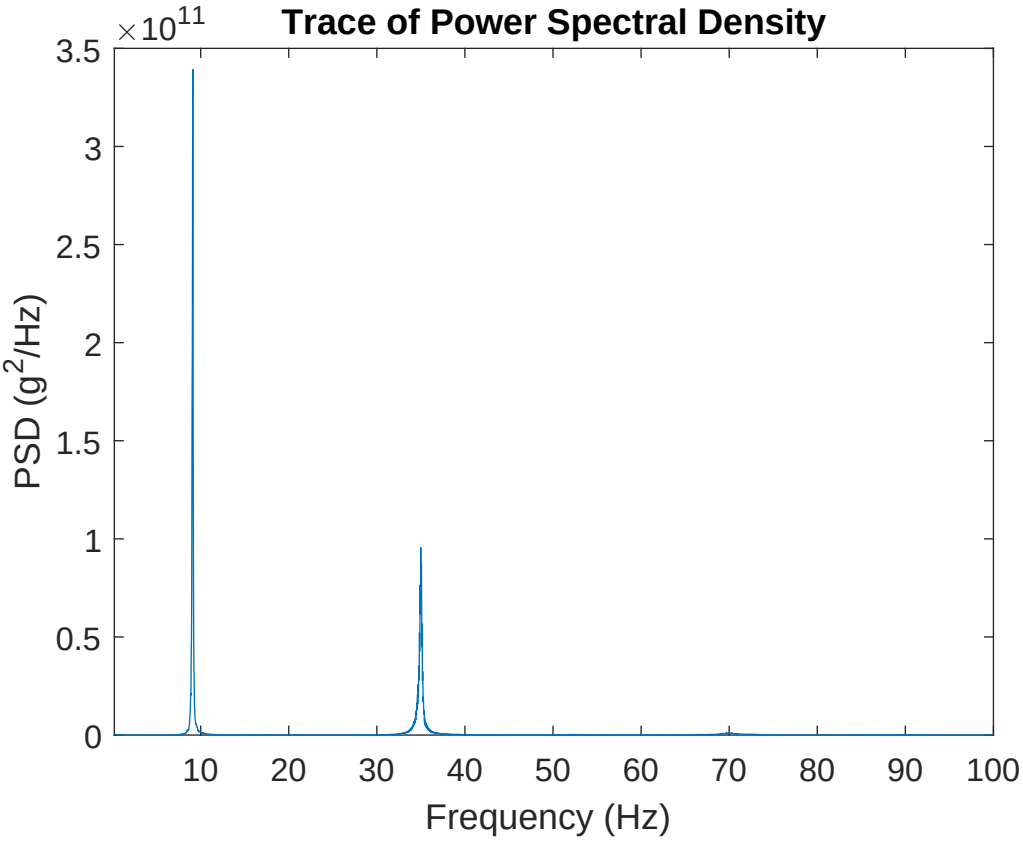

Figure 3.10 : Trace of the power spectral density matrices.

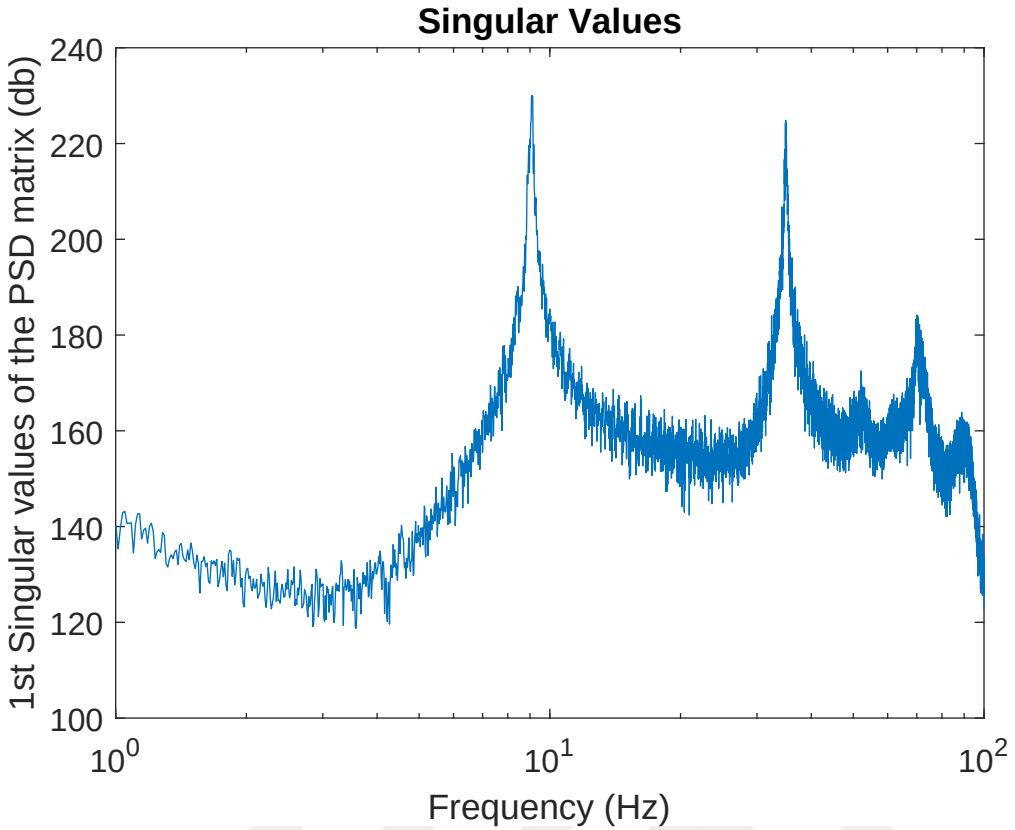

Figure 3.11 : Singular values of PSD.

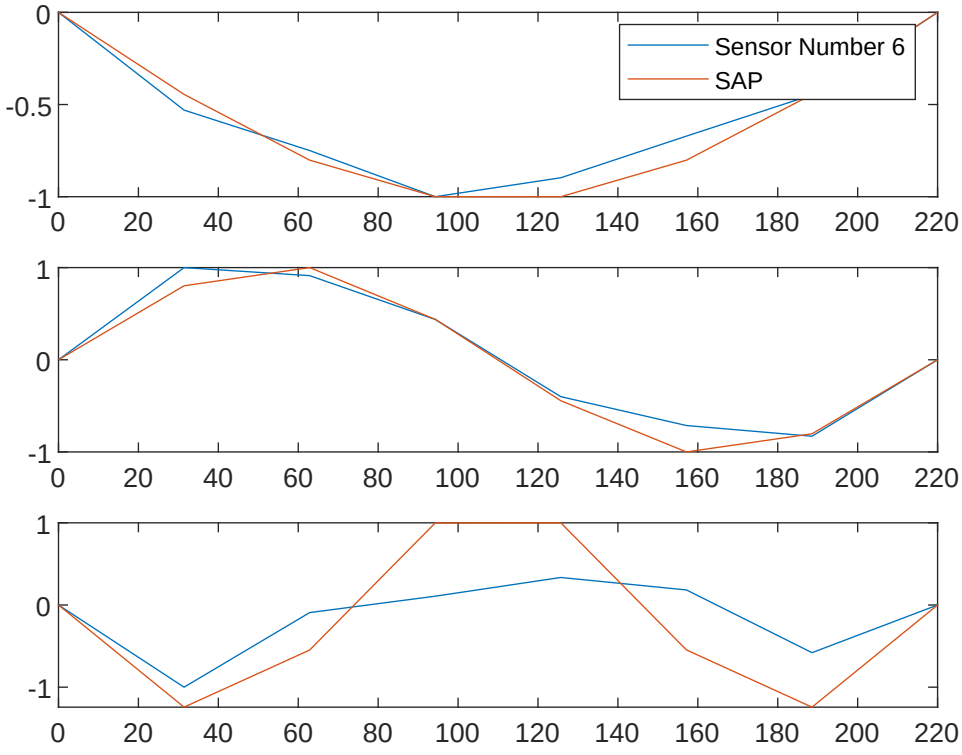

Figure 3.12 : Mode shapes for 6 sensors case.

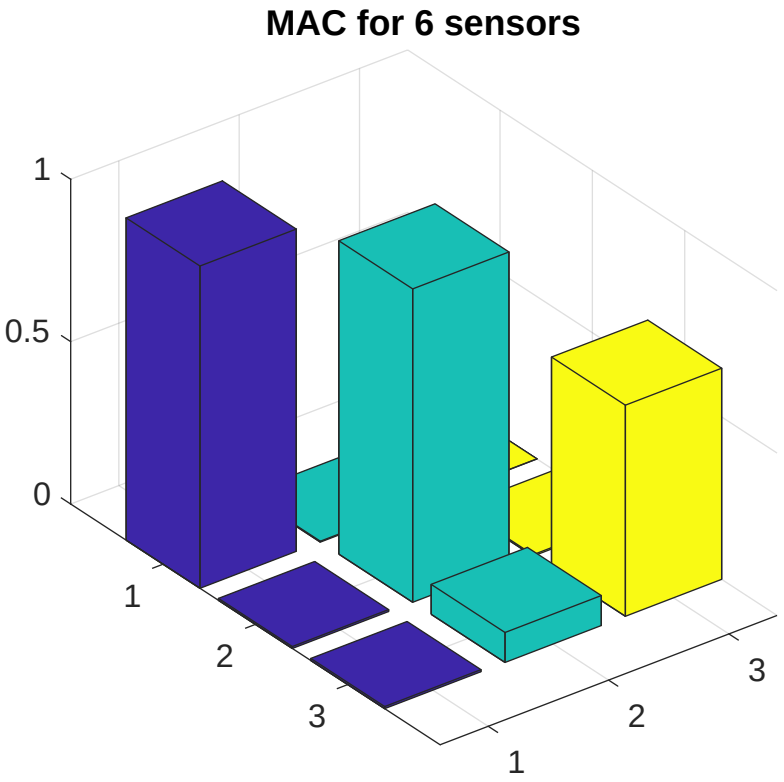

Figure 3.13 : MAC values for 6 sensors case

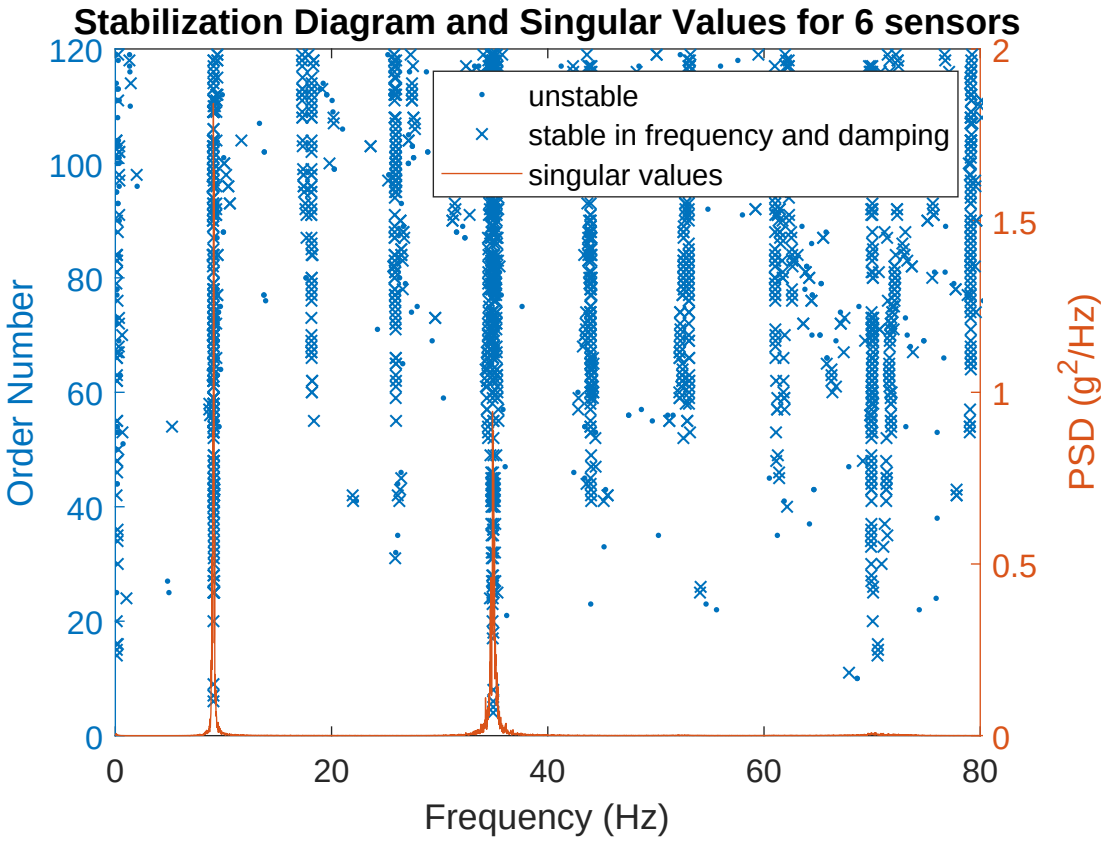

Figure 3.14 : Stabilization diagram and singular values for 6 sensors case.

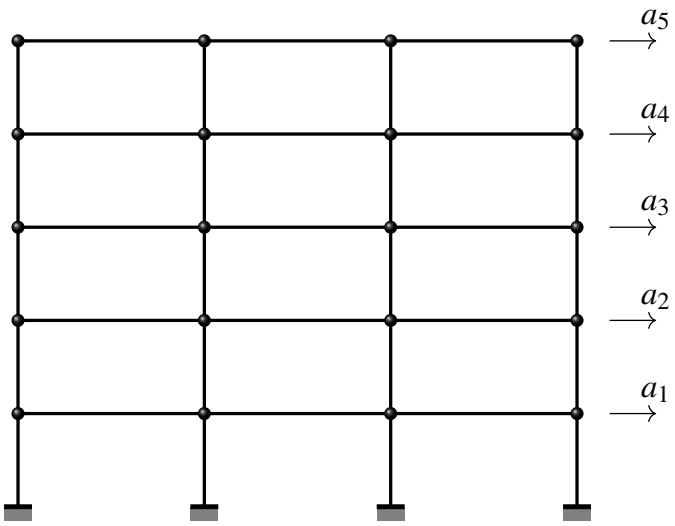

Figure 3.15 : Numerical model of the building and its verification.

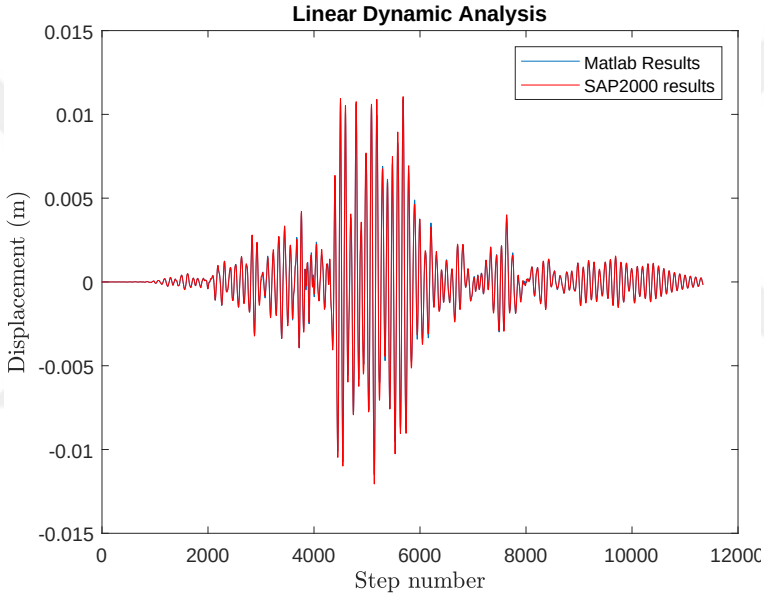

Figure 3.16 : Numerical model of the building and its verification.

input $U \sim \mathcal{N}(\mu = 0, \sigma^2 = g)$. A five story building was created, as shown in the figure 3.16. Moreover, each acceleration of the stories were used to determine the effects of noise to the output only system identification methods. The noise effects were presented according to ground acceleration Signal to Noise Ratio (SNR). Results of comparison of the SI methods in terms of noise level are reported in the Figures 3.18, 3.20, 3.22, and 3.24.

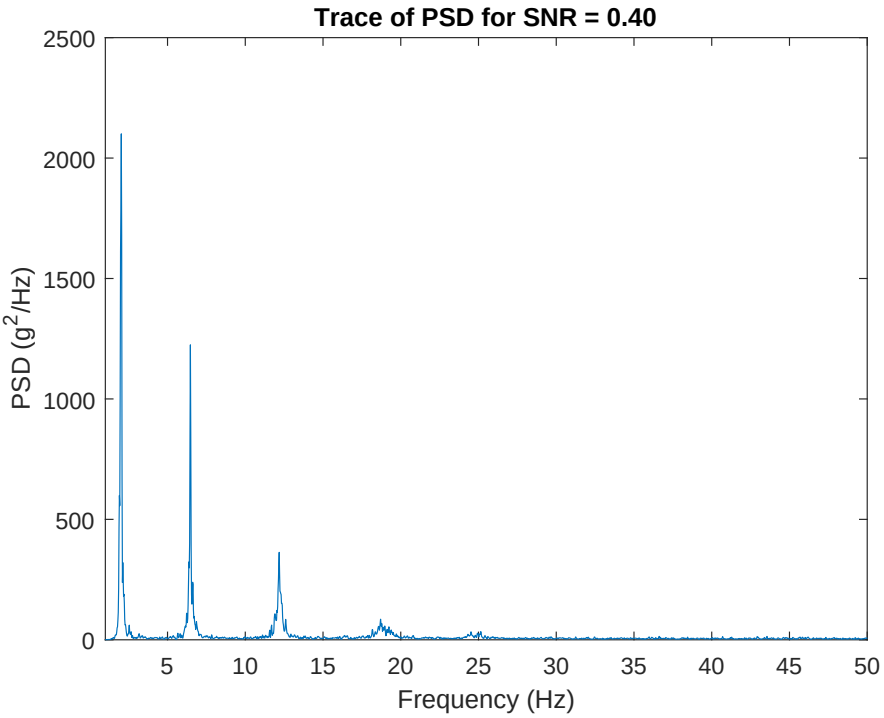

Figure 3.17 : Trace of PSD matrices for SNR=0.40.

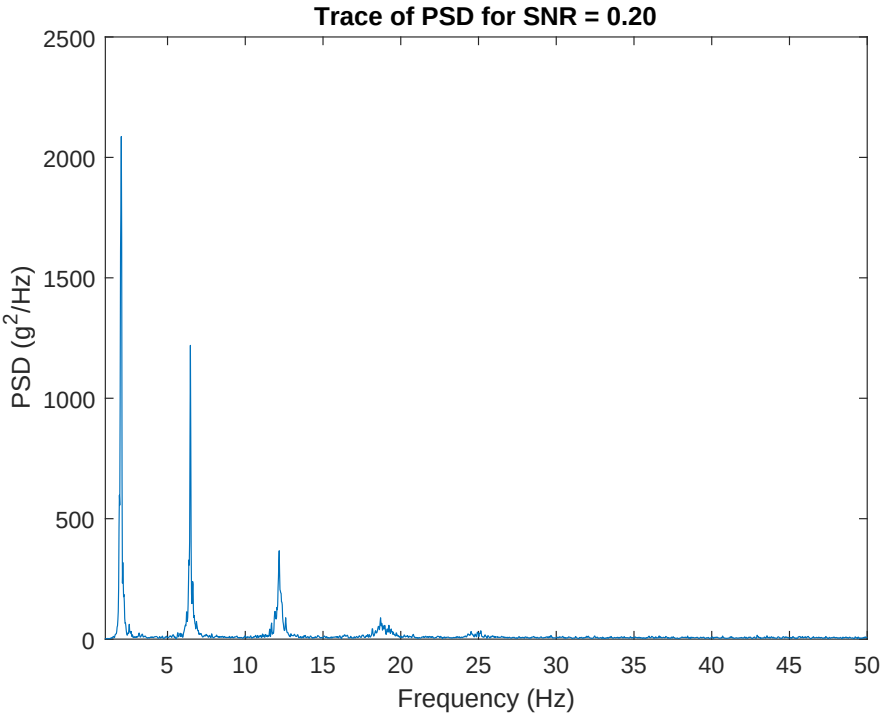

Figure 3.18 : Trace of PSD matrices for SNR=0.05.

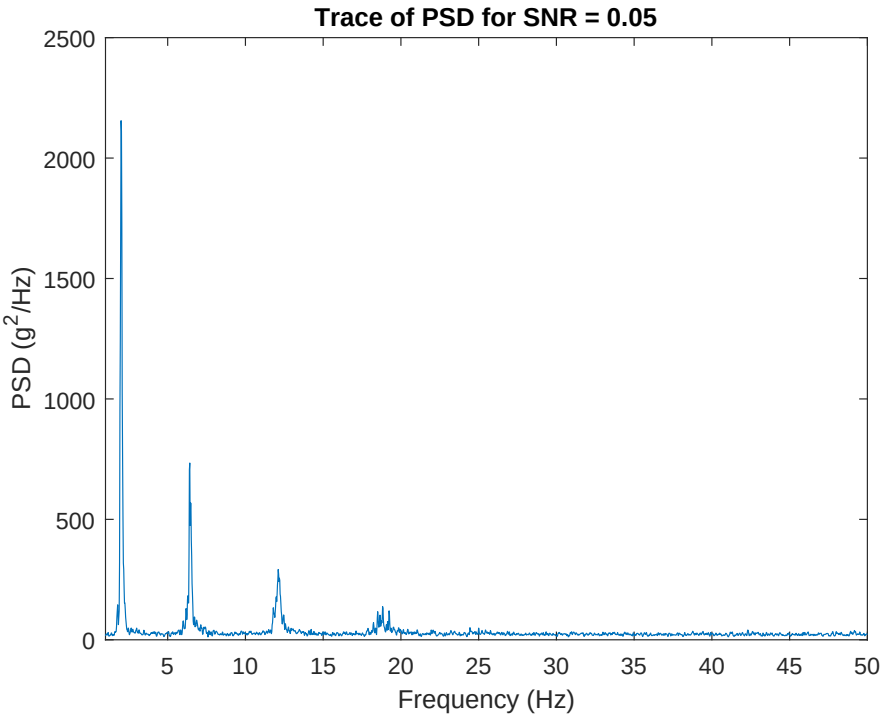

Figure 3.19 : Trace of PSD matrices for SNR=0.05.

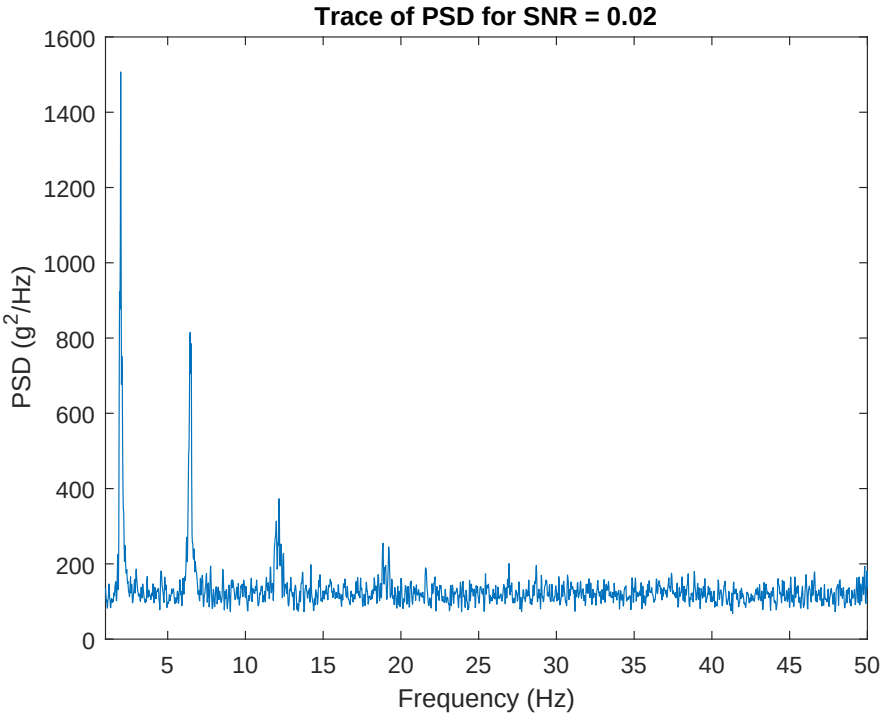

Figure 3.20 : Trace of PSD matrices for SNR=0.02.

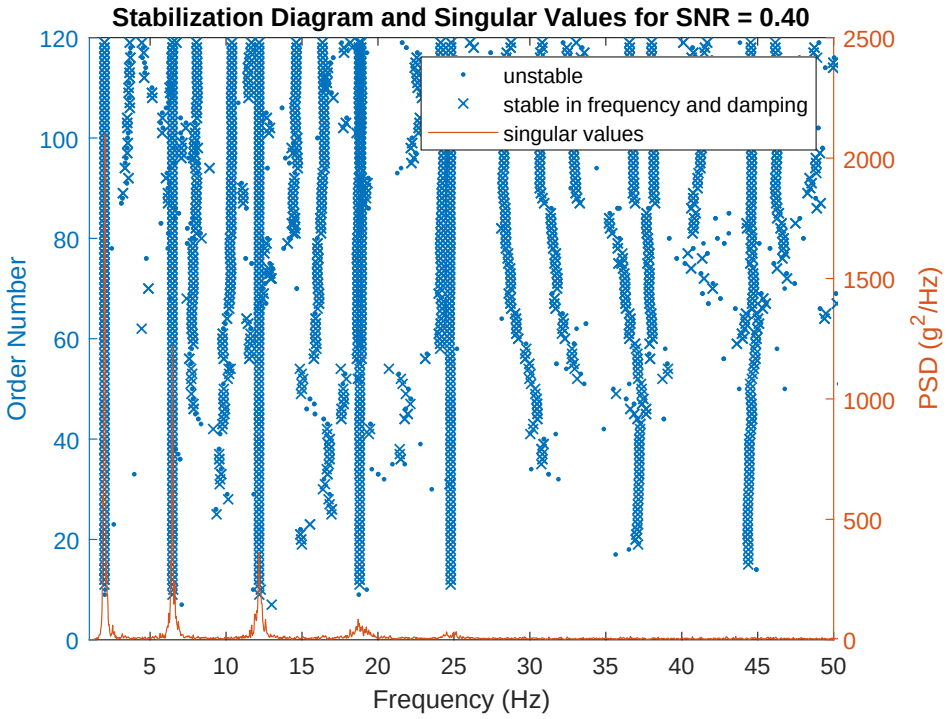

Figure 3.21 : Stabilization diagram and singular values for SNR=0.40.

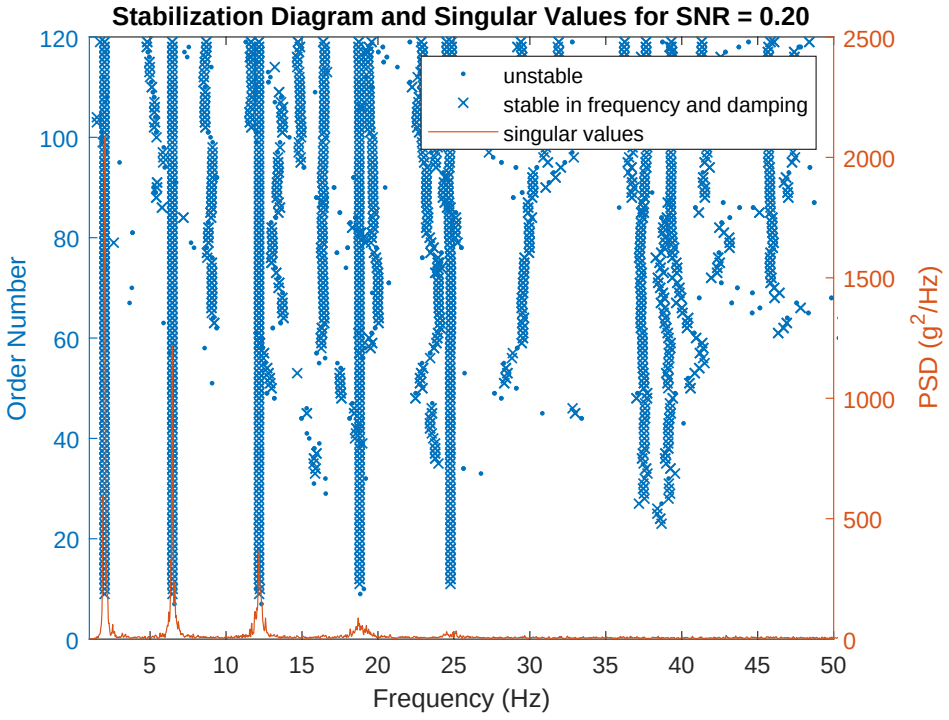

Figure 3.22 : Stabilization diagram and singular values for SNR=0.20.

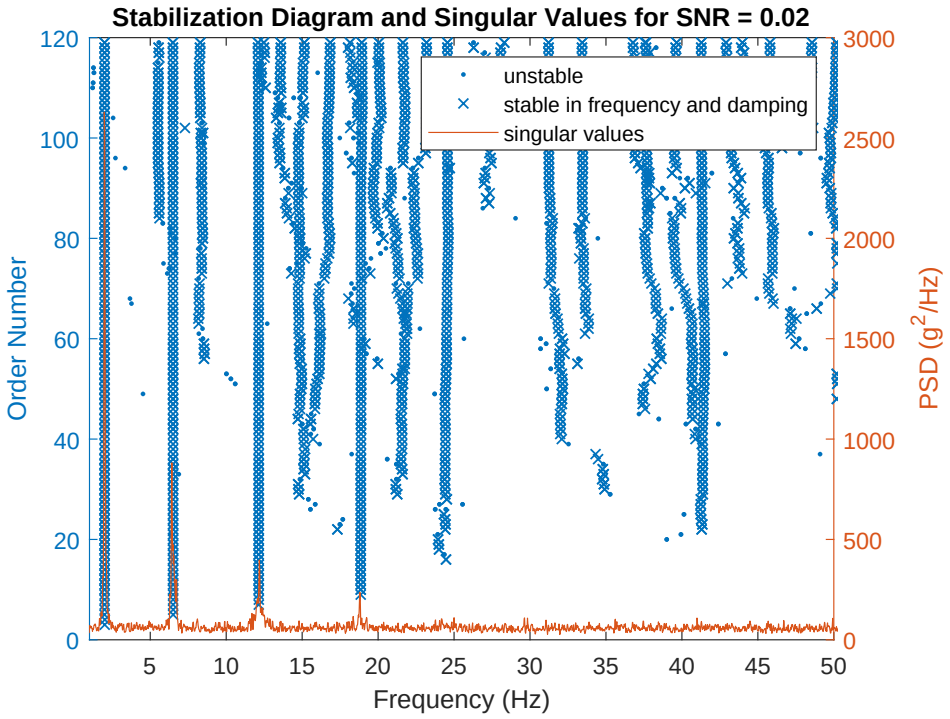

Figure 3.23 : Stabilization diagram and singular values for SNR=0.02.

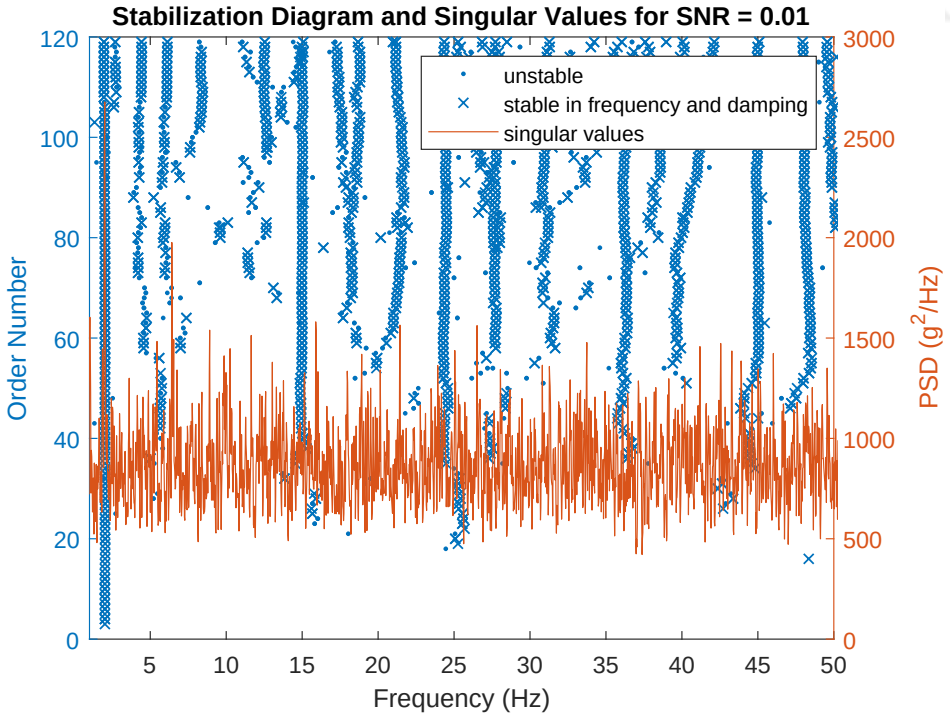

Figure 3.24 : Stabilization diagram and singular values for SNR=0.01.

4. SYSTEM IDENTIFICATION OF GOLDEN HORN METRO BRIDGE

4.1 Introduction

In this chapter, first a general review of the structural system of Golden Horn Metro Bridge (GHB) is given. Then, long-term and short-term monitoring system is explained. Third, methods employed for system identification are explained. Finally, results of the system identification are reported.

4.2 General Information

Golden Horn Metro-Crossing Bridge is cable-stayed bridge whose the construction stage was started in 2 January 2009 and finished in 9 January 2014. The opening of the bridge was 15 February 2014. The bridge located between the Yenikapi and Taksim districts in Istanbul was designed as overdosed cable-stayed bridge considering aesthetics concerns about historical peninsula . The bridge is the part of the M2 metro line operated by Metro Istanbul. According to Metro Istanbul, average number of passengers carried daily is approximately 320.000 [64].

4.3 Structural System

The GHB bridge involves five major parts:

- main cable-stayed bridge
- two approach bridges (Unkapanı and Beyoglu)
- swing bridge
- single-span bridge.

The swing bridge, cable-stayed bridge, and single-span bridge is steel structures and approach bridges are concrete structures. The span configurations of cable-stayed

bridge is 90 m +180 m + 90 m. Structural components of cable-stayed bridge are the pylons, deck, piers, and cables. The orthotropic deck consists of 3 cells shown in the Figure 4.4. The width of deck is 13.7 m, height is 3.5 m and its thickness is 40 mm. It is also approximately 17 m above water level. It is directly connected to the pylons whose height is about 54 m from the deck. Also, its sectional properties are varying, but the highest section properties are 5.4 m 2.5 m and its thickness is 70 mm. The deck and pylon section are illustrated in the Figure 4.4 and **??**. Moreover, the piers were designed as different number of tubular steel piles, also the piles filled with concrete by the last 50 m [1]. The design of the GHB is realized according to Load Resistance Factor Design specified by AASHTO-LRFD Bridge Design Specification. For the entire bridge, LRFD provides uniform safety level in terms of loads and the resistance. Each structures or structural components must satisfies the limit state specified. The bridge was examined considering different load combination and limit states determined as strength limit state, extreme limit state, service limit state, and fatigue limit state, according to AASHTO-LRFD. Load cases were determined in line with AASHTO loads definition as permanent load and transient forces. Permanent loads are dead load of structural and non-structural elements, superimposed dead load of wearing surfaces and utilities, downdrag, and accumulated locked-in forces from the construction process. Transient loads are vehicle live load, dynamic impact, nosing forces, braking and acceleration force, pedestrian live load uniform temperature, thermal gradient, settlement, wind load on structure, wind load on live load, water load and stream pressure, earthquake, ship impact, snow load, rupture of members. The Bridge should be checked for each possible load combinations, however, the earthquake resistance of the structure is assessed in this study. For this reason, the earthquake loads was explained [1].

Table 4.1 : Deck section properties

Deck		
Area		0.889 m^2
Moment of Inertia	x	1.27 m^4
Moment of Inertia	y	11.84 m^4
Radius of gyration)	x	1.198 m^4
Radius of gyration	y	3.648 m^4

Figure 4.1 : General view of Golden Horn Bridge.

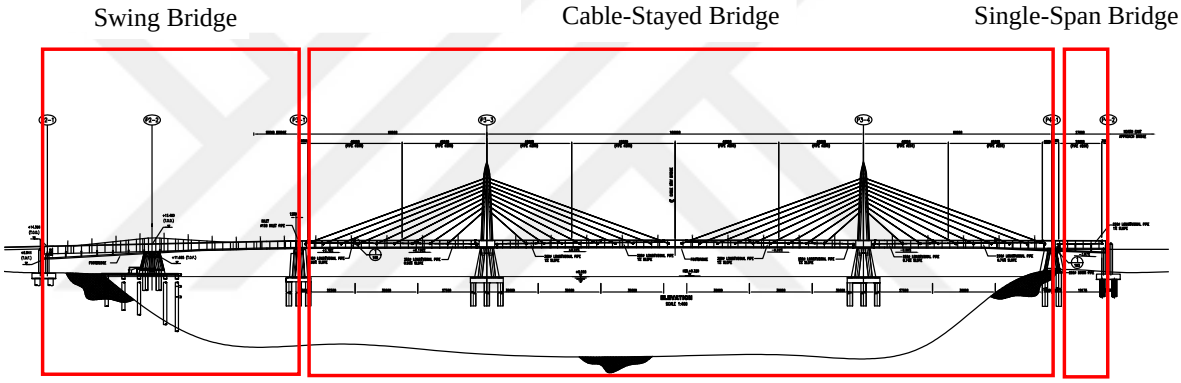

Figure 4.2 : Parts of the GHB.

Figure 4.3 : General view of Golden Horn Bridge

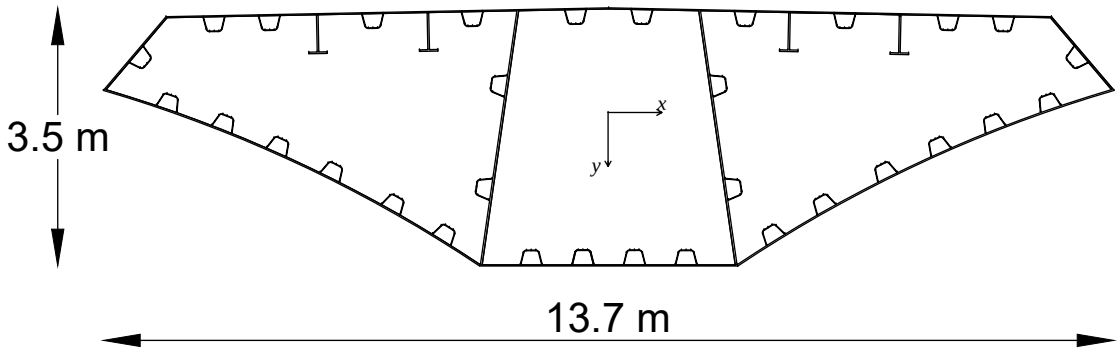

Figure 4.4 : Deck of the Golden Horn Bridge.

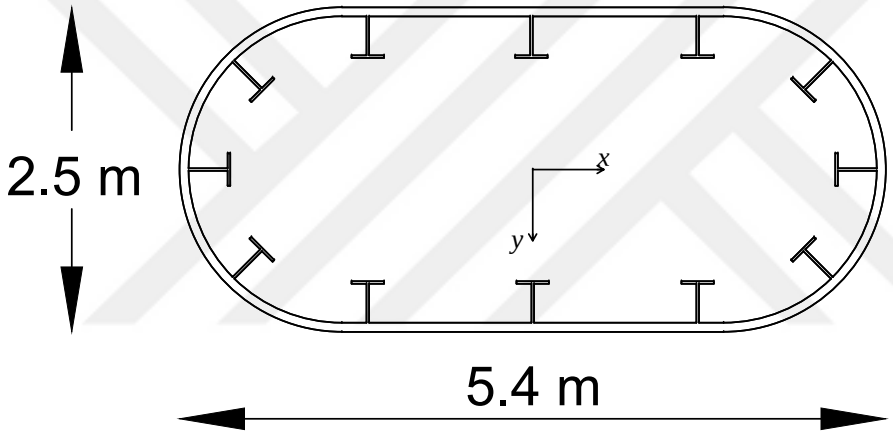

Figure 4.5 : Pylon of the Golden Horn Bridge.

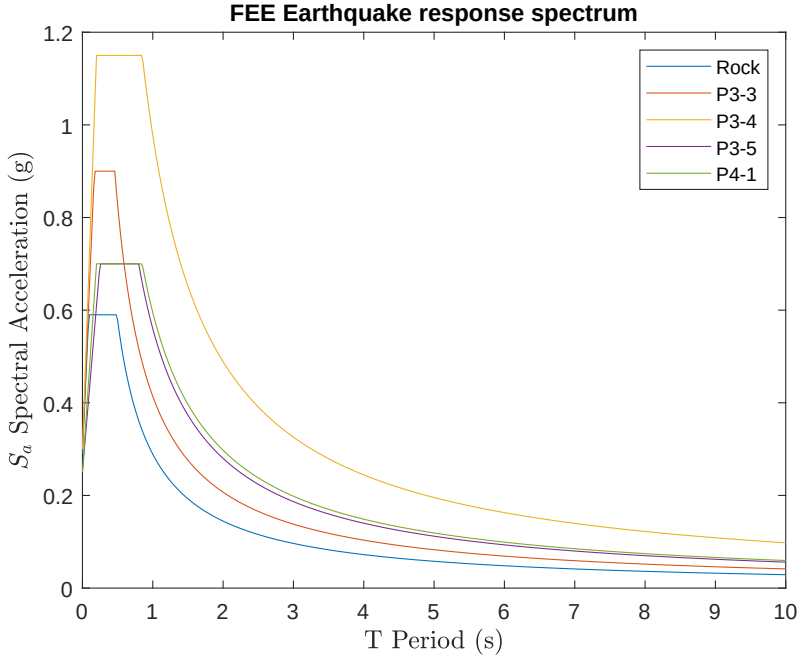

Figure 4.6 : FEE response spectra.

Seismic design objective was considered as safety for running train during earthquake and to make resumption of transportation possible as soon as the earthquake stops. Moreover, seismic design calculations carried out on the basis of geotechnical report for the area, AASHTO-Standard Specifications for Highways Bridges - Division IA Seismic Design for the approach viaducts, and EUROCODE 3. To provide an earthquake resistant design of GHB, two levels of ground motion are considered. One of them is functional evaluation of earthquake ground motion and the other one is safety evaluation of earthquake ground motion [1].

Functional evaluation of earthquake ground motion is the high probability earthquake that is generally defined as earthquake with 50% probability of exceedance in 50 years. Under the functional evaluation of earthquake (FEE) ground motion, the damage level of the GHB was taken into account as minimal and the bridge should continue without interruption. The different response spectra was used as shown the Figure **??** [1].

Other ground motion level was considered as the safety evaluation of earthquake (SEE) ground motion which has typically long return period. In the seismic design of the bridge, the earthquake with 2% probability of exceedance in 50 years is selected in line with site-specific probabilistic ground motion study. Under the SEE level ground motion, only repairable damage was allowed. Also, the damage allowed should be able to be repaired with a minimum risk of functionality and lives. The different response spectra was used for determination of the earthquake loads with respect to Figure 4.7 [1].

4.4 Finite Element Modeling

Finite element model of the Golden-Horn Bridge was created using technical drawing of the bridge provided by Istanbul Ulasim. The simplified mathematical model of the bridge consists of deck, pylons, cables, and piers. Pylons having variable cross sectional properties were represented as the elements which have parabolic variation between 6 different sections. Cables were taken into account as frame elements connected to pylons and deck with rigid elements. While the piers were considered as different number of same one dimensional elements, the soil behavior were modeled with spring elements having variable stiffness. Mode frequency and

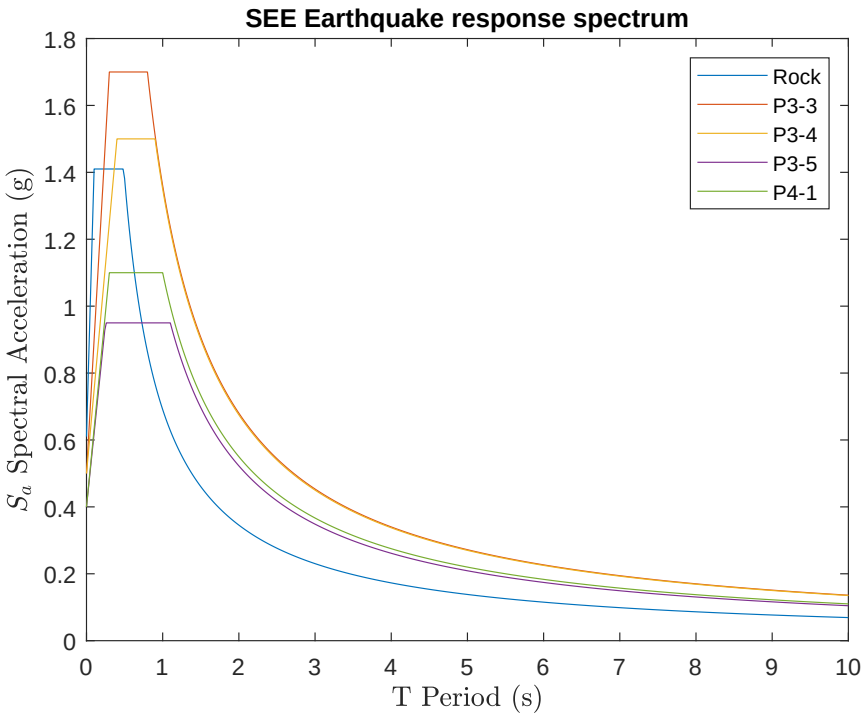

Figure 4.7 : SEE response spectra.

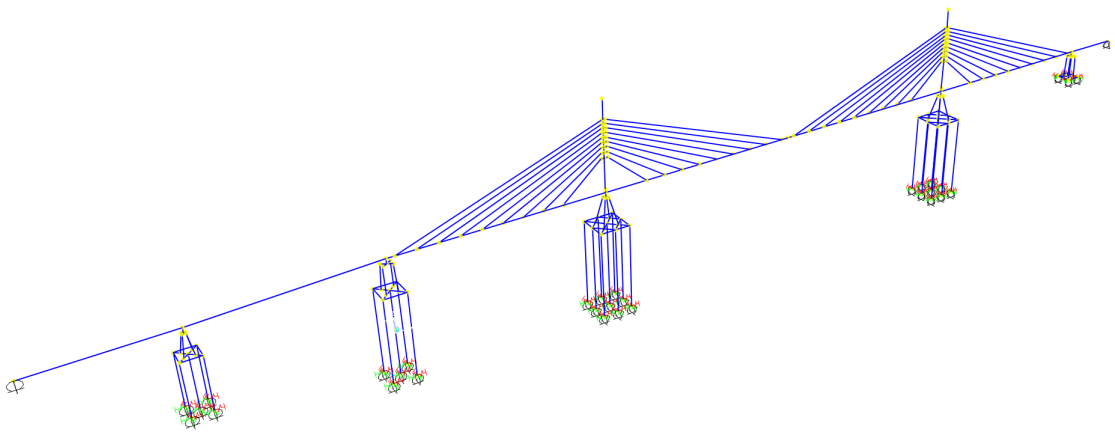

Figure 4.8 : Finite element model of the Golden Horn Bridge.

shapes of simplified model and design model comparison were illustrated in Figure 4.9.

Table 4.2 : Spring coefficients for ground modeling

	P2-2	P3-1	P3-3	P3-4	P4-1
k_y (kN/m)	9700	16000	11800	16200	38200

4.5 Golden Horn Metro Bridge Structural Health Monitoring System

When the structural health monitoring system is deployed, the permanent sensor measurements is validated using initial measurements by Vienna Consulting Engineers firm. Initial measurements were used for validating the permanent monitoring system. The measurements are recorded from the 80 different location for the deck and the 14 different location for the pylons. The sensor location were shown in the Figure 4.10 and 4.11 [2]. It also initial measurements structural parameter estimation results were illustrated in the Figure 4.12. The simplified finite elements model was also developed to check the system identification results by Vienna Consulting Engineers (VCE) firm.

4.6 Golden Horn Metro Bridge Permanent Structural Health Monitoring System

The permanent structural health monitoring system consists of 32 accelerometer, 4 meteorological, 12 temperature, 5 tilt meter, 4 displacement and 4 GPS sensors. The raw data of total 61 sensor measurements has been saved to the server located in the Metro Istanbul LTD. and sent to the VCE. Schematic view of the acceleration sensors are indicated in Figure 4.13.

The sensor data of the acceleration measurements were received from Metro Istanbul LTD. and the frequency analysis was applied for structural system identification purposes. Although the reasonable result from the system identification could not be reached. It has been decided that the measurements should be repeated with the existing facilities.

4.7 Golden Horn Bridge Acceleration Measurement

The acceleration measurements were carried out using aforementioned equipment in Chapter 3. Acceleration sensors were placed the 7 different location indicated in Figure

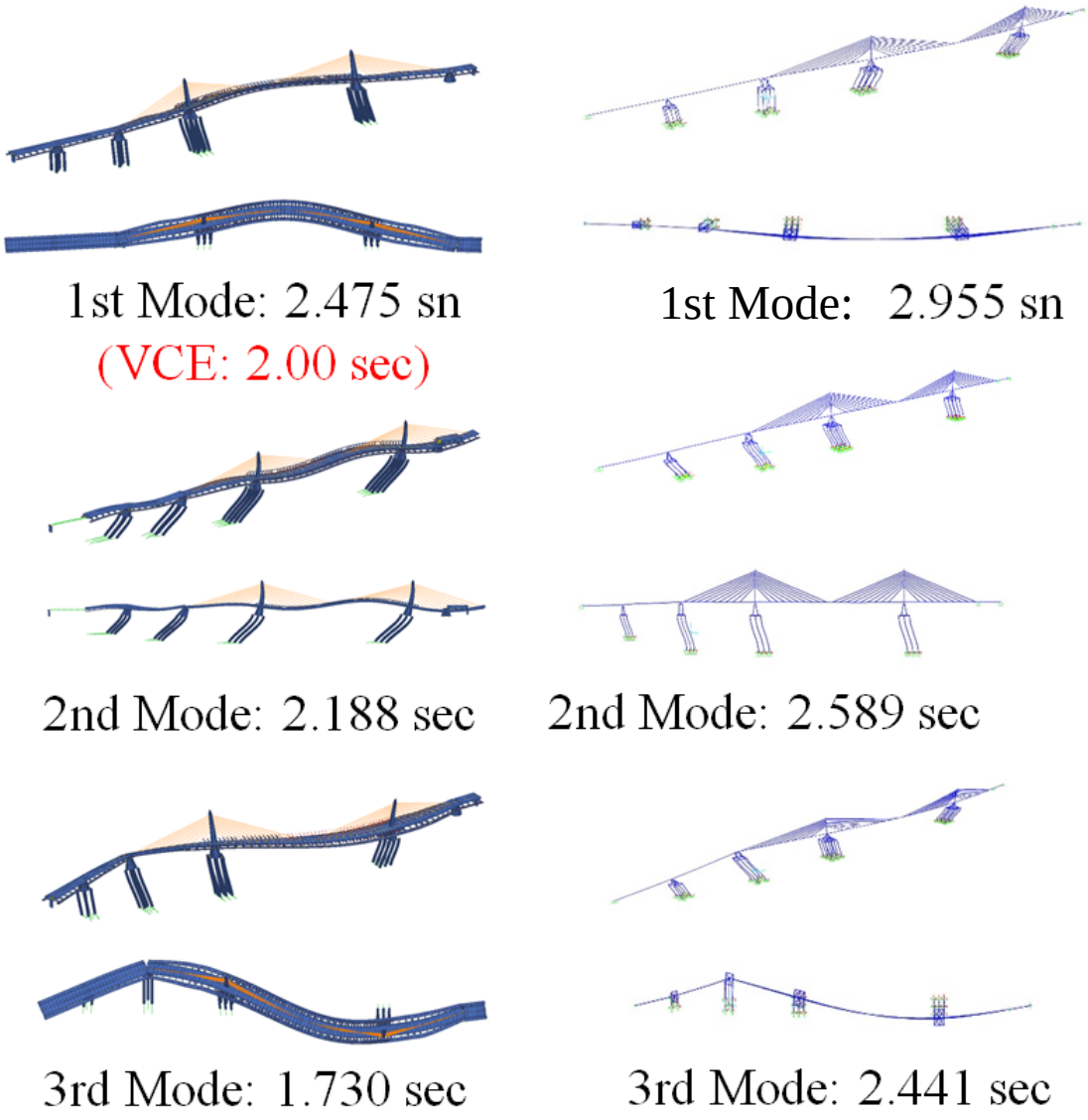

Figure 4.9 : Finite element model of the Golden Horn Bridge [1]

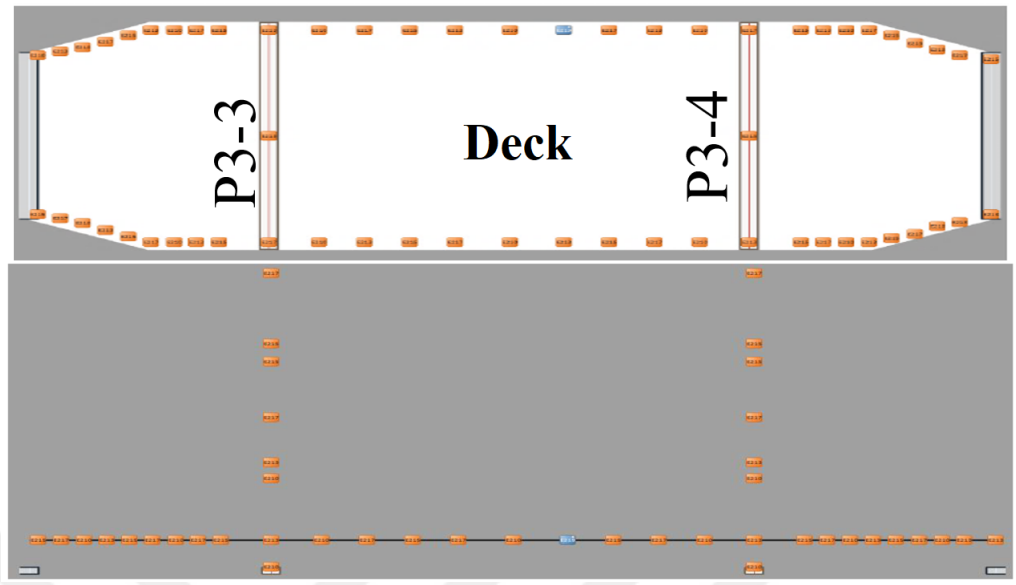

Figure 4.10 : Initial measurements location of deck and pylons

Figure 4.11 : Initial measurements location of deck and pylons

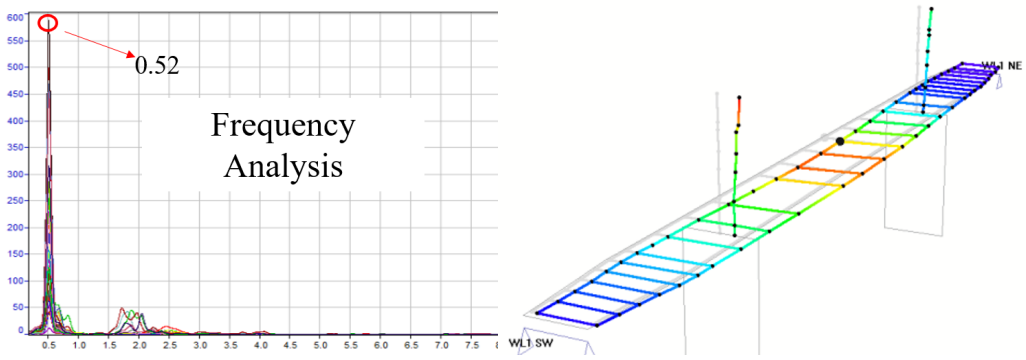

Eigen-frequencies	Vibration mode (Kind of loading)	BRIMOS Measurement [Hz]	FE Model [HZ]	Deviation [%]
1	1st bending mode	0,52	0,49	7,4
2	2nd bending mode	0,63	0,55	13,8
3	1st torsional mode	1,08	-	-
4	3rd bending mode	1,26	1,08	16,3
5	4th bending mode	1,82	-	-
6	2nd torsional mode	3,02	-	-
7	5th bending mode	4,23	-	-
mean deviation				**12,5**

Figure 4.12 : Initial measurements results [2]

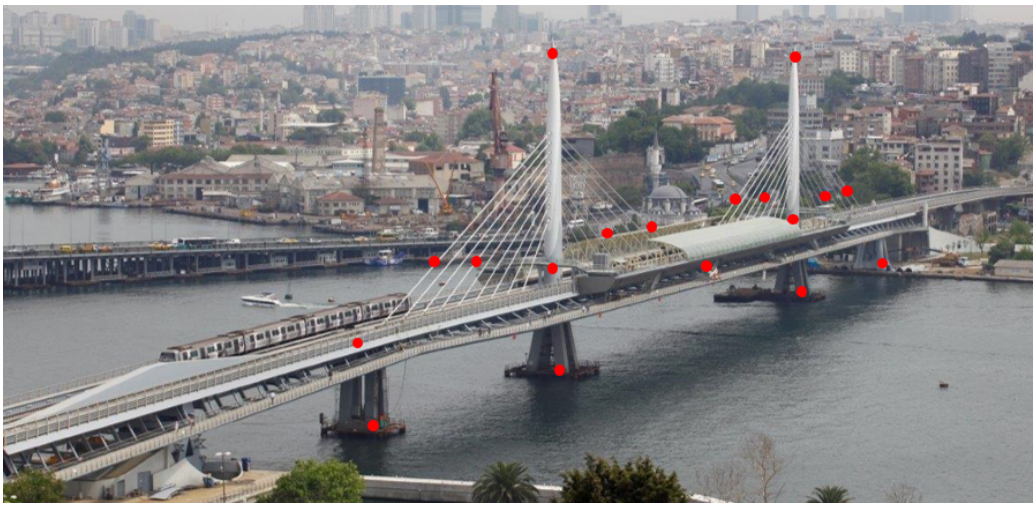

Figure 4.13 : Permanent acceleration sensors' location.

Figure 4.14 : GHB acceleration measurements.

4.15 on the deck. Distance between the accelerometer is 15 m. The measurements were realized in only main span where the train station is located. Acceleration records are measured in 200 Hz. In the Figure 4.14, the acceleration measurements are shown for the 7 channel. Also system identification results of the acceleration records is presented for the different system identification algorithms in the Figure 4.17, 4.18, and 4.19. As a system identification algorithm, trace of the PSD matrices, average normalized PSD, FDD, and SSI-DATA algorithms are used.

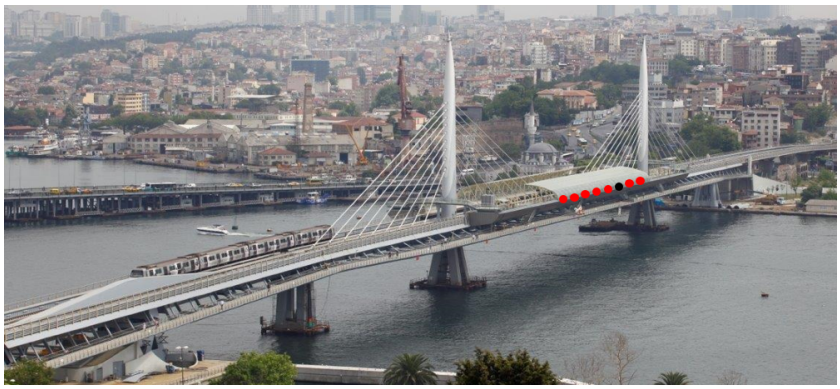

Figure 4.15 : Location of acceleration measurements.

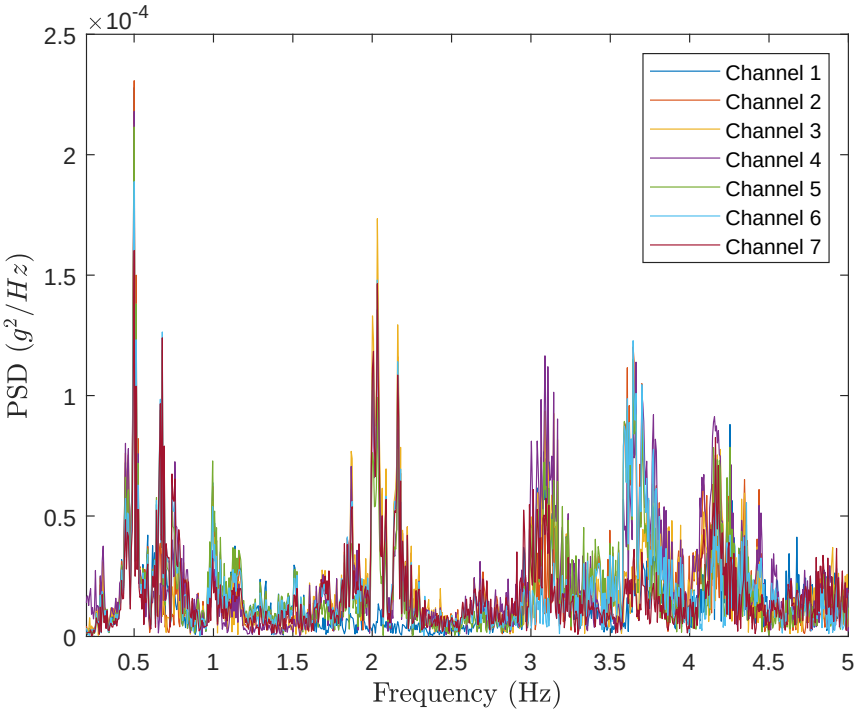

Figure 4.16 : Fourier spectra of acceleration measurements.

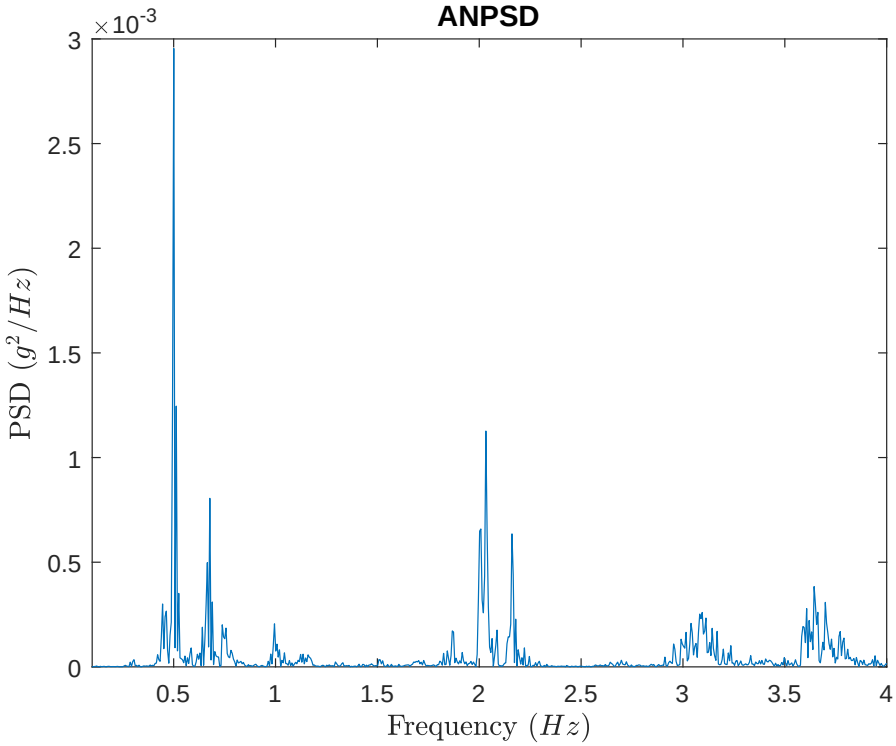

Figure 4.17 : ANPSD of acceleration records.

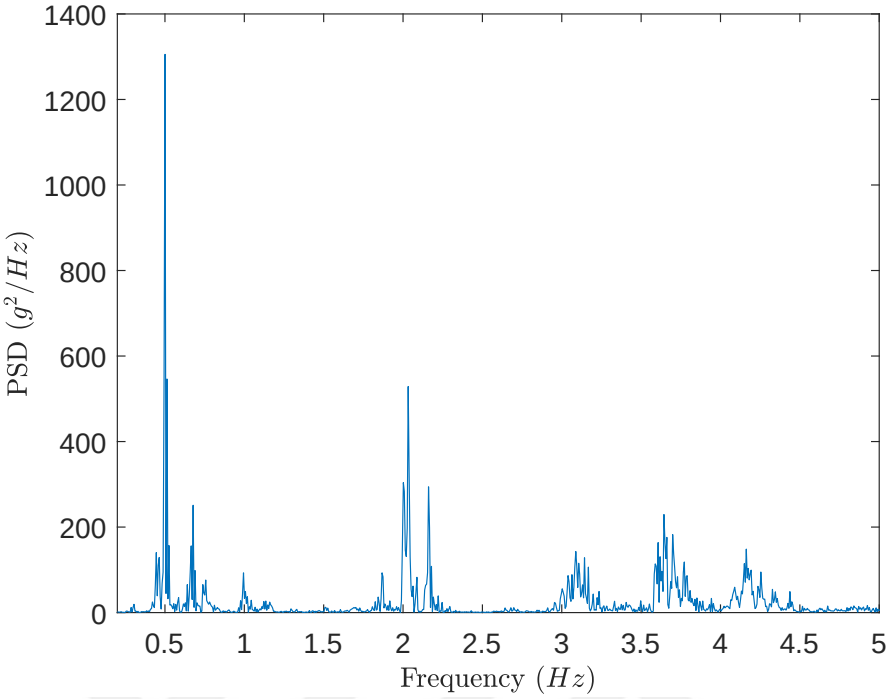

Figure 4.18 : Trace of the power spectral densities.

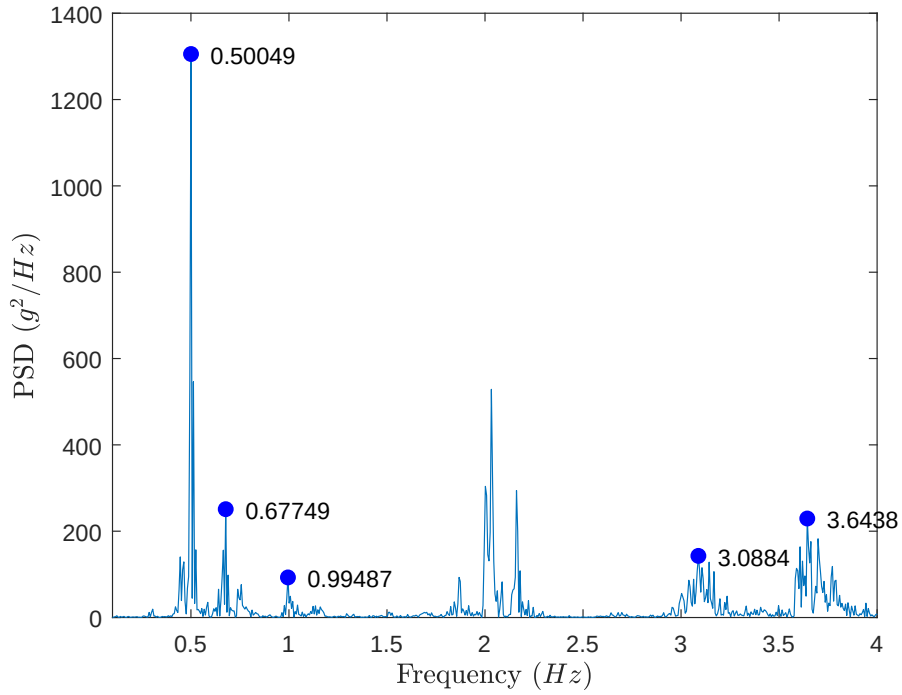

Figure 4.19 : SVD of power spectral densities and the chosen modal frequencies

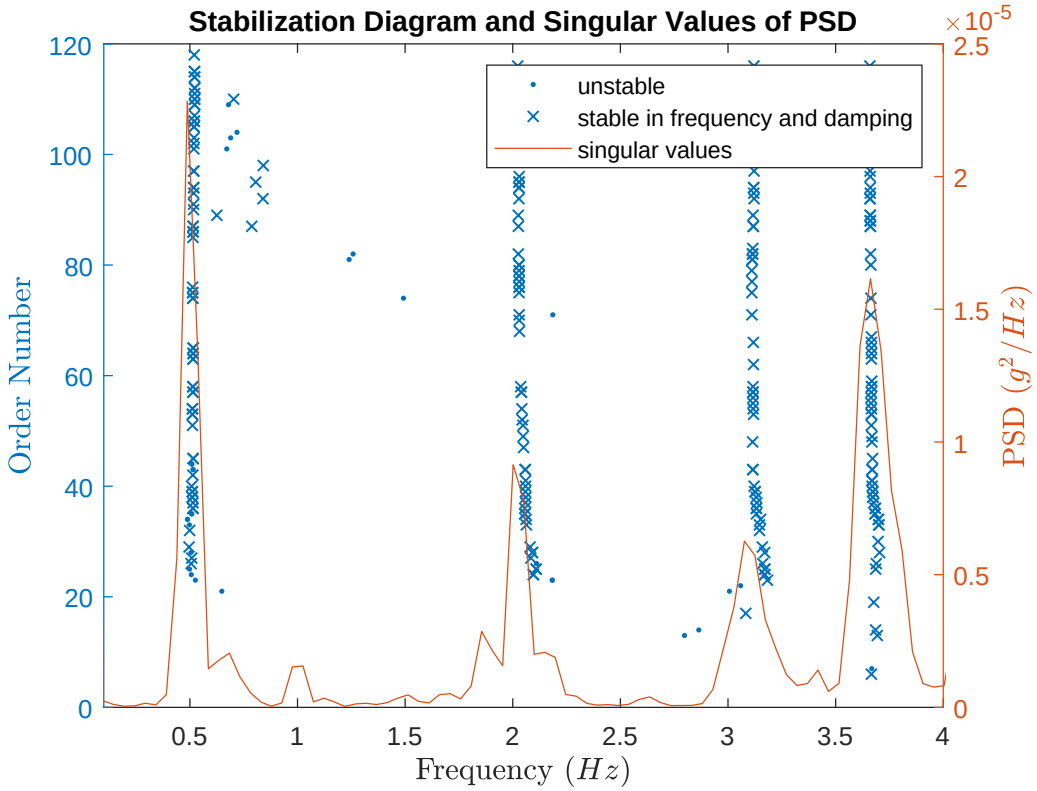

Figure 4.20 : Stabilization Diagram of acceleration records.

Damping estimation can be realized using aforementioned half power bandwidth method. According to this method, following relation can be written for the first mode;

$$\xi = \frac{\omega_b - \omega_a}{2\omega_n} = \frac{0.52 - 0.48}{2 \times 0.50} = 0.04 \tag{4.1}$$

Also, results of system identification methods for GHB measurements are presented in the Tables 4.3 and 4.4 and mode shapes obtained from different system identification algorithms are reported in Figure 4.21 and Tables 4.3,4.4

Table 4.3 : System Identification comparison

SI method	1st Mode	2nd Mode	3rd Mode	4th Mode	5th Mode
PP	0.50	0.68	0.99	3.09	3.64
FDD	0.50	0.68	0.99	3.09	3.64
SSI	0.52	-	-	3.12	3.66

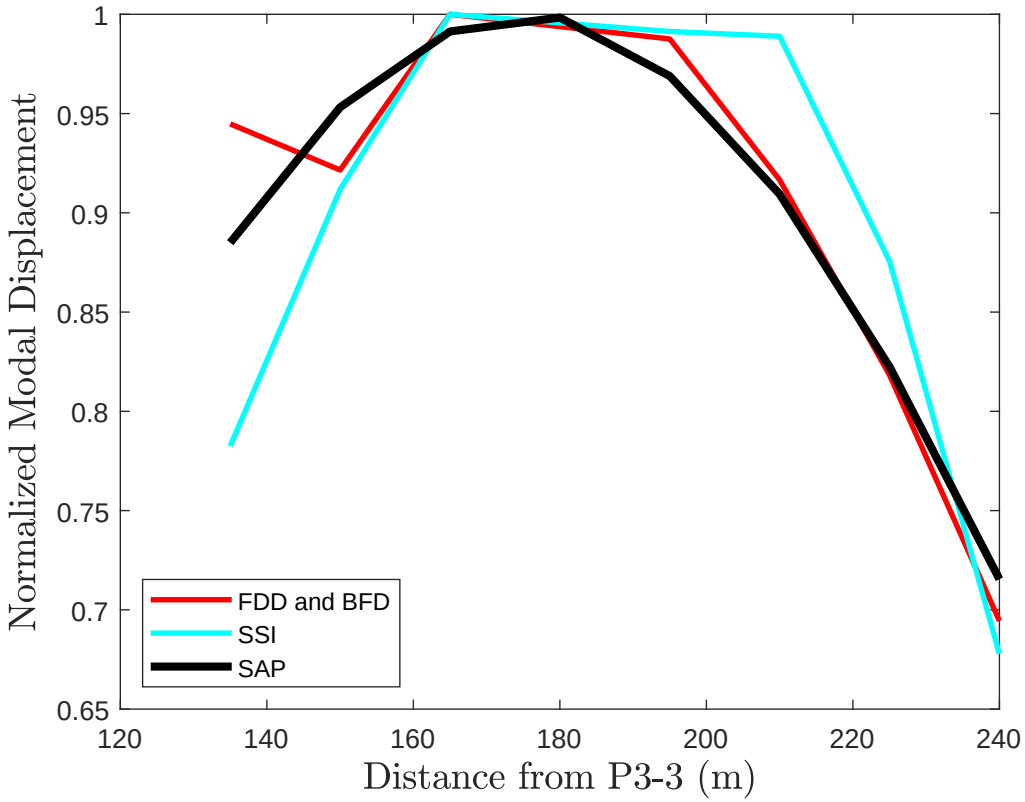

Figure 4.21 : Mode shape comparison.

Table 4.4 : MAC values for 1st mode

SI method	MAC (%)	ξ (%)
PP	99.75	4
FDD	99.75	4
SSI	84.00	2.45

5. PERFORMANCE ASSESSMENT OF GOLDEN HORN METRO BRIDGE

5.1 Introduction

The realistic finite element model through system identification methods is hitherto discussed. Although, the third step of damage identification is the quantification of damage level [4]. In other words, the performance of a structure needs to be assessed to define the structural health level after an earthquake. The performance assessment of GHB is carried out through nonlinear time history analysis.

For the nonlinear time history analysis, the expected plastic deformation location needs to be defined. The plastic deformations should be placed in the part of the visible of the bridge. So the plastic deformation allowed on the top of the piles.

5.2 Nonlinear Modeling of GHB

In order to capture the nonlinear behavior of the GHB, the cable-stayed bridge and the swing bridge were modeled together. Moreover, the soil structure interaction were taken into account through nonlinear soil spring. The below ground pile sections are the composite sections and group effects of piles are ignored.

In the nonlinear structural mathematical model, the soil behavior, geometric nonlinearity and the plastic deformation of piles are considered. The soil structure interactions are modeled based on geotechnical report and the pile analysis conducted [1]. Nonlinear soil springs are reported in Table C.2 for P2-2 as an example. The soil springs properties of other piles are indicated in Appendix A.3.

The second nonlinearity considered in this chapter is the plastic deformation on top of the piles. The plastic behavior of pile sections are obtained through moment-curvature relationships using SAP2000 section designer tool. To define the plastic behavior of the pile, rigid-plastic moment hinges are utilized based on the section properties found

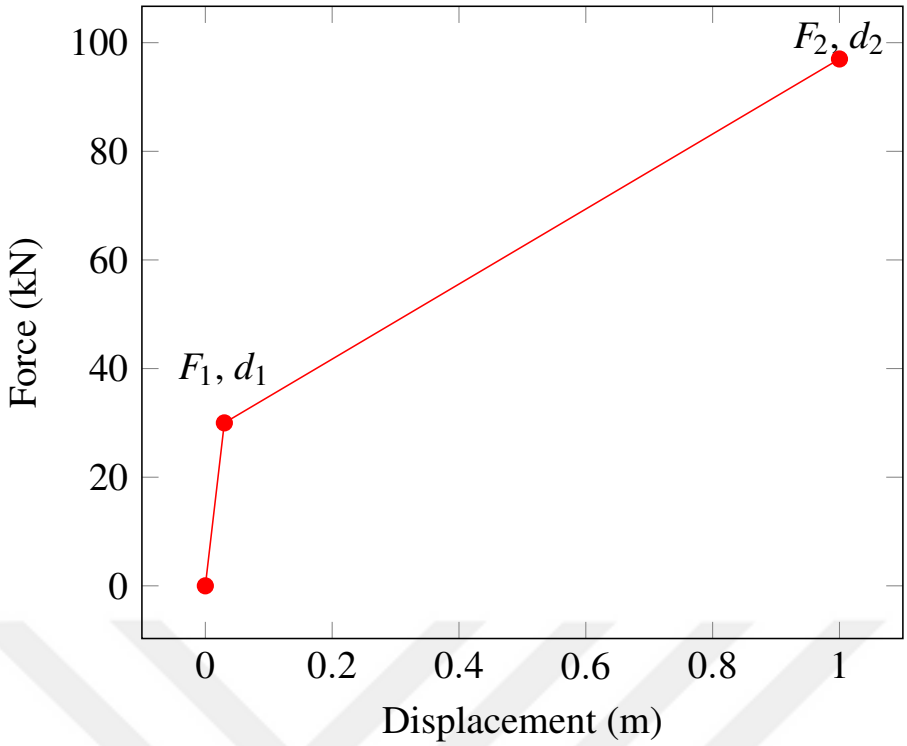

Figure 5.1 : Soil spring behavior

at moment-curvature analysis and these moment-curvature relationships are shown in Figure 5.2 and 5.3.

As already mentioned in Chapter 4, the GHB is designed that the only possible plastic deformations are allowed to occur on top of the piles. In the design stage of the superstructures, the pier, pylons, and deck sections are provided to be elastic limits. The superstructure is designed through maximum response spectra which is the P3-3 spectra for the assessment of internal forces in the SEE level earthquake design. While under the FEE level earthquake, the structure remains elastic, the top of the piles exhibits the plastic deformations due to the SEE level earthquake, according to substructure design report [65]. Moreover, for response spectrum analysis, the maximum response spectrum which is the response spectra belonging to P3-3 is chosen and the response spectrum could be seen in the figure 5.5.

Finite element model of GHB is indicated in the Figure 5.6. As it could be seen that the piles of the GHB is extended to the rock and also soil structure interaction behavior is represented with addition nonlinear soil spring. So the response spectra to be used for the time history analysis is the response spectra belonging to rock .

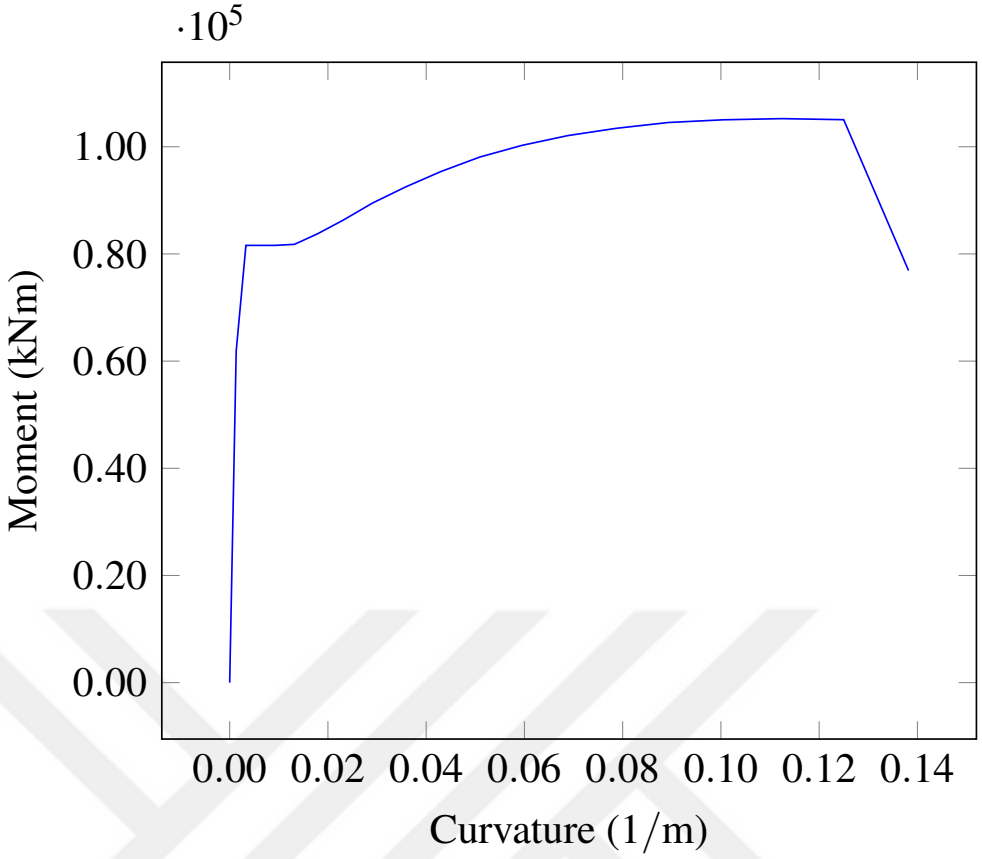

Figure 5.2 : Moment-Curvature relationship of single pile

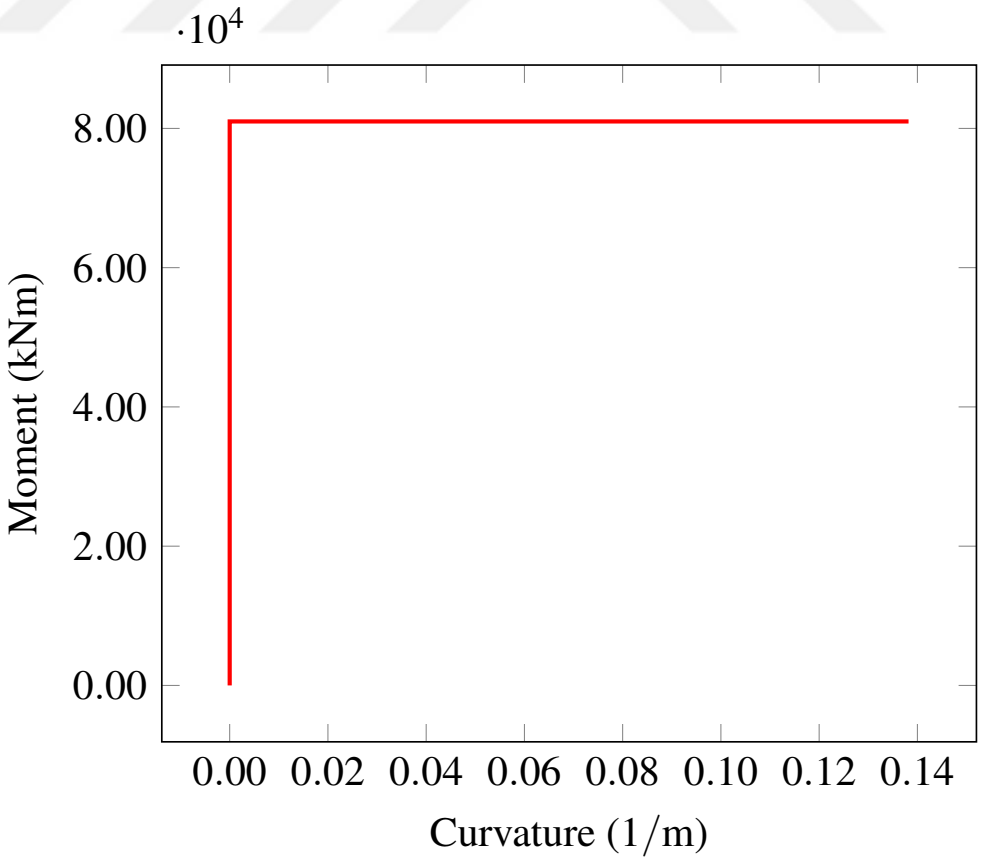

Figure 5.3 : Moment-Curvature relationship of rigid-plastic hinge

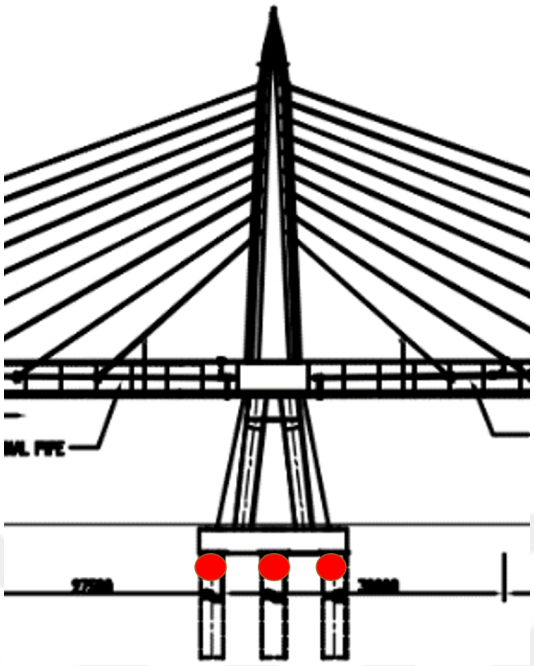

Figure 5.4 : Location of plastic hinges.

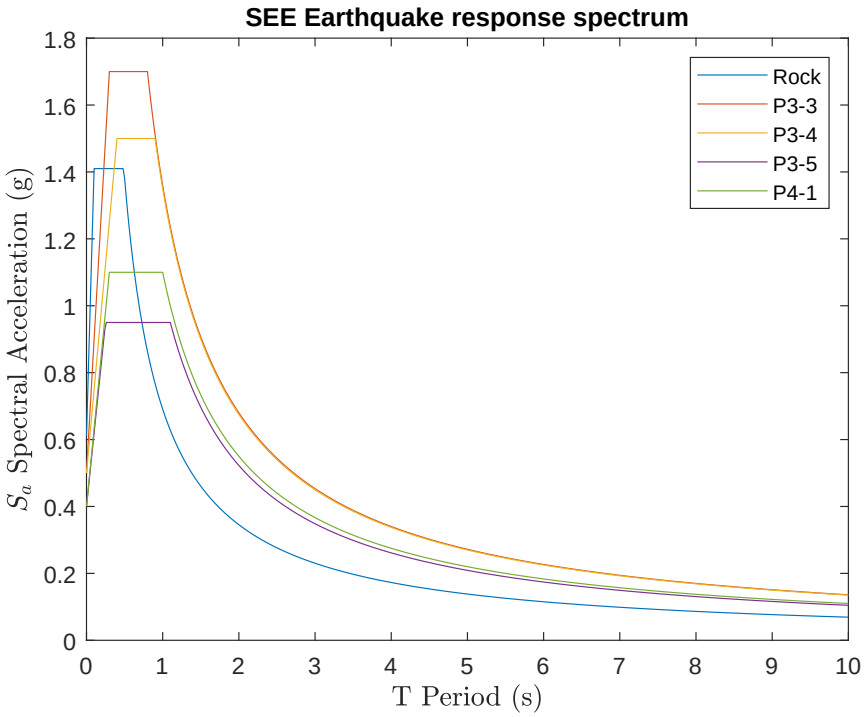

Figure 5.5 : SEE response spectra

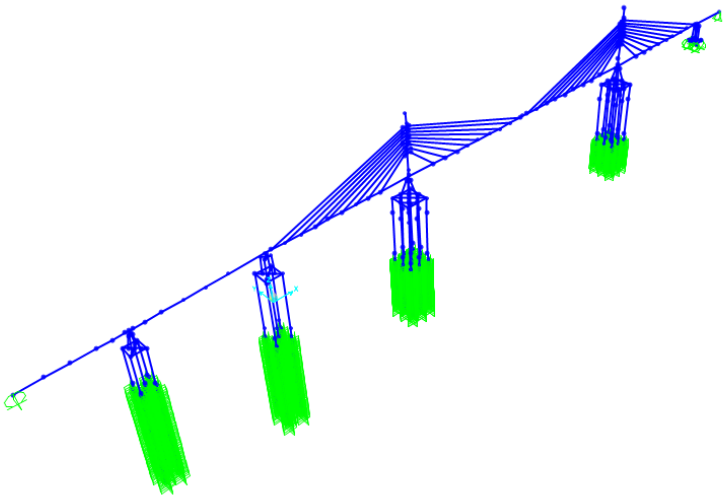

Figure 5.6 : SAP2000 model of GHB.

Table 5.1 : Earthquake records used in time history analysis

Record No	Earthquake	Fault Distance	Duration	Fault types
1605	Düzce	6.58	25.885	SS
1634	Manjil	75.58	29.5	SS
1165	Kocaeli	6.58	30	SS
1166	Kocaeli	30.73	30	SS
1176	Kocaeli	4.83	35	SS
1762	Hector	43.05	60	SS
1787	Hector	11.66	45.3	SS
5948	Sierra	222.36	65	SS
6953	Darfield	24.55	54	SS
836	Landers	87.94	50	SS
883	Landers	172.32	53.315	SS

5.3 Time History Acceleration Data

In the performance assessment of GHB, real acceleration records of earthquakes shall be used. Earthquake records used in this study was presented in Table 5.1. Moreover, the fault distances, duration, and fault types of earthquake were reported as well. More information on the selection of earthquake record may be found the study conducted by Fahjan [66]. Target spectrum is considered as spectrum which is belonging to the rock and its PGA is 0.61 g. In order to obtain the compatible earthquake records with the target spectrum, spectral matching is implemented using SeismoMatch software and matched response spectrum of the earthquake records is shown in Figure 5.7.

5.4 Performance Assessment of GHB

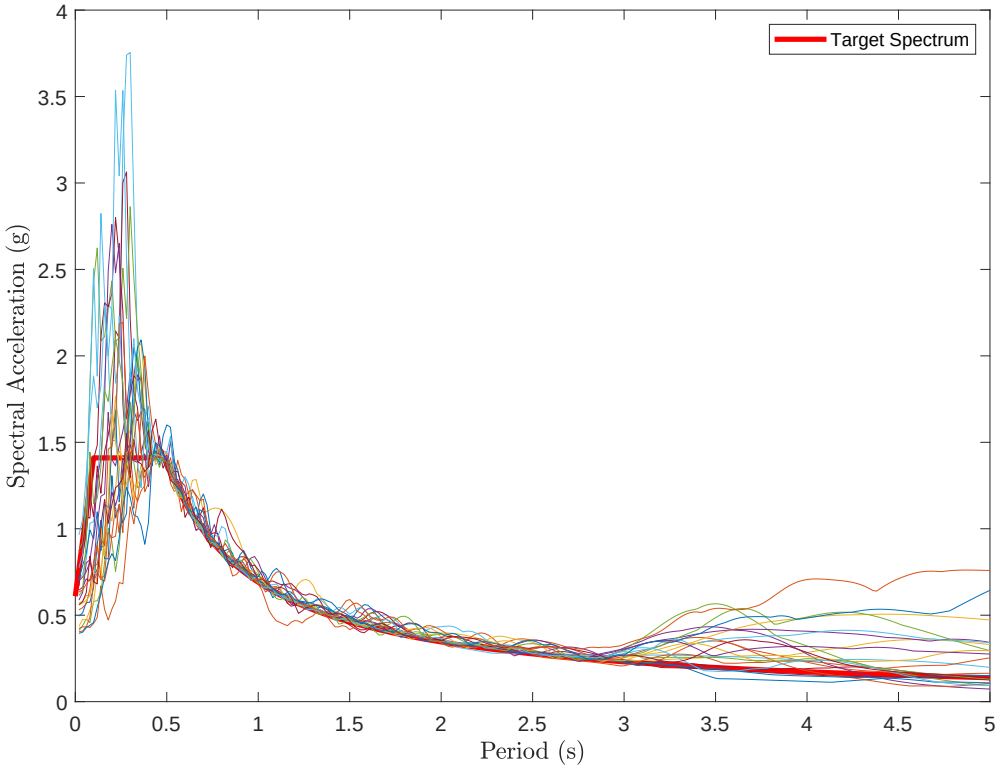

Figure 5.7 : Matched earthquake response spectrum

The nonlinear time history analyses were performed using the SAP2000 software. The nonlinear model of the structures were created by using aforementioned soil structure interaction springs, plastic hinges modeled as rigid-plastic hinge. 22 nonlinear time history analyses were performed for 11 different historical time history records. The maximum hysteresis of an hinge as a results of the nonlinear time history analysis are presented for the critical elements and compared with those given in the FEMA 356. Performance assessment of the critical elements is investigated. The performance of the structure is also investigated using fragility curve analysis for an earthquake. The earthquake used in this fragility curve analysis is RSN1762 earthquake time history. The fragility curve was implemented using earthquake scaled by coefficient ranging from 1.8 to 2.4. And results of the fragility curve analysis are indicated using average plastic rotation of the 54 hinges. For each nonlinear time history analyses, the each plastic rotation of the hinges were obtained and their averages were calculated. The calculated average plastic rotation of the hinges were indicated with respect to the maximum acceleration of piles and the results indicated Figure 5.10. Thanks to this

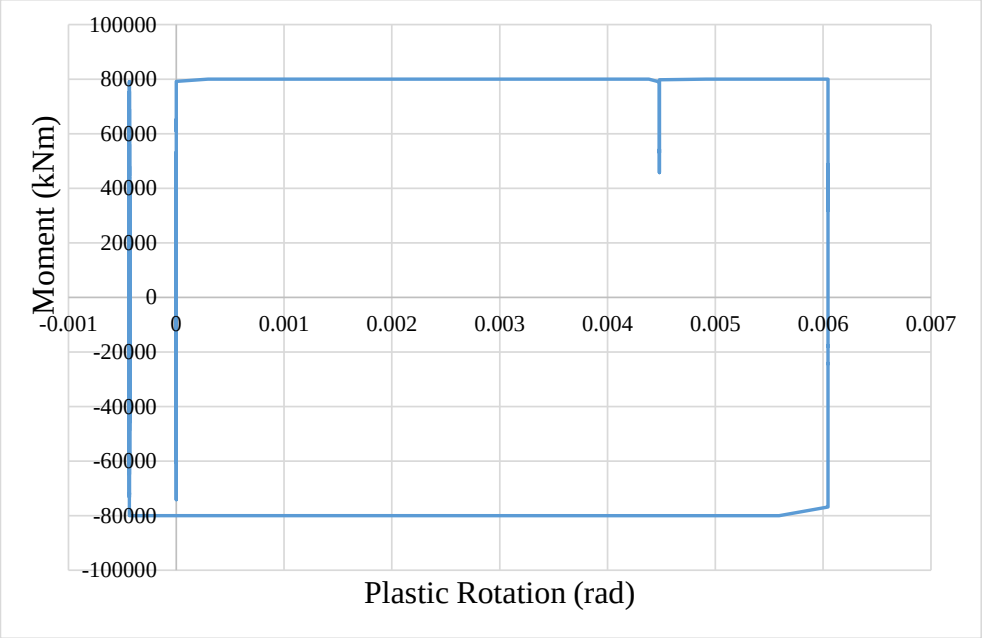

Figure 5.8 : Moment-Plastic rotation of elements of pile P3-3.

fragility curve study, the average maximum rotation can be obtained for the measured maximum acceleration of the top of piles, in the case of seismic event.

According to FEMA 356, the performance of the structural members can be evaluated using using 5.4 and the performance levels are indicated in Table 5.3.

Table 5.3 : Performance of piles P3-3 and P3-4.

Element	θ_{max}	θ_y	Performance level
1	0.006	0.07	IO
2	0.0012	0.07	IO

Table 5.4 : FEMA 356 performance criteria for columns.

For columns $P/P_{CL} < 0.20$	IO	LS	CP
Criteria	$1\theta_y$	$6\theta_y$	$8\theta_y$
	0.07	0.42	0.56

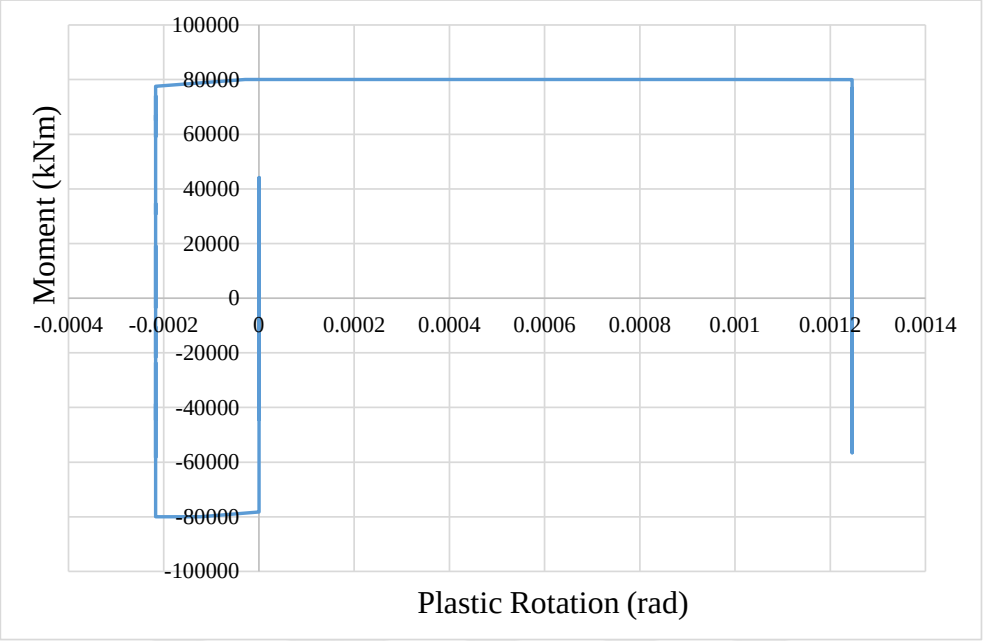

Figure 5.9 : Moment-Plastic rotation of elements of pile P3-4.

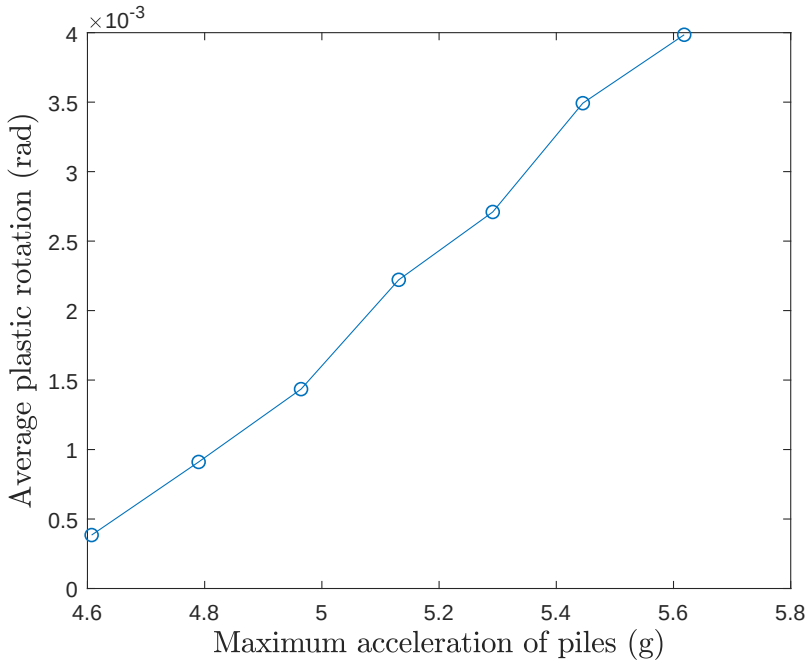

Figure 5.10 : Fragility curve.

Table 5.2 : Spring coefficients for ground modeling.

P2-2					
Spring No	Depth (m)	F1 (kN)	F2 (kN)	Delta 1 (m)	Delta 2 (m)
1	1.5	30	97	0.03	1
2	3	70	223	0.03	1
3	4.5	89	281	0.03	1
4	6	107	340	0.03	1
5	7.5	122	387	0.03	1
6	9	172	545	0.02	0.5
7	10.5	227	719	0.02	0.5
8	12	241	766	0.02	0.5
9	13.5	245	776	0.02	0.5
10	15	245	776	0.02	0.5
11	16.5	245	776	0.02	0.5
12	18	245	776	0.02	0.5
13	19.5	245	776	0.02	0.5
14	21	669	474	0.05	0.19
15	22.5	1094	172	0.05	0.19
16	24	1094	172	0.05	0.19
17	25.5	1094	172	0.05	0.19
18	27	1094	172	0.05	0.19
19	28.5	1094	172	0.05	0.19
20	30	1094	172	0.05	0.19
21	31.5	1094	172	0.05	0.19
22	33	1094	172	0.05	0.19
23	34.5	1094	172	0.05	0.19
24	36	1094	172	0.05	0.19
25	37.5	1094	172	0.05	0.19
26	39	1497	235	0.03	0.14
27	40.5	1900	298	0.03	0.14
28	42	1900	298	0.03	0.14
29	43.5	1900	298	0.03	0.14
30	45	1900	298	0.03	0.14
31	46.5	1900	298	0.03	0.14
32	48	1900	298	0.03	0.14
33	49.5	1900	298	0.03	0.14
34	51	1900	298	0.03	0.14
35	52.5	1900	298	0.03	0.14
36	54	8544	57534	0.01	0.09
37	55.5	15398	116613	0.01	0.09
38	57	15820	120300	0.01	0.09
39	58.5	16242	123986	0.01	0.09
40	60	9233	64896	0.01	0.09

6. CONCLUSION AND RECOMMENDATION

In this study, system identification methods were compared in terms of noise contamination using numerical model and sensor number using experimental setup. The experimental setup is also used for comparing data correcting methods that are implemented in order to obtain displacement signal such as filtering and baseline correction. Moreover, structural parameter estimation of Golden Horn Metro Bridge has been applied through three different system identification algorithms, namely basic frequency domain, frequency domain decomposition, and data-driven stochastic subspace identification. For these purposes, algorithms were implemented using the MATLAB environment. These algorithms were applied to the measured data on experimental setup, data from numerical model, and the measured acceleration of Golden Horn Metro Bridge which is cable-stayed bridge. Furthermore, the measured acceleration data were compared against the data measured from permanent structural health monitoring system. The measured response from the deck of the bridge were analyzed for system identification methods. These methods were investigated for structural parameter estimation to be compared against the mathematical model obtained from the first principle approaches. The mathematical model of the GHB was developed using the SAP2000 commercial software. The model of GHB is also evaluated against the structural modal properties obtained from the system identification methods. The main purpose of this thesis, is to investigate the utilization of the permanent structural health monitoring system to assess the performance of structure after an earthquake. The highlights of the result are listed as follows;

- System identification algorithms used in this study, are useful up to considerable noise magnitudes. Furthermore, number of the sensors affects the capturing the mode shapes significantly. The number of sensors to be used should be chosen considering the probable mode shapes of the structure specifically.

- It was observed that many sensors produce unreliable data in the permanent structural health monitoring system of GHB. The modal properties of the GHB could not be obtained using the existing sensors.
- Measured acceleration of the bridge deck, mode frequencies were obtained and these results were compatible with those extracted from the initial measurements. However, mode shapes belonging to the higher frequencies could not be acquired.
- As a result of performance assessment of the GHB, the maximum plastic rotation of the pile members were under the immediate occupancy limits in case of the structure subjecting to the increased earthquake acceleration.
- First stages of the fragility curve analysis is also implemented in order to compare the measured acceleration obtained from the GHB and the calculated from the mathematical model of the GHB.

Finally, the following modifications should be made to immediately assess the performance of the bridge after an earthquake through structural health monitoring.

- For the seismic use of structural health monitoring system, the number of sensors should be increased to capture the higher frequency mode shape with a high spatial resolution. Increasing resolution provides more information about mode shapes and the accuracy of damage identification is improved. Furthermore, sensors on the bridge are needed to be maintained.
- The sensors deployed on free field or ground which provides information about seismic excitation are necessary, since under the known seismic excitation, performance of GHB can be assessed more accurately with the measured response. Therefore, the performance assessment of GHB can be realized real-time after an earthquake, and decision may be made about the structural health of GHB.
- For the sensor locations of the structural health monitoring system need to be chosen carefully considering expected nonlinear behavior of the structure in order to compare the expected nonlinear behavior of the structure and the real response during an earthquake.

- The finite element model of the structure is required to be improved with the utilization of two or three dimensional elements model to provide more realistic structural responses.
- The earthquake levels used in the fragility curve analysis need to be more frequent in that range to increase resolution of the analyses.

REFERENCES

[1] **Wiecon** (2011). Golden Horn Metro Crossing Project, Superstructure-Detail Design Report, **Technical Report**.

[2] **VCE** (2011). Golden Horn Metro Crossing Permanent Monitoring System, **Technical Report**.

[3] **Doebling, S.W.**, **Farrar, C.R.**, **Prime, M.B. and Shevitz, D.W.** (1996). Damage identification and health monitoring of structural and mechanical systems from changes in their vibration characteristics: a literature review, **Technical Report**, Los Alamos National Lab., NM (United States).

[4] **Rytter, A.** (1993). Vibrational based inspection of civil engineering structures, *Ph.D. thesis*, Dept. of Building Technology and Structural Engineering, Aalborg University.

[5] **Sohn, H.**, **Farrar, C.R.**, **Hemez, F.M.**, **Shunk, D.D.**, **Stinemates, D.W.**, **Nadler, B.R. and Czarnecki, J.J.** (2003). A review of structural health monitoring literature: 1996–2001, *Los Alamos National Laboratory, USA*.

[6] **Carden, E.P. and Fanning, P.** (2004). Vibration based condition monitoring: a review, *Structural health monitoring*, *3*(4), 355–377.

[7] **Fan, W. and Qiao, P.** (2011). Vibration-based damage identification methods: a review and comparative study, *Structural health monitoring*, *10*(1), 83–111.

[8] **Reynders, E.** (2012). System identification methods for (operational) modal analysis: review and comparison, *Archives of Computational Methods in Engineering*, *19*(1), 51–124.

[9] **Felber, A.J.** (1994). Development of a hybrid bridge evaluation system, *Ph.D. thesis*, University of British Columbia.

[10] **Brincker, R.**, **Zhang, L. and Andersen, P.** (2000). Modal identification from ambient responses using frequency domain decomposition, *Proc. of the 18*'International Modal Analysis Conference (IMAC), San Antonio, Texas*.

[11] **Shih, C.**, **Tsuei, Y.**, **Allemang, R. and Brown, D.** (1988). Complex mode indication function and its applications to spatial domain parameter estimation, *Mechanical systems and signal processing*, *2*(4), 367–377.

[12] **Rainieri, C. and Fabbrocino, G.** (2014). Operational modal analysis of civil engineering structures, *Springer, New York*, *142*, 143.

[13] **James, G.**, **Carne, T.G.**, **Lauffer, J.P.** *et al.* (1995). The natural excitation technique (NExT) for modal parameter extraction from operating structures, *Modal Analysis-the International Journal of Analytical and Experimental Modal Analysis*, *10*(4), 260.

[14] **Ibrahim, S.** (1977). Random decrement technique for modal identification of structures, *Journal of Spacecraft and Rockets*, *14*(11), 696–700.

[15] **Brincker, R. and Ventura, C.E.** (2015). *Introduction to Operational Modal Analysis*, John Wiley & Sons, Ltd.

[16] **Juang, J.N. and Pappa, R.S.** (1985). An eigensystem realization algorithm for modal parameter identification and model reduction, *Journal of guidance, control, and dynamics*, *8*(5), 620–627.

[17] **Ho, B. and Kálmán, R.E.** (1966). Effective construction of linear state-variable models from input/output functions, *at-Automatisierungstechnik*, *14*(1-12), 545–548.

[18] **Zeiger, H.p. and McEwen, A.** (1974). Approximate linear realizations of given dimension via Ho's algorithm, *IEEE Transactions on Automatic Control*, *19*(2), 153–153.

[19] **Juang, J.N.**, **Phan, M.**, **Horta, L.G. and Longman, R.W.** (1993). Identification of observer/Kalman filter Markov parameters-Theory and experiments, *Journal of Guidance, Control, and Dynamics*, *16*(2), 320–329.

[20] **Akaike, H.** (1974). Stochastic theory of minimal realization, *IEEE Transactions on Automatic Control*, *19*(6), 667–674.

[21] **Benveniste, A. and Fuchs, J.J.** (1985). Single sample modal identification of a nonstationary stochastic process, *IEEE Transactions on Automatic Control*, *30*(1), 66–74.

[22] **Overschee, P. and Moor, B.** (1996). *Subspace Identification for Linear Systems. [electronic resource] : Theory - Implementation - Applications.*, Boston, MA : Springer US, 1996.

[23] **Peeters, B. and De Roeck, G.** (1999). Reference-based stochastic subspace identification for output-only modal analysis, *Mechanical systems and signal processing*, *13*(6), 855–878.

[24] **Kaynardağ, K. and Soyöz, S.** Structural health monitoring of a tall building.

[25] **Şafak, E. and Celebi, M.** (1991). Seismic response of Transamerica building. II: system identification, *Journal of Structural Engineering*, *117*(8), 2405–2425.

[26] **Çelebi, M. and Şafak, E.** (1991). Seismic Response of Transamerica Building. I: Data and Preliminary Analysis, *Journal of Structural Engineering*, *117*(8), 2389–2404.

[27] **Sun, H. and Büyüköztürk, O.** (2018). The MIT Green Building benchmark problem for structural health monitoring of tall buildings, *Structural Control and Health Monitoring*, *25*(3), e2115.

[28] **Shimpi, V.**, **Sivasubramanian, M.V.**, **Singh, S.**, **Zhang, J.**, **Liu, K.**, **Gao, C.**, **Wu, Z.**, **Zheng, Y.**, **Gao, D.**, **Li, S.** *et al.* (2019). System Identification of Heritage Structures Through AVT and OMA: A Review, *System*, *13*(1).

[29] **Wenzel, H.** (2008). *Health monitoring of bridges*, John Wiley & Sons.

[30] **Sabamehr, A.**, **Lim, C. and Bagchi, A.** (2018). System identification and model updating of highway bridges using ambient vibration tests, *Journal of Civil Structural Health Monitoring*, *8*(5), 755–771.

[31] **Feng, M.Q.**, **Fukuda, Y.**, **Chen, Y.**, **Soyoz, S.**, **Lee, S.** *et al.* (2006). Long-term structural performance monitoring of bridges, *Phase II: Development of Baseline Model and Methodology—Report to the California Department of Transportation*.

[32] **Chatzis, M.N.**, **Chatzi, E.N. and Smyth, A.W.** (2015). An experimental validation of time domain system identification methods with fusion of heterogeneous data, *Earthquake Engineering & Structural Dynamics*, *44*(4), 523–547.

[33] **Sun, H. and Büyüköztürk, O.** (2015). Identification of traffic-induced nodal excitations of truss bridges through heterogeneous data fusion, *Smart Materials and Structures*, *24*(7), 075032.

[34] **Siringoringo, D.M.**, **Abe, M. and Fujino, Y.** (2004). System Identification of Instrumented Bridge Using Earthquake-induced Record, *Proceedings of 22nd IMAC Conference and Exposition 2004: A Conference and Exposition on Structural Dynamics*, pp.26–29.

[35] **Smyth, A.W.**, **Pei, J.S. and Masri, S.F.** (2003). System identification of the Vincent Thomas suspension bridge using earthquake records, *Earthquake Engineering & Structural Dynamics*, *32*(3), 339–367.

[36] **Bas, S.**, **Apaydin, N.M.**, **Ilki, A. and Catbas, F.N.** (2018). Structural health monitoring system of the long-span bridges in Turkey, *Structure and Infrastructure Engineering*, *14*(4), 425–444.

[37] **Soyoz, S.**, **Dikmen, U.**, **Apaydin, N.**, **Kaynardag, K.**, **Aytulun, E.**, **Senkardasler, O.**, **Catbas, N.**, **Lus, H.**, **Safak, E. and Erdik, M.** (2017). System identification of Bogazici suspension bridge during hanger replacement, *Procedia Engineering*, *199*, 1026–1031.

[38] **Apaydin, N. and Erdik, M.**, (2001). Structural vibration monitoring system for the Bosporus Suspension Bridges, Strong motion instrumentation for civil engineering structures, Springer, pp.343–367.

[39] **Temur, E.**, **Pınar, Ö.G.**, **Erkuş, B. and Özden, B.** (2017). Haliç Köprüsü Sağlık İzleme Sisteminin Geliştirilmesi.

[40] **Furtner, P.**, **Stöger, M. and Fritz, M.** Structural health monitoring of Golden Horn Metro Crossing Bridge in Istanbul–initial assessment and permanent monitoring.

[41] **Aydınoğlu, M.** (2007). Deprem Katsayısından Performansa Göre Tasarıma: Bir Mühendisin Bakış Açısından Deprem Mühendisliğinin 40 Yılı, *İstanbul Bülten TMMOB İnşaat Mühendisleri Odası İstanbul Şubesi Aylık Yayın Organı*, *97*(2008), 10–29.

[42] **Housner, G.W.** (1952). Spectrum intensities of strong-motion earthquakes.

[43] **Code, U.B.**, (1958), International Council of Building.

[44] **SEAOC.** (1995). Performance Based Seismic Engineering of Buildings, Vision 2000, *Structural Engineers Association of California*.

[45] **ATC** (1996). Seismic Evaluation and Retrofit of Concrete Buildings, ATC 40, Vol. 1., *Applied Technology Council.*

[46] **Ghobarah, A.** (2001). Performance-based design in earthquake engineering: state of development, *Engineering structures*, *23*(8), 878–884.

[47] **FEMA, F.**, (1997), NEHRP guidelines for the seismic rehabilitation of buildings.

[48] **ATC, A.T.C.** (2010). Modeling and acceptance criteria for seismic design and analysis of tall buildings.

[49] **Kolmogorov, A.N.** (1965). Three approaches to the quantitative definition ofinformation', *Problems of information transmission*, *1*(1), 1–7.

[50] **Papoulis, A. and Pillai, S.U.** (2002). *Probability, Random Variables, and Stochastic Processes*, McGraw-Hill Higher Education, 4 edition.

[51] **Erkus, B.** (2003). A Report on Nonstationary Response of Nonlinear MDOF Systems using Equivalent Linearization and Compact Analytical Model of the Excitation Process.

[52] **Stark, H. and Woods, J.W.** (1986). *Probability, Random Processes, and Estimation Theory for Engineers*, Prentice-Hall, Inc., Upper Saddle River, NJ, USA.

[53] **Bendat, J. and Piersol, A.** (1980). *Engineering applications of correlation and spectral analysis*, Wiley, New York, NY [u.a.].

[54] **Oppenheim, A.V.**, **Willsky, A.S. and Nawab, S.H.** (1996). *Signals and Systems (2Nd Ed.)*, Prentice-Hall, Inc., Upper Saddle River, NJ, USA.

[55] **Chopra, A.K.** (2014). *Dynamics of structures : theory and applications to earthquake engineering.*, Prentice-Hall international series in civil engineering and engineering mechanics, Boston : Pearson, 2014.

[56] **Clough, R. and Penzien, J.** (1993). *Dynamics of Structures*, Civil Engineering Series, McGraw-Hill.

[57] **Celep, Z.** (2011). *Yapı dinamiği.*, İstanbul : Beta, 2001.

[58] **Peeters, B. and De Roeck, G.** (2001). Stochastic system identification for operational modal analysis: a review., *Journal of Dynamic Systems, Measurement, and Control*, (4), 659.

[59] **Felber, A.J.** (1993). Development of a hybrid bridge evaluation system, *Ph.D. thesis*, The University of British Columbia.

[60] **Brincker, R.**, **Zhang, L. and Andersen, P.** (2001). Modal identification of output-only systems using frequency domain decomposition, *Smart Materials and Structures*, *10*(3), 441–445.

[61] **Ljung, L.** (2012). System Identification: Theory for the User, *IEEE Robotics & Automation Magazine, Robotics & Automation Magazine, IEEE, IEEE Robot. Automat. Mag*, (2), 95.

[62] **Peeters, B.** (2000). System Identification and Damage Detection in Civil Engineering, *Ph.D. thesis*, Katholieke Universiteit Leuven.

[63] **Peeters, B. and Roeck, G.D.** (1999). Reference-Based Stochastic Subspace Identification for Output-Only Modal Analysis, *Mechanical Systems and Signal Processing*, *13*(6), 855 – 878.

[64] **Istanbul, M.**, (2019), M2 Metro Line information, `https://www.metro.istanbul/Hatlarimiz/HatDetay?hat=M2`.

[65] **Wiecon** (2011). Golden Horn Metro Crossing Project, Substructure-Detail Design Report, **Technical Report**.

[66] **Fahjan, Y.M.** (2008). Türkiye Deprem Yönetmeliği (DBYBHY, 2007) Tasarım İvme Spektrumuna Uygun Gerçek Deprem Kayıtlarının Seçilmesi ve Ölçeklenmesi, *İMO Teknik Dergi*, *292*, 4423–4444, `http://dergipark.gov.tr/download/article-file/136649`.

APPENDICES

APPENDIX A : Experimental Results
APPENDIX B : System Identification of GHB
APPENDIX C : Performance Assessment of GHB

APPENDIX A: Experimental Studies

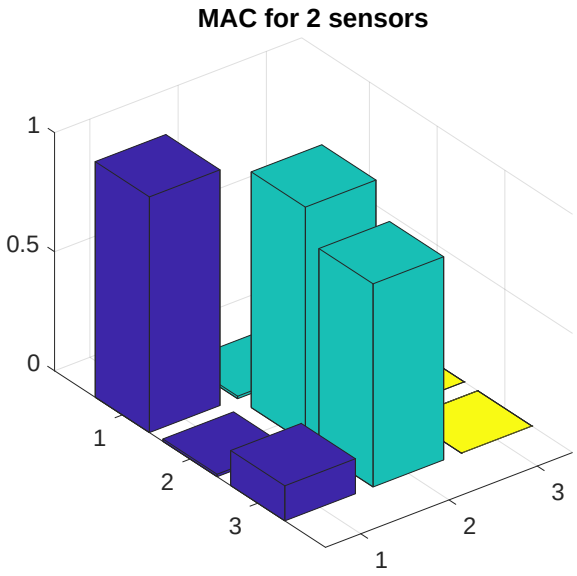

Figure A.1 : MAC values for 2 sensors case

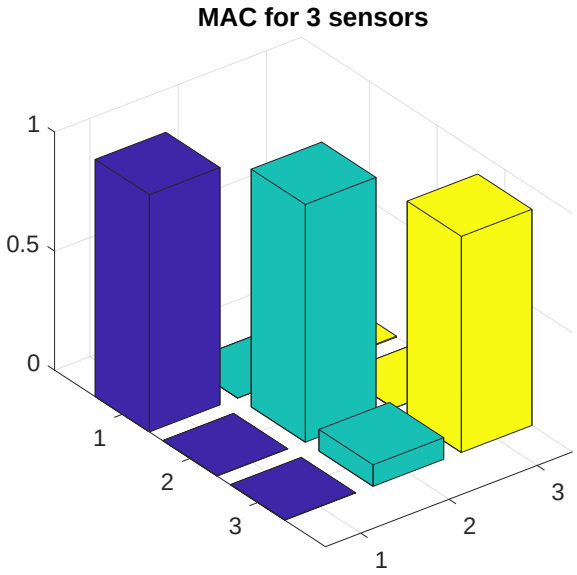

Figure A.2 : MAC values for 3 sensors case

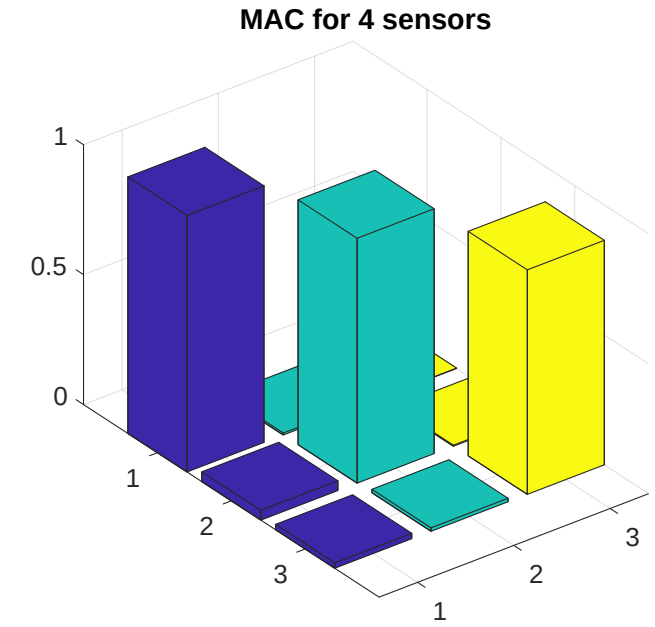

Figure A.3 : MAC values for 4 sensors case

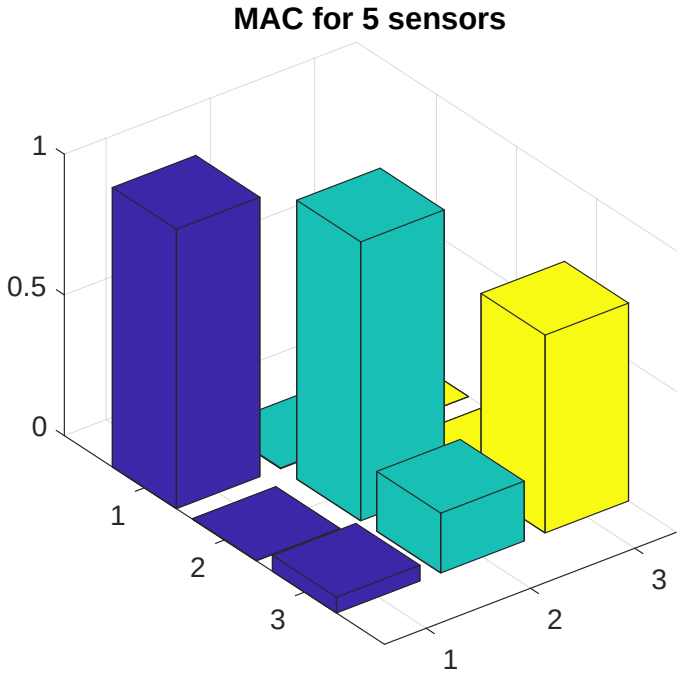

Figure A.4 : MAC values for 5 sensors case

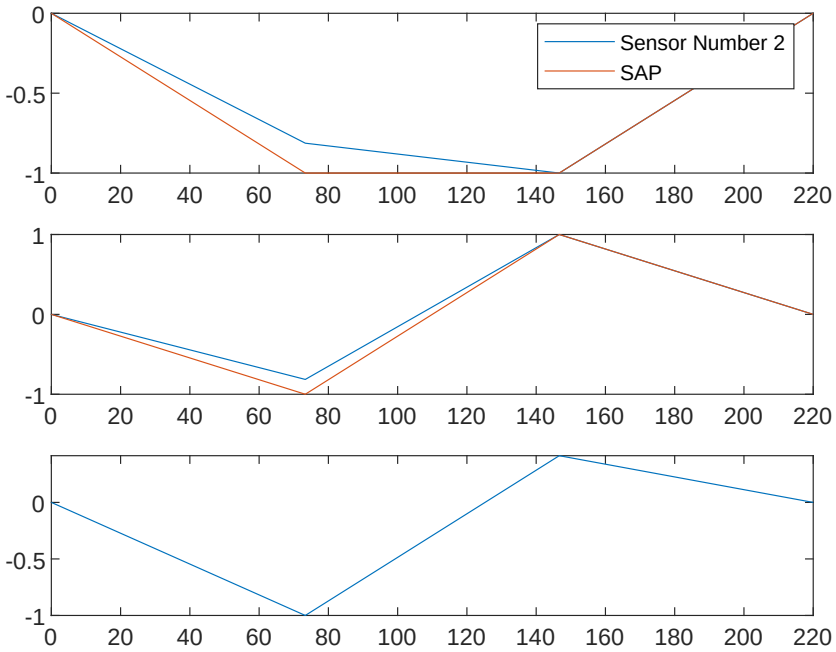

Figure A.5 : Mode shapes for 2 sensors case

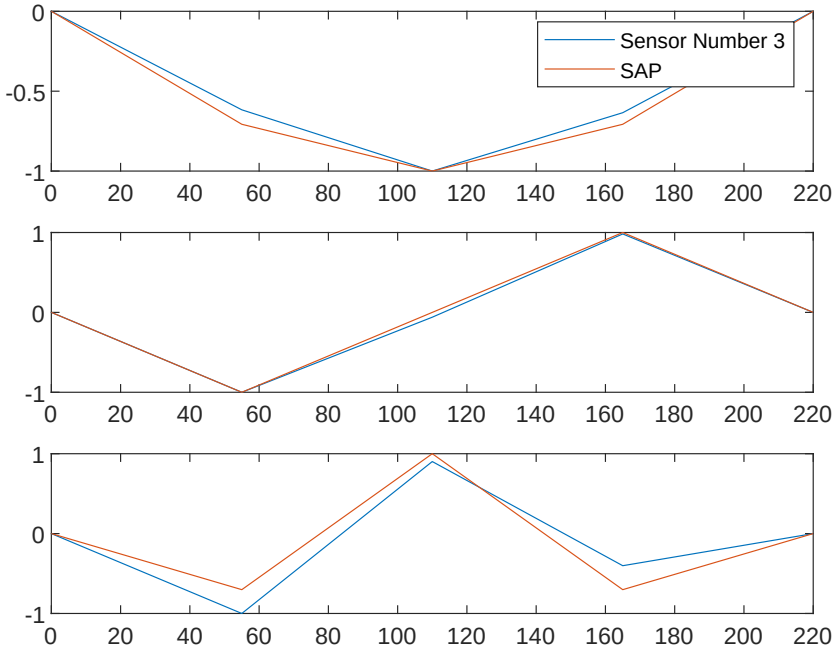

Figure A.6 : Mode shapes for 3 sensors case

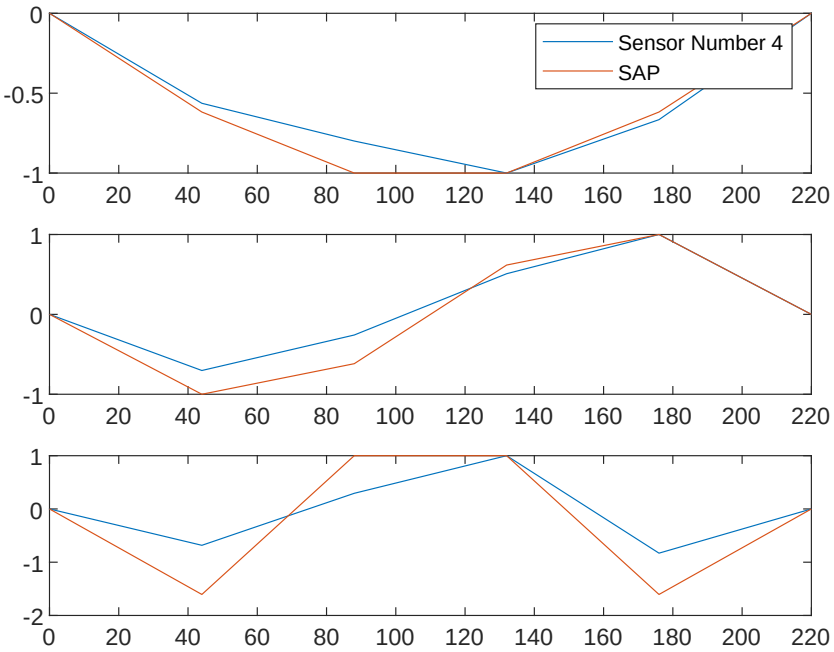

Figure A.7 : Mode shapes for 4 sensors case

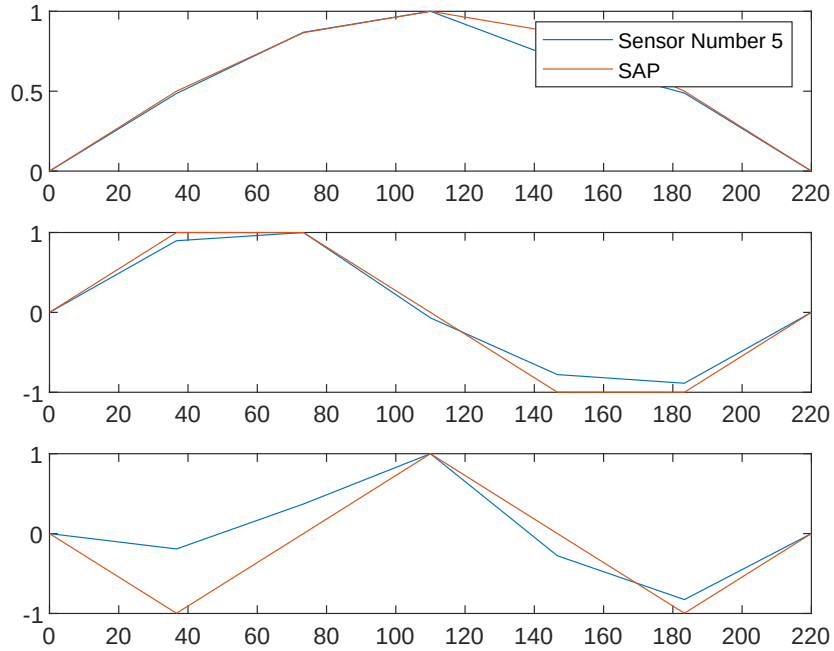

Figure A.8 : Mode shapes for 5 sensors case

APPENDIX B: System Identification of GHB

In this part, the comparisons of measurements recorded in sensor deployed by VCE firm and carried out by the Advanced Structural Systems (ITU) study group. For this purposes, time history plots are presented for both sensor measurement. Moreover, averaged normalized power spectral density, and the singular values of power spectral density matrices are also indicated in the following figures. Additionally, the Fourier spectra of the sensors placed in similar locations are presented in the figure B.11 and B.12. The figures B.1 and B.2 representing the time history plot of the measurement results. The records carried by ITU-AST study group was realized in 25th april 2019 and the records given for comparison were measured in 10th october 2018 and both of the records are measured in approximately 05:00 pm.

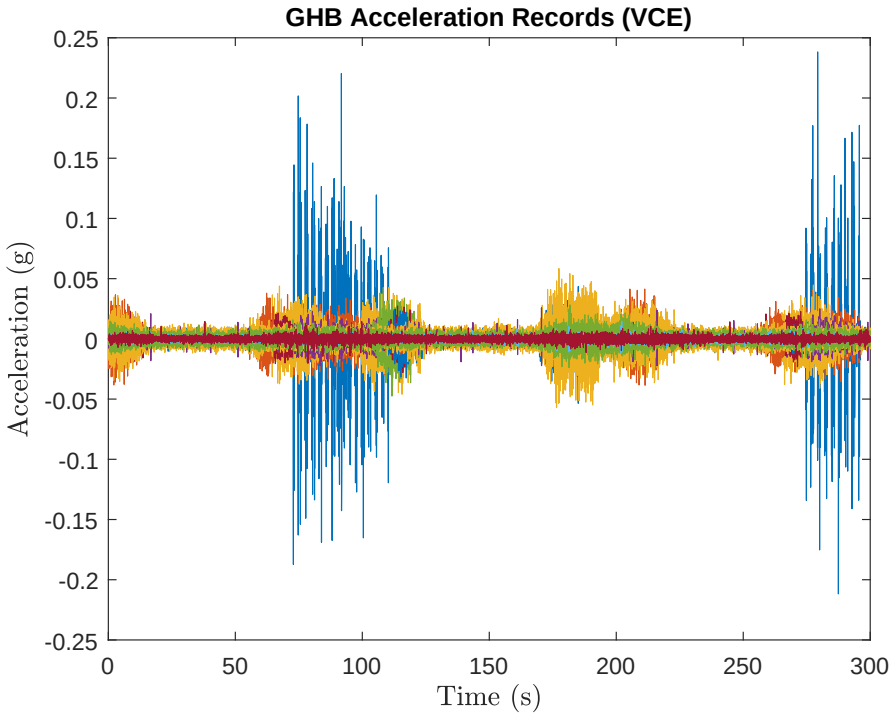

Figure B.1 : VCE acceleration records

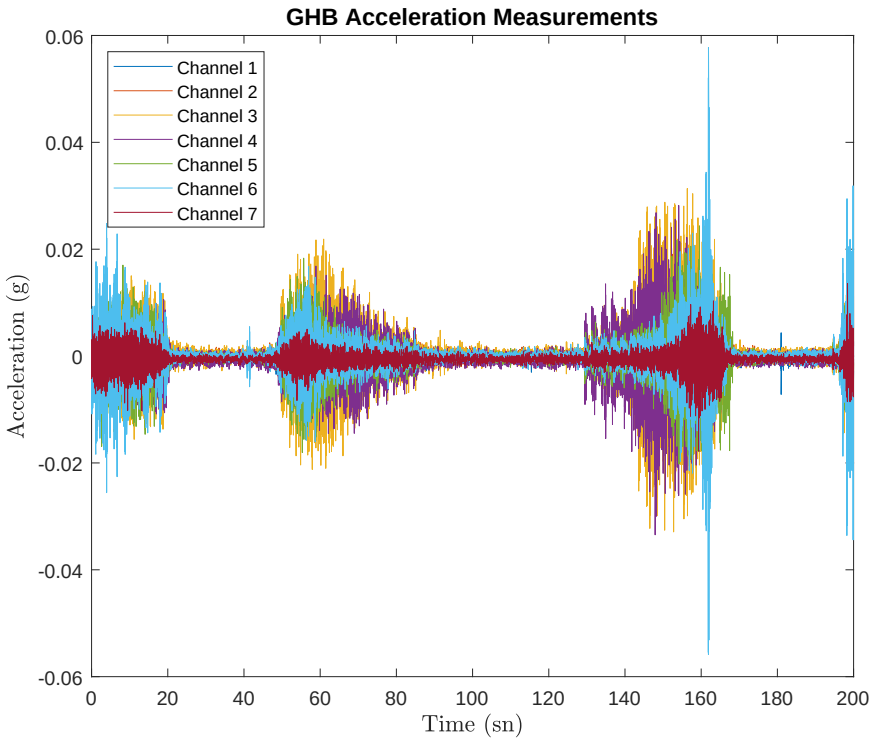

Figure B.2 : AST acceleration measurements

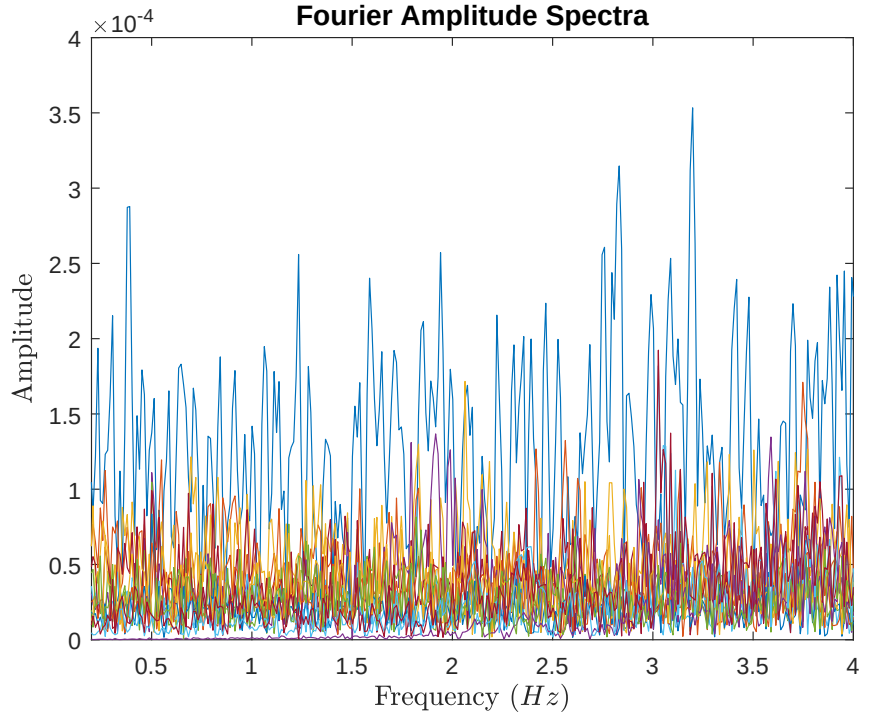

Figure B.3 : VCE Fourier spectra of acceleration measurements

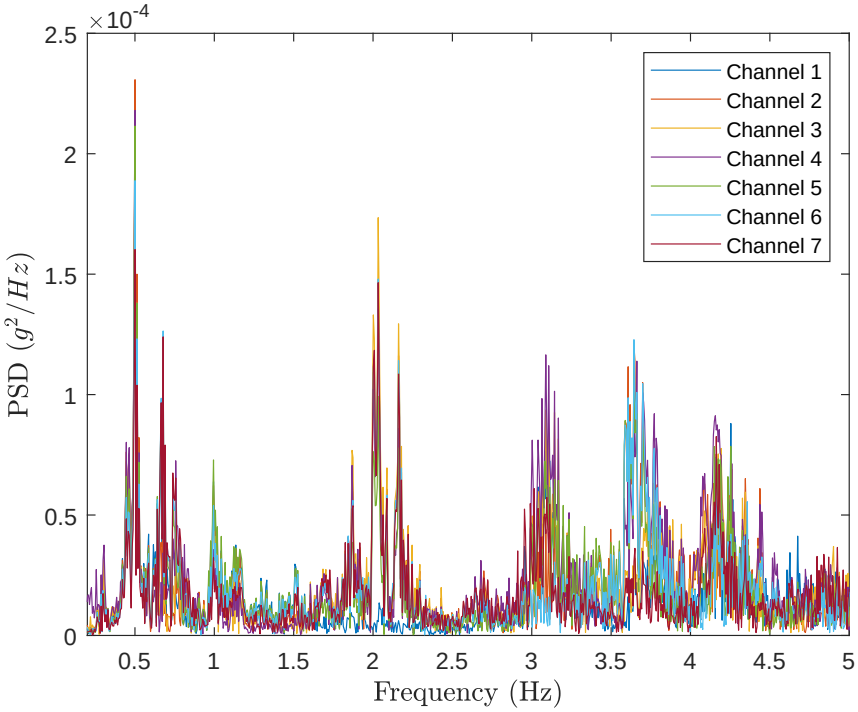

Figure B.4 : AST Fourier spectra of acceleration measurements

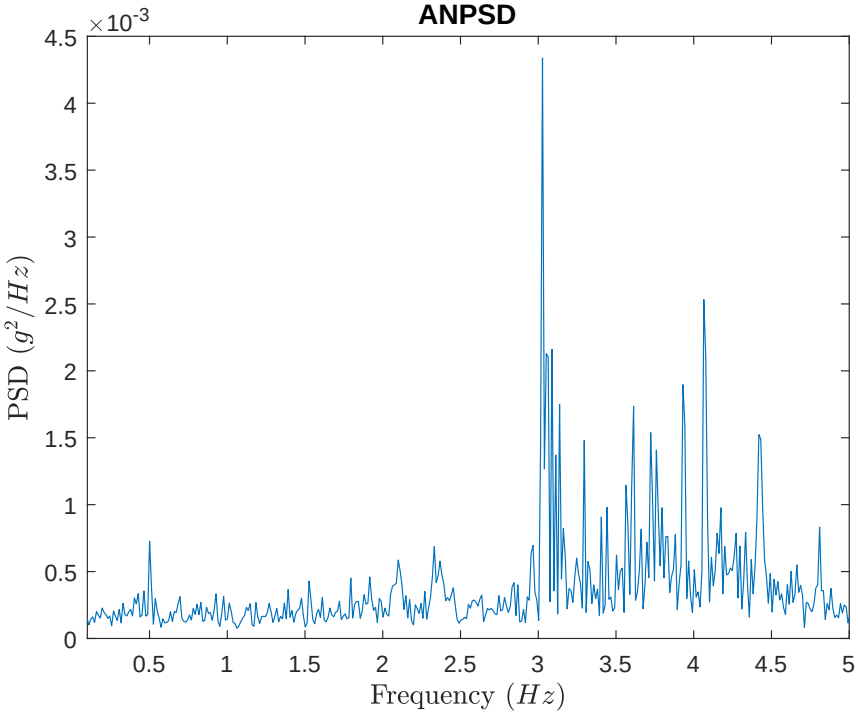

Figure B.5 : VCE ANPSD of acceleration measurements

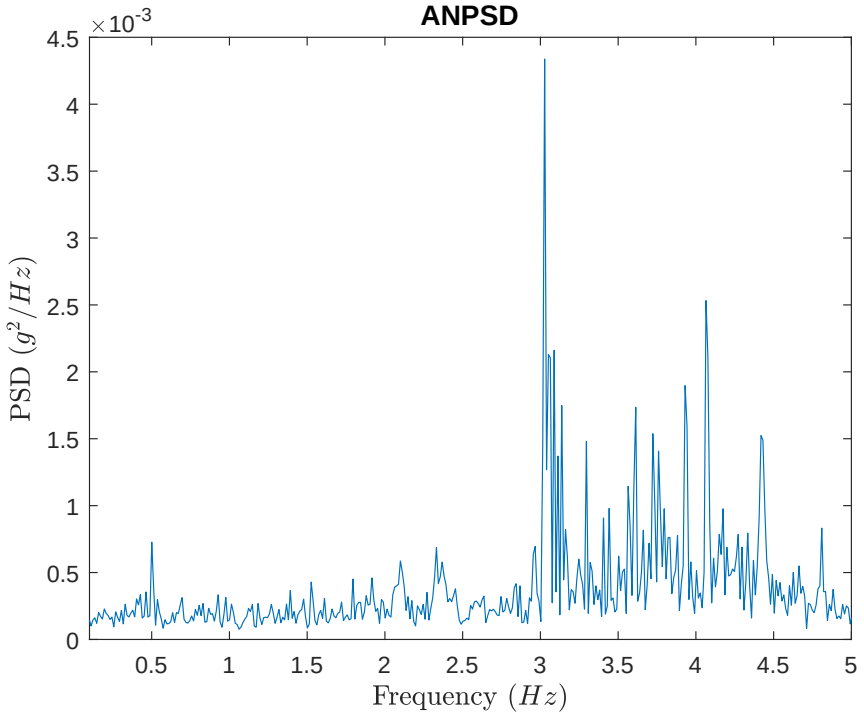

Figure B.6 : VCE ANPSD of acceleration measurements

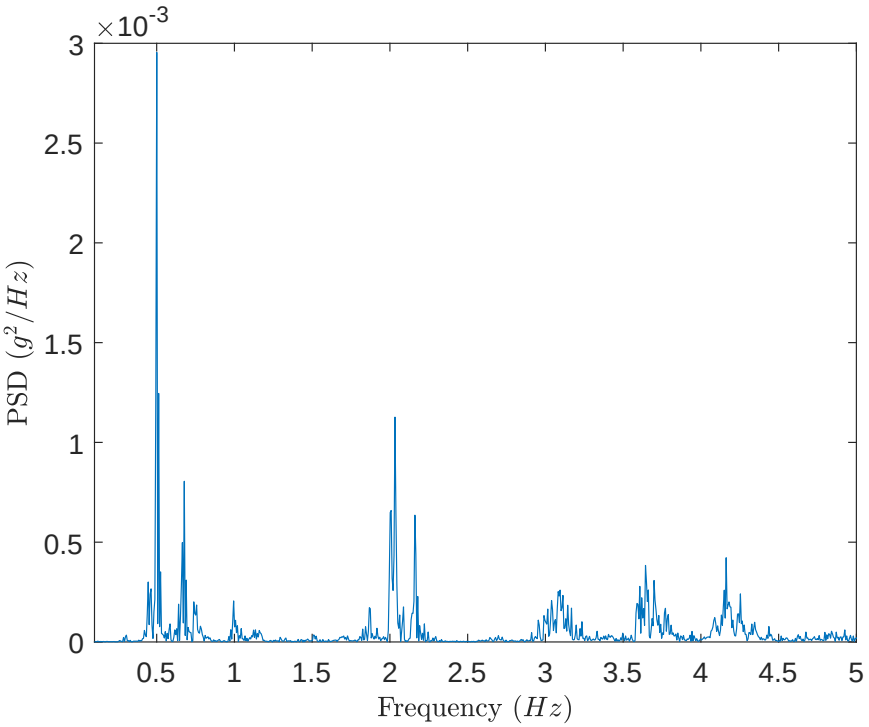

Figure B.7 : AST acceleration measurements

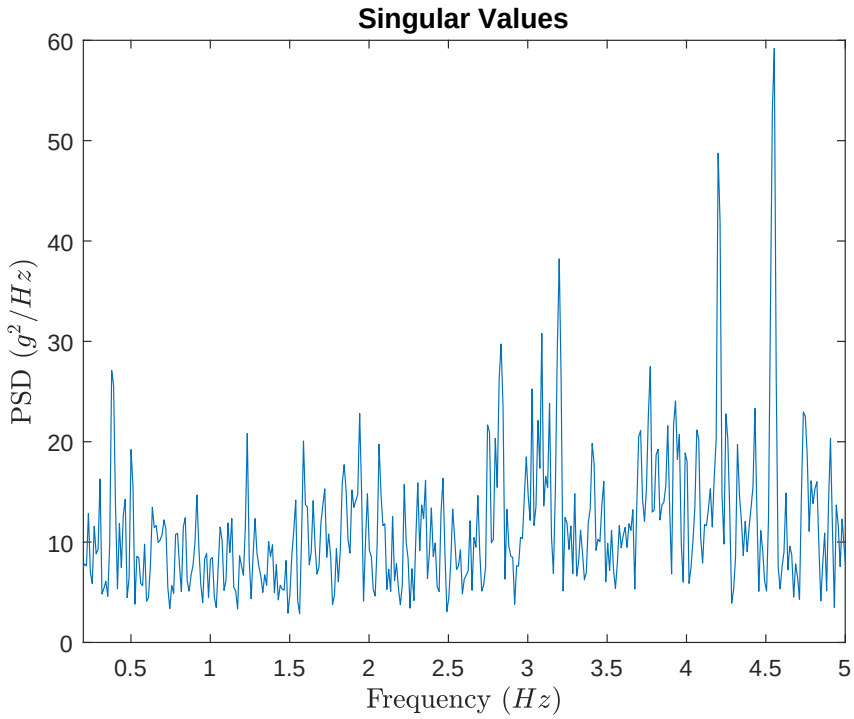

Figure B.8 : VCE Singular values of acceleration measurements

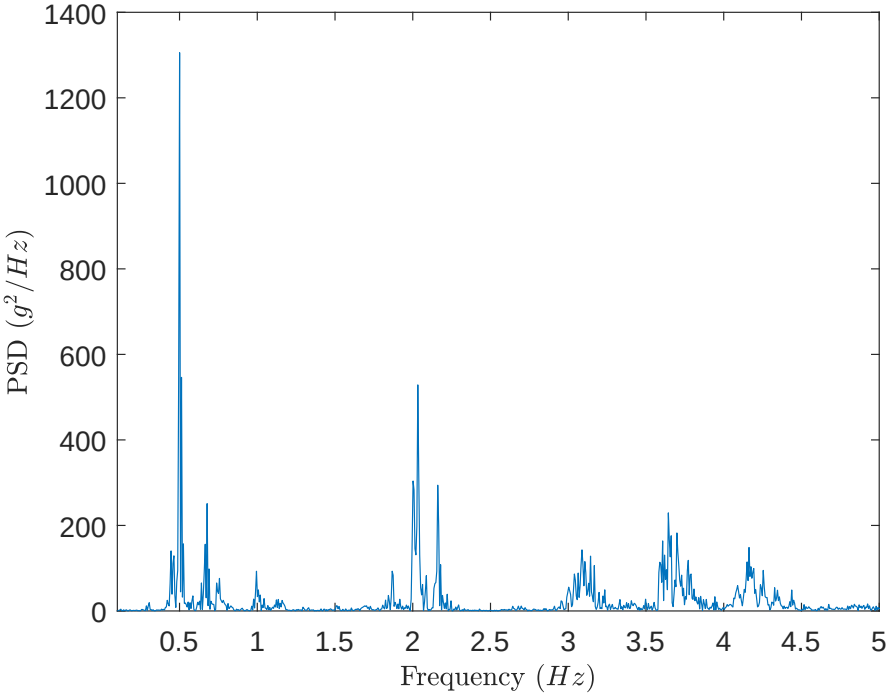

Figure B.9 : AST acceleration measurements

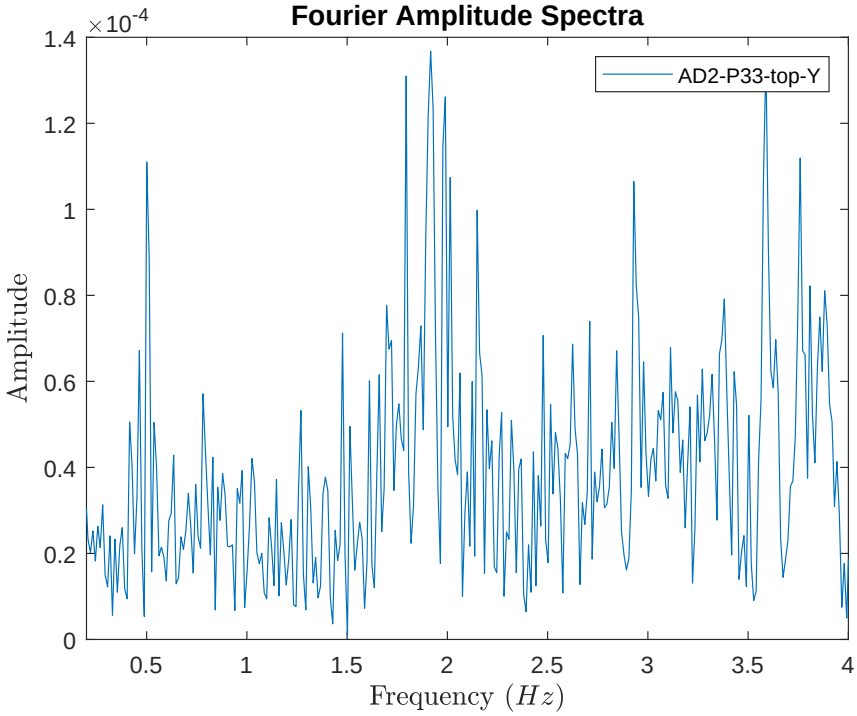

Figure B.10 : VCE Fourier spectra of AD2-P33-top_Y sensor data

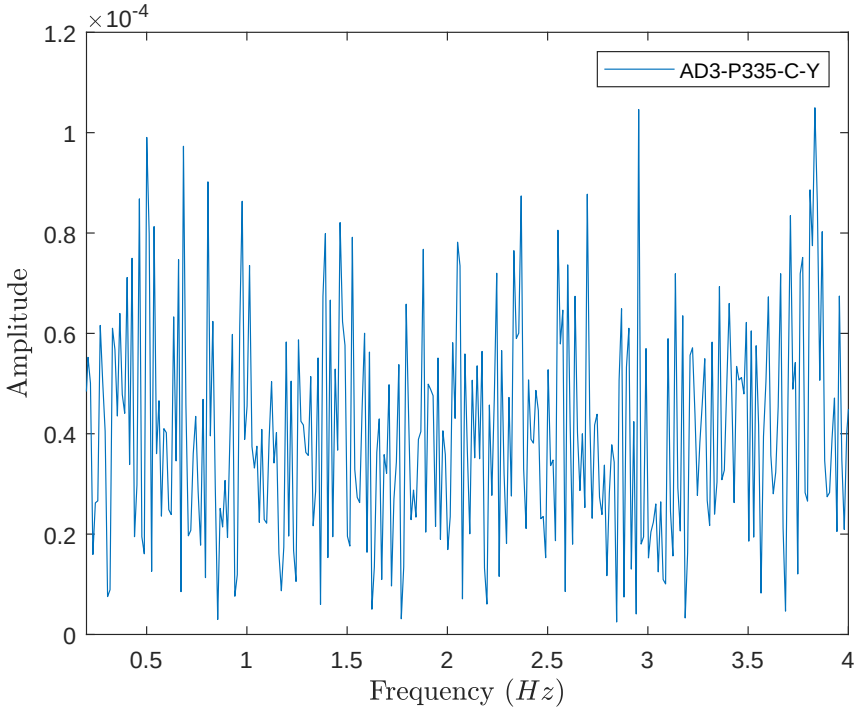

Figure B.11 : VCE Fourier spectra of AD3-P335-C_Y sensor data

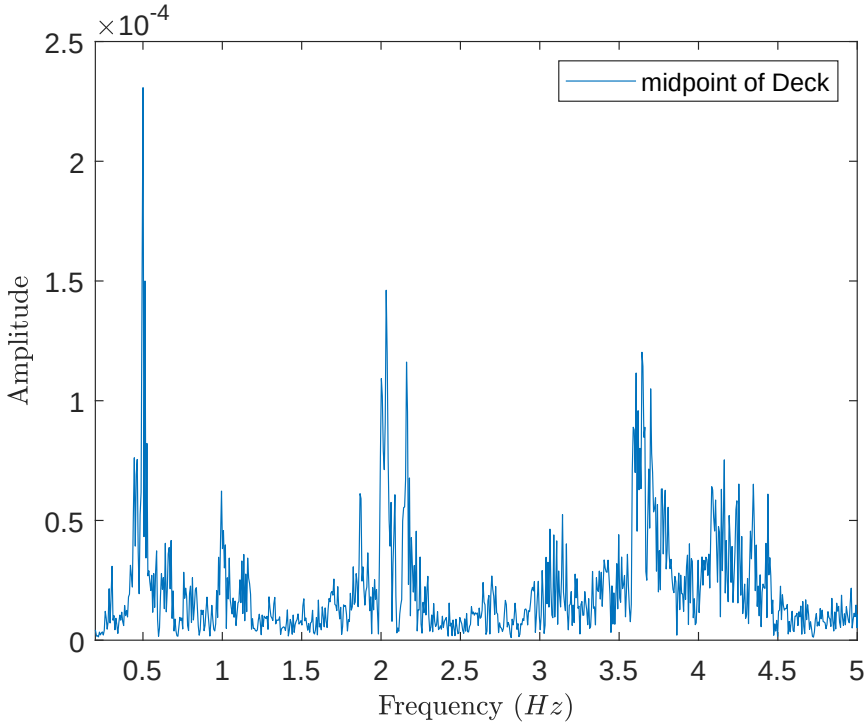

Figure B.12 : AST Fourier spectra of acceleration recorded from midpoint of the deck

APPENDIX C: Performance Assessment of GHB

‘

Table C.1 : Spring coefficients of P3-4

P3-4					
Spring No	Depth (m)	F1 (kN)	F2 (kN)	Delta 1 (m)	Delta 2 (m)
1	1.5	27	84	0.03	1
2	3	62	197	0.03	1
3	4.5	80	253	0.03	1
4	6	97	309	0.03	1
5	7.5	106	338	0.03	1
6	9	138	439	0.03	1
7	10.5	170	540	0.03	1
8	12	170	540	0.03	1
9	13.5	170	540	0.03	1
10	15	170	540	0.03	1
11	16.5	170	540	0.03	1
12	18	1222	2507	0.01	0.09
13	19.5	3691	7264	0.01	0.09

Table C.2 : Spring coefficients of P3-1

P3-1					
Spring No	Depth (m)	F1 (kN)	F2 (kN)	Delta 1 (m)	Delta 2 (m)
1	1.5	30	97	0.03	1
2	3	70	223	0.03	1
3	4.5	89	281	0.03	1
4	6	107	340	0.03	1
5	7.5	122	387	0.03	1
6	9	186	890	0.02	0.5
7	10.5	256	812	0.02	0.5
8	12	280	889	0.02	0.5
9	13.5	295	936	0.02	0.5
10	15	298	945	0.02	0.5
11	16.5	298	945	0.02	0.5
12	18	298	945	0.02	0.5
13	19.5	298	945	0.02	0.5
14	21	298	945	0.02	0.5
15	22.5	298	945	0.02	0.5
16	24	298	945	0.02	0.5
17	25.5	298	945	0.02	0.5
18	27	298	945	0.02	0.5
19	28.5	298	945	0.02	0.5
20	30	298	945	0.02	0.5
21	31.5	298	945	0.02	0.5
22	33	298	945	0.02	0.5
23	34.5	298	945	0.02	0.5
24	36	298	945	0.02	0.5
25	37.5	298	945	0.02	0.5
26	39	298	945	0.02	0.5
27	40.5	298	945	0.02	0.5
28	42	298	945	0.02	0.5
29	43.5	6266	39937	0.01	0.09
30	45	12445	81958	0.01	0.09
31	46.5	12867	88126	0.01	0.09
32	48	13289	94195	0.01	0.09
33	49.5	13711	98968	0.01	0.09
34	51	14133	102654	0.01	0.09
35	52.5	14555	106341	0.01	0.09
36	54	14977	110027	0.01	0.09
37	55.5	8769	58249	0.01	0.09
38	57	3416	6723	0.01	0.09

Table C.3 : Spring coefficients of P3-3

P3-3					
Spring No	Depth (m)	F1 (kN)	F2 (kN)	Delta 1 (m)	Delta 2 (m)
1	1.5	44	140	0.03	1
2	3	99	313	0.03	1
3	4.5	120	380	0.03	1
4	6	141	446	0.03	1
5	7.5	161	512	0.03	1
6	9	182	579	0.03	1
7	10.5	197	627	0.03	1
8	12	202	641	0.03	1
9	13.5	202	641	0.03	1
10	15	202	641	0.03	1
11	16.5	202	641	0.03	1
12	18	202	641	0.03	1
13	19.5	202	641	0.03	1
14	21	202	641	0.03	1
15	22.5	202	641	0.03	1
16	24	202	641	0.03	1
17	25.5	202	641	0.03	1
18	27	202	641	0.03	1
19	28.5	271	861	0.02	0.5
20	30	340	1080	0.02	0.5
21	31.5	340	1080	0.02	0.5
22	33	1528	3213	0.01	0.09
23	34.5	3900	7676	0.01	0.09

CURRICULUM VITAE

Name Surname: Eray Temur

Place and Date of Birth: Kayseri, 1990

E-Mail: temureray@gmail.com

EDUCATION:

- **B.Sc.:** 2015, Istanbul Technical University, Environmental Engineering,
- **B.Sc.:** 2016, Istanbul Technical University, Civil Engineering.

PUBLICATIONS ON THE THESIS:

- **Temur, E. , Pınar, Ö. G., Erkus, B., and Caglayan, B. Ö.** (2017) "Development of Structural Health Monitoring System of Golden Horn Bridge. (in Turkish)" 7 th Steel Structures Symposium, Gaziantep, Turkey.
- **Temur, E. and Erkus, B.** (2019) “Seismic Performance Assessment of Golden Horn Metro Bridge Through Structural Health Monitoring System” 5th International Conference On Earthquake Engineering and Seismology, Ankara, Turkey.